Characterization and Improvement of Interferon-γ Glycosylation in Chinese Hamster Ovary Cell Culture

by

Xuejun (Sherry) Gu

B. S. Chemistry
Pittsburg State University, 1992

SUBMITTED TO THE DEPARTMENT OF CHEMICAL ENGINEERING IN PARTIAL FULFILLMENT OF THE REQUIREMENT FOR THE DEGREE OF

DOCTOR OF SCIENCE IN CHEMICAL ENGINEERING

at the
MASSACHUSETTS INSTITUTE OF TECHNOLOGY
September 1997

Signature of Author: _____
Department of Chemical Engineering
September, 1997

Certified by: _____
Daniel I. C. Wang
Institute Professor
Thesis Supervisor

Accepted by: _____
Robert E. Cohen
Professor of Chemical Engineering
Chairman, Committee for Graduate Students

Characterization and Improvement of Interferon-γ Glycosylation in Chinese Hamster Ovary Cell Culture

by

Xuejun (Sherry) Gu

Submitted to the Department of Chemical Engineering on September, 1997 in Partial Fulfillment of the Requirement for the Degree of Doctor of Science in Chemical Engineering

ABSTRACT

Glycoproteins, representing an important category of therapeutics for human health care, generally exist as a set of glycosylated variants exhibiting heterogeneity with respect to both the proportion of potential glycosylation sites that are occupied (*i.e.*, macroheterogeneity) and the oligosaccharide structures observed at each glycosylation site (*i.e.*, microheterogeneity). Therefore, it is essential to characterize and, if possible, optimize the glycosylation profiles of recombinant glycoproteins to ensure their quality and consistency as effective pharmaceuticals and to meet increasing regulatory demands.

In this study, the two potential N-linked glycosylation sites (*i.e.*, Asn^{25} and Asn^{97}) of recombinant human interferon-γ (IFN-γ) derived from Chinese hamster ovary (CHO) cell culture were characterized by a sensitive (~ 1 μg) and rapid (~ 3 h) analytical methodology employing a variety of tandem chromatographic techniques, capillary electrophoresis and mass spectrometry. Although complex biantennary glycans were the predominant structures at both glycosylation sites, Asn^{25}-linked glycans possessed higher proportions of tri- and tetraantennary structures and were exclusively fucosylated compared to glycans at Asn^{97}. Although the proportions of glycan antennary structures were found to be relatively invariable throughout typical CHO batch cultures, the oligosaccharide structures were selectively altered by the introduction of various inhibitors of intracellular glycosylation pathways. For example, the use of dexamethasone, an inhibitor of the enzyme responsible for oligosaccharide branching, was found to decrease the proportions of tri- and tetraantennary glycan structures and, thus, improve the glycosylation homogeneity of CHO-derived IFN-γ.

A critical aspect of glycosylation is sialylation since the presence of sialic acid can dramatically extend a glycoprotein's circulatory lifetime. The sialylation patterns of CHO-derived IFN-γ were characterized by RP-HPLC separations of glycosylation site-specific tryptic glycopeptides. IFN-γ displayed both site- and branch-specific differences in sialic acid content as Asn^{25}-linked glycans and the Man(α1-3) branch of the predominant complex biantennary glycan structures at

each site were preferentially sialylated. Both incomplete intracellular sialylation and extracellular desialylation resulting from release of sialidase during cell lysis were found to determine the sialic acid content of the final product. Primatone RL, an animal tissue hydrolysate commonly employed as a serum substitute to stimulate cell growth, was found to have an adverse impact on intracellular sialylation of CHO-derived IFN-γ in both batch and fed-batch cultures. However, incomplete intracellular sialylation was minimized through feeding of N-acetylmannosamine (ManNAc), a synthetic precursor of sialic acid. Feeding of 20 mM ManNAc reduced the proportion of undersialylated glycan structures by 50%. Radiolabeled ManNAc was utilized to confirm that the supplemental ManNAc was incorporated into IFN-γ as sialic acid. The intracellular pool of CMP-sialic acid, the nucleotide sugar substrate for sialyltransferase, was also extracted and quantitated by RP-HPLC. Although feeding of 20 mM ManNAc increased the intracellular pool of CMP-sialic acid nearly 30-fold, *in vitro* incubation of isolated Golgi with radiolabeled CMP-sialic acid revealed a limitation for transport of the substrate to the site of sialylation

Thesis Supervisor Dr Daniel I. C Wang
Title: Institute Professor

Acknowledgments

Although I am listed as the only author of this thesis, there are many people who have contributed greatly to my thesis, who have been very helpful and kind to me during my years at MIT.

First of all, I would like to thank my undergraduate advisor, Prof. Clarence E. Pfluger, at Pittsburg State University, who granted me a scholarship seven years ago. Without this scholarship, I would have had no chance to come to this country and take any advanced education. His guidance and wisdom has extended beyond my years at PSU. We still keep in good contact and I am looking forward to visiting him again after my thesis defense. Mrs. Pfluger cooks the best Matzo ball soup I have ever had.

I would also like to thank my thesis advisor, Dr. Daniel I. C Wang, for not only giving me insightful guidance on research but also letting me understand how to build up my self-esteem for future career development. I would also like to thank my committee members, Prof. Lodish, Prof. Regnier, Prof Stephanopoulos and Prof. Griffith, for their constructive advice as well as valuable information.

Many of my coworkers at BPEC have made my stay at MIT enjoyable as well as unforgettable: Gregg, Steve, Marc, Joydeep, Araba, Robert, Brian, Inn, Chandrea, Anna, Jifeng, Audrey, Chris, Lynn, Darlene and John. Thank you guys for everything, and I hope to bump into some of you some day. I will see if you can still remember my name then.

I would also like to thank some of my Chinese Buddies at MIT, Lei, Tani, Jane, Gene, and Jianfeng, for the tradition of Monday lunch and keeping my life entertained.

I would also like thank my Mom Xianglian, brother Xuedong and sister Xueming for letting me living in this wonderful family ever since I came to this world. Of course, nothing would be good enough for me to thank my research collaborator and husband, Bryan Harmon, for his love and effort. I am looking forward to sharing my life with him.

Finally, I would like to dedicate this thesis to my father, Yishou Gu, from a daughter he never had a chance to be proud of, and for a father that the daughter never had the chance to know enough.

TABLE OF CONTENTS

ABSTRACT **2**

ACKNOWLEDGMENTS **4**

TABLE OF CONTENTS **6**

LIST OF FIGURES **9**

LIST OF TABLES **13**

CHAPTER ONE: INTRODUCTION **15**

1.1 Introduction 15

1.2 Thesis Objective 16

1.3 Thesis Organization 16

CHAPTER TWO: LIETERATURE REVIEW **18**

2.1 N-linked glycosylation pathway 18

2.2 Fuctions of carbohydrates in glycoproteins 23

2.3

2.2.1 Influence on protein solubility and thermal stability 23

2.2.2 Protection from protease attack 24

2.2.3 Influence on biological activity and immunogenicity 24

2.2.4 Influence on glycoprotein *in vivo* circulatory half-life 26

2.3 Factors influencing protein glycosylation 26

2.3.1 Influence of protein 27

2.3.2 Influence of expression system 28

2.3.3 Culture environment 30

2.3.3.1 Cell culture medium composition 30

2.3.3.2 Other intracellular events 32

2.3.3.3 Physical parameters of culture 34

2.3.3.4 Degradation of product glycosylation 35

2.4 Analytical techniques for protein glycosylation determination 35

2.4.1 Analytical techniques for glycosylation macroheterogeneity 36

2.4.2 Analytical techniques for detailed glycan analysis 37

2.4.2.1 Analysis of free glycans 37

2.4.2.2 Analysis of glycopeptides 38

2.5 Model system: IFN-γ and γ-CHO cell culture 44

CHAPTER THREE: MATERIALS AND METHODS 47

3.1 CHO cell culture 47
3.1.1 CHO cell stock preparation 47
3.1.2 CHO cell batch cultures 48
3.1.3 CHO cell cultures containing deocymannojirimycin 49
3.1.4 CHO cell cultures containing 2,3-dehydro-2-deoxy-N-acetylneuraminic acid 49
3.1.5 CHO cell cultures containing Primatone RL 49
3.1.6 CHO cell cultures containing ammonia 50
3.1.7 CHO cell cultures using JRH PF-CHO medium 50
3.1.8 CHO cell cultures containing dexamethasone 50
3.1.9 CHO cell cultures containing N-acetyl-mannosamine (ManNAc) 51
3.1.10 Fed-batch CHO cultures 51

3.2 IFN-γ glycosylation characterization 52
3.2.1 IFN-γ purification by immunoaffinity chromatography 52
3.2.2 Characterization of IFN-γ macroheterogeneity 53
3.2.3 Digestion of IFN-γ and fractionation of glycopeptides 54
3.2.4 MALDI/TOF mass spectrometry 55
3.2.5 Enzymatic digestions 56
3.2 6 Site- and branch-specific quantitation of sialylation 56
3.2.7 Identification of monosialylated biantennary glycopeptide fractions 57

3.3 Nucleotide sugar extraction and quantitation of intracellular CMP-sialic acid 58

3.4 Determination of incorportion of radiolabeled ManNAc 59

3.5 Isolation of Golgi from CHO cells and study of CMP-NANA *in vitro* transport through Golgi membrane 60

CHAPTER FOUR: CHARACTERIZATION OF IFN-γ GLYCOSYLATION 63

4.1 Purification of IFN-γ 65

4.2 Determination of IFN-γ glycosylation macroheterogeneity 67

4.3 Determination of IFN-γ glycosylation microheterogeneity 77

4.4 Determination of IFN-γ sialylation 97

CHAPTER FIVE: THE INFLUENCE OF CELL CULTURE CONDITIONS ON IFN-γ GLYCOSYLATION 115

5.1 Changes of glycosylation pattern throughout culture process 115

5.2 Influence of medium composition on sialylation of recombinant human IFN-γ in Chinese hamster ovary cell culture 126

5.2.1 Sialylation of IFN-γ from batch CHO culture using different serum-free media 128

5.2.2 Sialylation of IFN-γ from fed-batch CHO culture with and without Primatone RL feeding 138

CHATPER SIX: IMPROVEMENT OF IFN-γ GLYCOSYLATION IN CHO CELL CULTURE 147

6.1 Improvement of antennarity homogeneity by dexamethasone feeding 147

6.2 Improvement of sialylation by feeding of N-acetylmannosamine 153

6.2.1 Effect of supplemental ManNAc on intracellular CMP-sialic acid 156

6.2.2 Incorporation of supplemental ManNAc 159

6.2.3 Effect of supplemental ManNAc on product sialylation 161

6.2.4 Transport of CMP-sialic acid through Golgi vesicles 167

CHAPTER SEVEN: CONCLUSIONS AND RECOMMENDATIONS 172

REFERENCES 178

List of Figure

Figure 2.1 The biosynthesis of core N-linked oligosaccharide 20

Figure 2.2 N-linked glycosylation 21

Figure 2.3 Structures of the major types of asparagine-linked oligosaccharide 22

Figure 2.4 Matrix-assisted laser desorption ionization/time-of-flight mass spectrometry (MALDI/TOF) 40

Figure 2.5 Matrix-assisted laser desorption ionization (MALDI) 41

Figure 2.6 Time of flight (TOF) detector 43

Figure 4.1 Rapid characterization of interferon-γ glycosylation macro- and microheterogeneity 64

Figure 4.2 Immunoaffinity chromatography of interferon-γ from CHO supernatant 66

Figure 4.3 Calibration curve for quantitation of interferon-γ by immunoaffinity chromatography 68

Figure 4.4 On-line concentration enhancement of interferon-γ by solid-phase extraction using perfusion reversed-phase chromatography 70

Figure 4.5 Mechanism of interferon-γ separation by micellar electrokinetic chromatography (MEKC) 72

Figure 4.6 Determination of interferon-γ macroheterogeneity by micellar electrokinetic chromatography (MEKC) 74

Figure 4.7 Monitoring of interferon-γ with PNGase F digestion with time 76

Figure 4.8 MALDI/TOF mass spectrum of intact immunopurified IFN-γ from day seven of suspension γ-CHO batch culture 78

Figure 4.9 On-line proteolysis of immunopurified interferon-γ by immobilized trypsin cartridge 81

Figure 4.10 Reversed-phase HPLC chromatogram of tryptic peptides of recombinant human IFN-γ 83

Figure 4.11 MALDI/TOF mass spectra of tryptic glycopeptides of (A) Asn^{97} (fraction A of Figure 4.10) and (B) Asn^{25} (fraction B of Figure 4.10) glycosylation sites of recombinant human IFN-γ 85

Figure 4.12 MALDI/TOF mass spectra of PNGase F-treated tryptic glycopeptides of (A) Asn^{97} and (B) Asn^{25} glycosylation sites of recombinant human IFN-γ 86

Figure 4.13 MALDI/TOF mass spectra of sialidase-treated tryptic glycopeptides of (A) Asn^{97} and (B) Asn^{25} glycosylation sites of recombinant human IFN-γ 93

Figure 4.14 Inhibition of glycoprotein processing by deoxymannojirimycin 95

Figure 4.15 MALDI/TOF mass spectra of tryptic glycopeptides of (A) Asn^{97} and (B) Asn^{25} glycosylation sites of recombinant human IFN-γ from γ-CHO culture in presence of 2.5 mM deoxymannojirimycin 96

Figure 4.16 Neutral pH/borate complexation reversed-phase HPLC separation of Asn^{97}-linked IFN-γ tryptic glycopeptides following 168 h of suspension batch CHO cell culture 102

Figure 4.17 MALDI-TOF mass spectra of complex biantennary peaks of Asn^{97}-linked tryptic glycopeptides of IFN-γ eluted from neutral pH/borate complexation reversed-phase HPLC chromatography 105

Figure 4.18 MALDI-TOF mass spectra of Monosialo isomers treated with galactosidase and N-acetylhexoaminidase 107

Figure 4.19 MALDI-TOF mass spectra of Monosialo isomers treated with galactosidase, N-acetylhexoaminidase and mannosidase.....108

Figure 5.1 Viable cell density and interferon-γ concentration in a suspension batch CHO cell culture.....116

Figure 5.2 Monitoring of interferon-γ macroheterogeneity in CHO batch culture 118

Figure 5.3 Antennarity of CHO-derived interferon-γ during batch culture 119

Figure 5.4 Effect of culture time on site-specific sialylation of complex biantennary glycans of interferon-γ in a suspension batch CHO cell culture 120

Figure 5.5 Effect of sialidase inhibitor 2,3-dehydro-2-deoxy-N-acetylneuraminic acid on site-specific sialylation of complex biantennary glycans of interferon-γ in a suspension batch CHO cell culture 122

Figure 5.6 Effect of culture time on branch-specific sialylation of (a) Asn^{25}- and (b)Asn^{97}-linked complex biantennary glycans of interferon-γ in a suspension batch CHO cell culture 125

Figure 5.7 Neutral-pH/borate-complexation reversed-phase HPLC separations of (a) Asn^{25}- and (b)Asn^{97}-linked interferon-γ tryptic glycopeptides following 96 h of suspension batch CHO culture using SFM-CHO-II medium (Gibco) 131

Figure 5.8 Neutral-pH/borate-complexation reversed-phase HPLC separations of (a) Asn^{25}- and (b)Asn^{97}-linked interferon-γ tryptic glycopeptides following 96 h of suspension batch CHO culture using PF-CHO medium (JRH Bioscience) 132

Figure 5.9 Cell growth for fed-batch CHO cultures. A and B indicate cultures utilizing Primatone RL-supplemented and non-Primatone RL-supplemented feeding media, respectively 140

Figure 5 10 Interferon-γ concentrations for fed-batch CHO cultures. A and B indicate cultures utilizing Primatone RL-supplemented and non-Primatone RL-supplemented feeding media, respectively 141

Figure 5 11 Sialylation indices of (b) Asn^{25}- and (b) Asn^{97}-linked glycans of IFN-γ produced by fed-batch CHO cultures. A and B indicate cultures utilizing Primatone RL-supplemented and non-Primatone RL-supplemented feeding media, respectively 142

Figure 5 12 Viability profiles for fed-batch CHO cultures. A and B indicate cultures utilizing Primatone RL-supplemented and Primatone RL-free feeding media, respectively 144

Figure 5.13 Ammonia concentrations for fed-batch CHO cultures. A and B indicate cultures utilizing Primatone RL-supplemented and non-Primatone RL-supplemented feeding media, respectively 145

Figure 6.1 Oligosaccharide braching reactions in Golgi 149

Figure 6.2 Dexamethasone can alter the Asn^{97}-associated antennary structure distribution of interferon-γ in CHO cell culture 152

Figure 6.3 Synthetic pathway of CMP-sialic acid 155

Figure 6.4 Reversed-phase HPLC separations of nucleotide sugars extracted from CHO cells cultured in medium supplemented with a) 0, b) 0.2, c) 2, and d) 20 mM ManNAc 158

Figure 6.5 Neutral pH/borate-complexation reversed-phase HPLC separations of Asn^{97}-linked IFN-γ tryptic glycopeptides from CHO batch cultures supplemented with a) 0, b) 2, c) 20 mM ManNAc 163

Figure 6.6 Percentage of interferon-γ sialylation originating from supplemental ManNAc throughout four days of batch CHO cell culture 166

Figure 6.7 *in vitro* CMP-sialic acid transport into trans-Golgi vesicles 170

List of Tables

Table 3.1 The incubation of Golgi vesicles with radio-labeled CMP-sialic acid with or without the presence of CMP 61

Table 4.1 Amino acid sequence and expected tryptic peptides of human interferon-γ 79

Table 4.2 Tryptic glycopeptides of Asn^{97} glycosylation site of recombinant human interferon-γ from γ-CHO batch culture observed by MALDI/TOF mass spectrometry 89

Table 4.3 Tryptic glycopeptides of Asn^{25} glycosylation site of recombinant human interferon-γ from γ-CHO batch culture observed by MALDI/TOF mass spectrometry 90

Table 4.4 Tryptic glycopeptides of Asn^{97} and Asn^{25} glycosylation site of recombinant human interferon-γ from γ-CHO batch culture containing 2.5 mM deoxymannojiromycin observed by MALDI/TOF mass spectrometry 98

Table 4.5 Comparison of methods to quantify Asn^{97}- associated sialylation of interferon-γ from γ-CHO cell culture 100

Table 4.6 Oligosaccharide structures for Asn^{97}-linked glycopeptides fractions (Figure 4.16) identified by MALDI-TOF mass spectrometry..... 103

Table 4.7 Results of exoglycosidases treatment of mass-degenerate glycopeptides of IFN-γ 109

Table 4.8 Structures of mass-degenerate glycopeptides of IFN-γ..... 110

Table 5.1 Effect of two serum-free media on cell growth, product titer and product sialylation (96-h batch CHO culture) 129

Table 5.2 Effect of Primatone RL supplementation on cell growth, product titer and product sialylation using SFM-CHO-II serum-free medium (96-h batch CHO culture) 136

Table 5.3 Effect of ammonia on product sialylation using SFM-CHO-II serum-free medium (96-h batch CHO culture) 137

Table 6.1 Effect of 1 mM dexamethasone on cell growth, product yield and antennary structure distribution of CHO-derived IFN-γ 151

Table 6.2 Effect of supplemental ManNAc on cell growth and IFN-γ production of CHO batch cultures using SFM-CHO-II serum-free medium (96 h) 157

Table 6.3 Effect of supplemental ManNAc on sialylation of CHO-derived IFN-γ (96 h of batch culture using SFM-CHO-II serum-free medium) 157

CHAPTER ONE: INTRODUCTION

1.1 Introduction

Mammalian cells culture is now widely used for the production of proteins that are important as pharmaceuticals or diagnostic agents. In the past, much research has been focused on how to increase cell density as well as maximize product quantity. However, the quality of protein being produced is equally important . One critical aspect of protein qualilty is protein glycosylation, which will be the focus of this thesis.

Glycosylation is the attachment and modification of oligosaccharide structures to the polypeptide chain during the process of protein formation inside the endoplasmic reticulum (ER) and Golgi vesicles. It is initiated by the transfer of an oligosaccharide precursor onto a nascent polypeptide chain inside the ER, followed by multi-step tailoring and modification of the oligosaccharide structure inside both the ER and the Golgi vesicles. The presence and structure of carbohydrates have an important impact on the biological and pharmocokinetic properties of a glycoprotein.

Glycoproteins generally exist as a set of heterogeneous glycoforms in terms of the fraction of potential glycosylation sites which are occupied as well as the oligosaccharide structures at each site. The heterogeneity of glycoproteins can be influenced by cell culture conditions. Therefore, it is desirable to produce glycoprotein with glycosylation homogeneity for better product quality and consistency.

Recombinant human interferon-γ (IFN-γ), produced by Chinese Hamster Ovary cell culture, which possesses two potential N-linked glycosylation sites, serves as the model glycoprotein in this study. The study of protein glycosylation in cell culture requires a complete and accurate characterization of the glycosylation patterns of the product. However, traditional analytical methodologies are neither sensitive nor rapid enough to provide the glycosylation information required for this study.

1.2 Thesis Objective

The objective of this thesis is to develop an analytical scheme to characterize the glycosylation pattern of IFN-γ in CHO cell culture, assess the influence of cell culture condition upon IFN-γ glycosylation and,ultimately, explore cell culture strategies to improve product glycosylation homogeneity

1.3 Thesis Organization

This thesis consists of seven chapters in total. Following a brief introduction in Chapter One, a literature review of protein glycosylation is presented in Chapter Two. Chapter Three gives a full description of the materials and experimental protocols for all of the analytical procedures and cell culture experiments described in this thesis. A full presentation and discussion of the analytical methodology which was developed to characterize both macro- and microheterogeneity of IFN-γ in CHO cell culture is given in Chapter Four. This analytical scheme was then utilized to assess the influence of cell culture

conditions upon product glycosylation, and Chapter Five describes the results of those experiments, particularly the changes in product glycosylation throughout the batch culture process and the negative impact of serum substitute Primatone RL on product sialylation. Chapter Six explores cell culture strategies to improve product quality by maximizing glycosylation homogeneity, including the effects of N-acetylmannosamine, which improves product sialylation, and dexamethasone, which minimizes glycosylation antennarity are discusses there. Finally, conclusions as well as suggestions for future work are offered in Chapter Seven.

CHAPTER TWO: LITERATURE REVIEW

Glycosylation, the addition of sugar residues to a peptide backbone, is the most extensive post-translational modification made to proteins by eukaryotic cells. Most glycans are attached to the polypeptide in one of the three ways: N-linked, O-linked or glycosylphosphatidylinositol (GPI) anchored. N-glycosylation occurs exclusively at the tripeptide sequence Asn-X-Ser/Thr (where X can be any amino acid). The specificity of O-glycosylation is less well-defined but must occur at a serine or threonine residue and is enhanced by clusters of these amino acids. GPI anchor sites are indicated by a hydrophobic carboxyl-terminal peptide which is concurrently cleaved when the GPI is transferred from the rough endoplasmic reticulum (ER) to the nascent polypeptide (Hart, 1992).

Since N-linked glycosylation represents the majority of the glycosylation occurring in mammalian cell-derived glycoproteins, and the synthetic pathways as well as structure of N-glycosylation account for the dominant body of current knowledge in this field, this thesis will be focused on characterization, understanding and improvement of N-linked glycosylation of recombinant proteins in mammalian cell culture.

2.1 N-linked glycosylation pathway

The synthesis of N-linked oligosaccharides involves a series of enzyme-catalyzed events localized in several intracellular compartments. In summary, N-linked glycosylation begins with the synthesis of a lipid-linked oligosaccharide

moiety ($Glc_2Man_9GlcNAc_2$-P-P-Dol) (Kornfeld and Kornfeld, 1985). This precursor is assembled in the ER on the lipid carrier dolichol phosphate. The sugars are added in a stepwise manner with the first seven monosaccharides derived from nucleotide sugars and the next seven derived from lipid intermediates, as shown in Figure 2.1 (Abeijon and Hirschberg, 1992).

A schematic representation of the pathway for N-glycosylation is presented in Figure 2.2 (Kornfeld and Kornfeld, 1985). The complete oligosaccharide is transferred intact from the lipid carrier to a nascent polypeptide chain in a process catalyzed by oligosaccharyltransferase in the luminal surface of the ER. Attachment occurs through asparagine, generally at the tripeptide recognition sequence Asn-X-Ser/Thr. Further post-translational processing of N-linked oligosaccharides by mammalian cells continues in the compartments of the Golgi where a sequence of exoglycosidase- and glycosyltransferase-catalyzed reactions generate the high-mannose, hybrid and complex structures shown in Figure 2.3. These structures contain a common pentasaccharide core of $(GlcNAc)_2Man_3$ but differ in the structures of outer arms. Complex type structures include oligosaccharides containing the disaccharide Galβ(1,4)GlcNAc in the antennae while oligomannose type is designated for glycans with mannose only present in the outer arms. However, hybrid structures contain the oligosaccharides with only mannose residues in one arm and complex structure(containing Galβ(1,4)GlcNAc) on the other arm. The glycosyltransferases responsible for N-linked oligosaccharide synthesis are very specific in the glycosidic bonds they construct, and each utilizes a specific

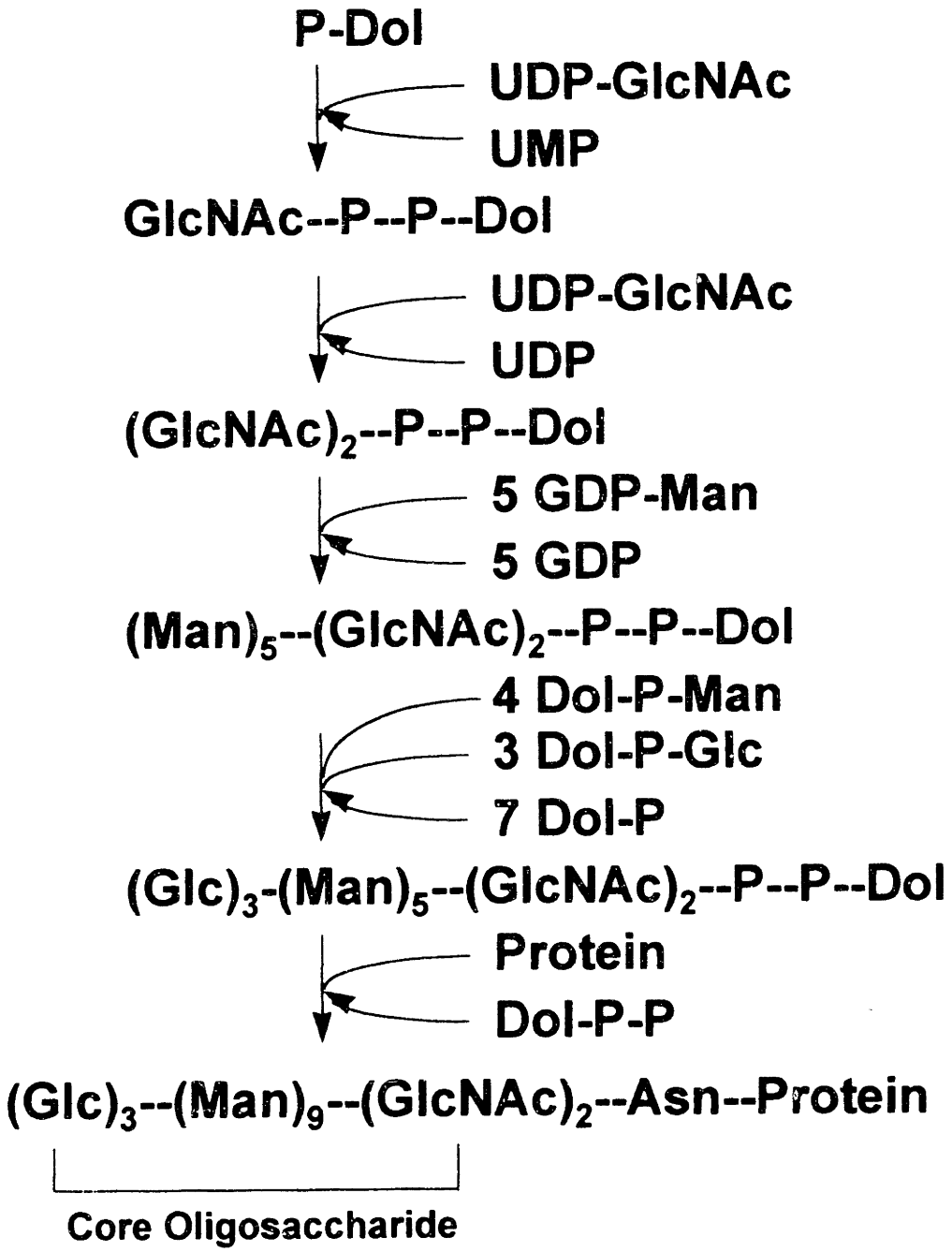

Figure 2.1: The biosynthesis of core N-linked oligosaccharide.

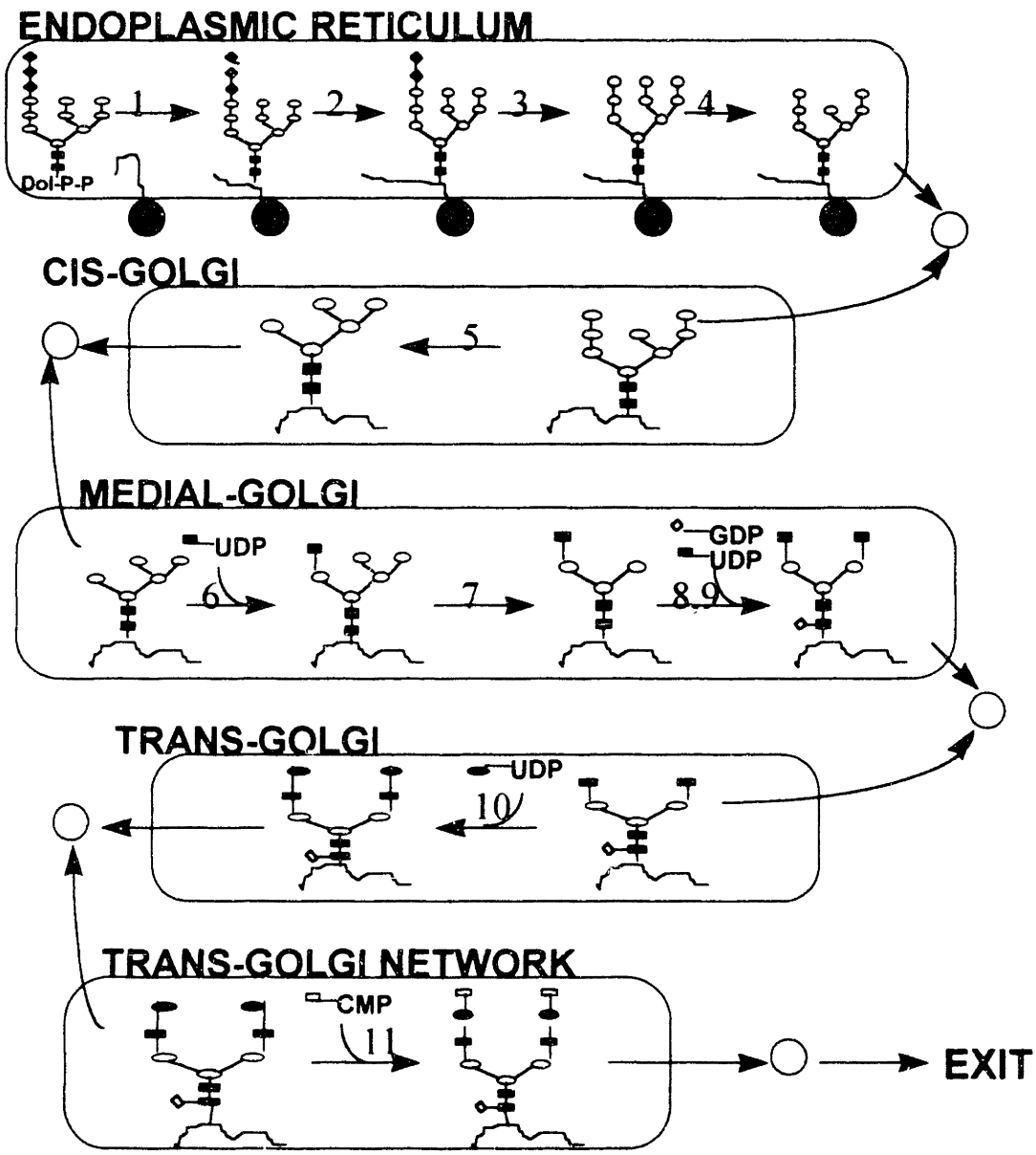

Figure 2.2: N-linked glycosylation

These enzymes are: (1) oligosaccharyltransferase (2) α-glucosidase I (3) α-glucosidase II (4) ER α(1,2)mannosidase (5) Golgi α-mannosidase I (6) N-acetylglucosaminyltransferase I (7) Golgi a-mannosidase II (8) N-acetylglucosaminyltransferase II (9) α(1,6) fucosyltransferase (10) β(1,4) galactosyltransferase (11) α(2,3) sialytransferase

These symbols are: ▬, N-acetylglucosamine; ○, mannose; ●, glucose; ◆fucose; ●galactose; ▭ , sialic acid. (Derived from figure 3 of Kornfeld and Kornfeld, 1985).

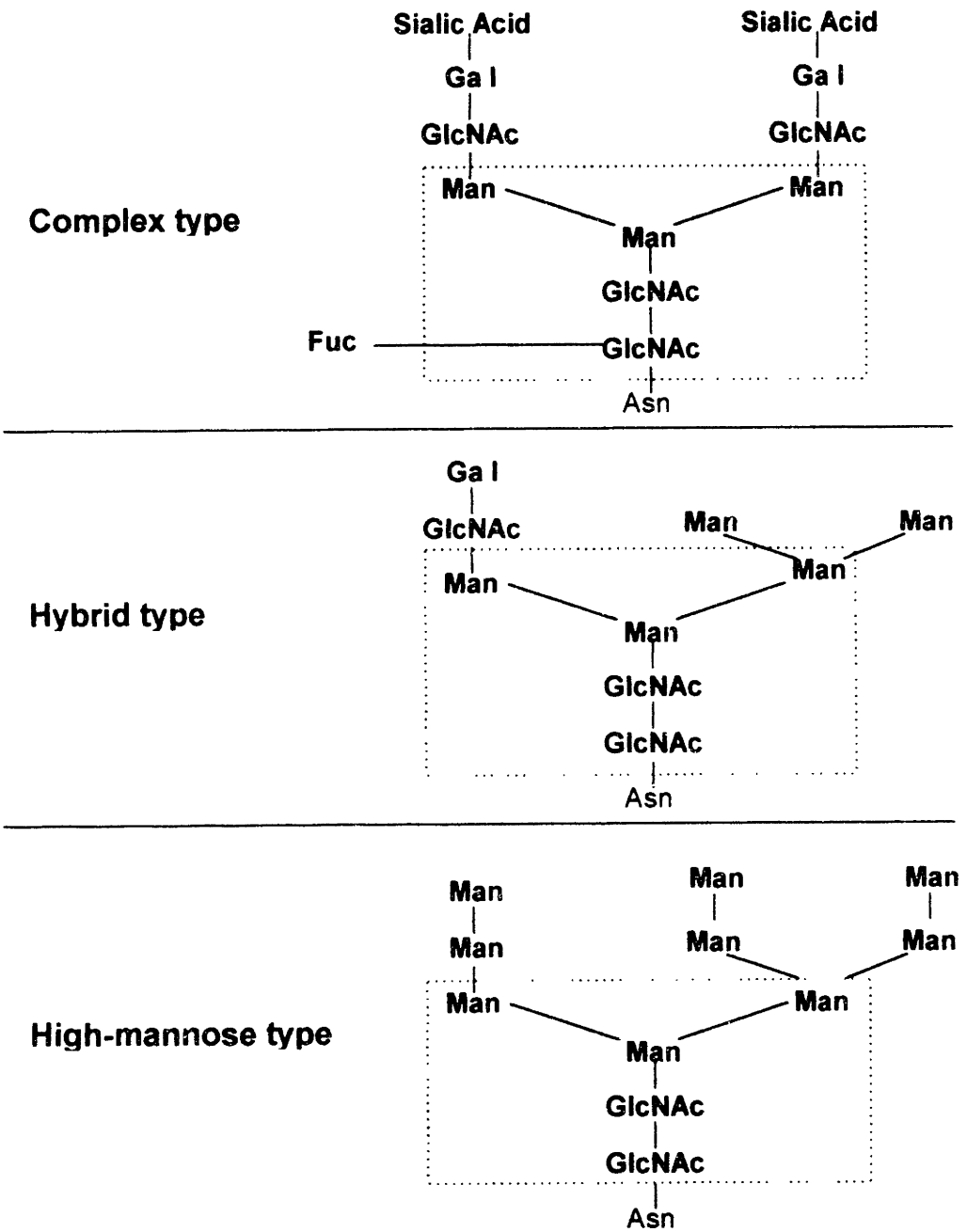

Figure 2.3: Structures of the major types of asparagine-oligosaccharides. The boxed area encloses the pentasaccharic core common to all N-linked structures.

nucleotide sugar as a cosubstrate to generate a defined carbohydrate linkage.

Due to the multiple steps involved in glycosylation, glycoproteins generally exhibit both macro- and microheterogeneity in their glycan structures. Macroheterogeneity, also termed as "variable site occupancy", refers to variability in the location and number of glycosyl attachment sites. On the other hand, microheterogeneity, also termed as "site microheterogeneity", refers to variability in the oligosaccharide structure at specific glycosylation sites. Due to both macro- and microheterogeneity in glycosylation, glycoproteins generally exist as a set of glycoforms, all of which share an identical amino acid backbone but are dissimilar in the structure and /or the disposition of their carbohydrate units. This heterogeneity leads to different physical and biochemical properties and, therefore, functional diversity for every set of glycoforms.

2.2 Functions of carbohydrates in glycoproteins

The majority of secreted proteins produced by mammalian cells, including many proteins of potential therapeutic importance, are glycoproteins. The carbohydrate moieties of glycoproteins have been found to strongly influence many aspects of protein properties.

2.2.1 Influence on protein solubility and thermal stability

The presence of the oligosaccharide can dramatically increase the protein's solubility and prevent aggregation. For example, the removal of oligosaccharides decreases the solubility of erythropoietin (EPO) (Dordal *et al.*, 1985) and results in increased protein aggregation for granulocyte colony-stimulating factor (G-

CSF) (Oheda *et al.*, 1990). These influences can be explained by the contribution of oligosaccharide to the decreased glycoprotein hydrophobicity and increased glycoprotein solubility by covering the hydrophobic protein surface as well as by strong affinity of the oligosaccharides for water (Parekh *et al.*, 1989).

The presence of oligosaccharide can also dramatically increase glycoproteins' resistance to thermal denaturation. For example, complete removal of N- and O-linked oligosaccharides results in an increase in the rate of EPO thermal denaturation (Tsuda *et al.*, 1990). It was suggested by Puett (1973) that the oligosaccharides contributed 0.3 to 0.4 kcal/mol to the thermal stability of bovine pancreatic ribonuclease.

2.2.2 Protection from protease attack

Oligosaccharide always plays a role in protecting glycoproteins from proteolytic attack. Porcine pancreatic ribonuclease is more vulnerable to the attack by trypsin and subtilisin when its carbohydrate portion is removed (Wang and Hirs, 1977), and unglycosylated fibronectin from chicken embryo fibroblasts is more susceptible to pronase digestion (Olden *et al.*, 1979). Furthermore, removal of terminal sialic acid from EPO results in increased susceptibility to proteolysis by trypsin (Goldwasser *et al.*, 1974). It has been proposed that oligosaccharides protect glycoproteins from proteolytic attack by masking potential cleavage sites on the protein surface (Yet and Wold, 1990).

2.2.3 Influence on biological activity and immunogenicity

Complete glycosylation of a protein in general is associated with the full biological activity of the protein. For example, factor IX completely loses its

clotting activity after the removal of its sialic acid (Yan *et al.*, 1990); deglycosylation of HIV-1 envelope glycoprotein gp120 reduces its binding affinity to CD4 receptors (Fennie and Lasky, 1989). However, they are quite a few exceptions. For example, unglycosylated EPO showed very similar specific activity compared to its native counterpart *in vitro* (Yamaguchi *et al.*, 1991); *E. Coli*-derived human IFN-γ has full antiviral and anti-proliferative activity *in vitro* (Rinderknecht *et al.*, 1984). For tissue plasminogen activator (tPA), glycosylation of Asn^{184} inhibits the proteolytic conversion of tPA-I (single chain form) to tPA-II (double chain form) (Wittwer and Howard, 1990). Since tPA-II has 20-30% greater activity than tPA-I (Berg *et al.*, 1993), glycosylation of Asn^{184} therefore decreases the biological activity of tPA.

Oligosaccharide can mask existing antigenic sites on the peptide backbone and thus affect the immunogenicity of a protein. For example, a mutant form of H3 influenca virus can escape monoclonal antibody recognition by forming a new glycosylation site (Skehel *et al.*, 1984). On the other hand, oligosacchride can also act as an immunogen itself and many mammalian circulating antibodies can target specific oligosaccharide determinants. For example, about 1% of human IgG is specific for the terminal Galα(1,3)Galβ(1,4)GlcNAc epitope (Galili *et al*, 1985). Meanwhile, the presence of oligosaccharides may indirectly impact the glycoproteins' antigenicity. Consequenly, the immunogenicity of glycoprotein could be altered as a result of oligosaccharide-protein interactions. For example, there are differences in antigenicity between glycosylated and unglycosylated

Semliki forestvirus protein (Kaluza *et al.*, 1980) and ovine luteinizing hormone (Sairam *et al.*, 1988).

2.2.4 Influence on glycoprotein in vivo *circulatory half-life*

The presence of oligosaccharide plays a dominant role in defining *in vivo* clearance rate of glycoproteins. The circulatory half-life is a very critical aspect of injected therapeutic glycoproteins since high *in vitro* specific activity will be of no significance if the injected protein is eliminated from the circulatory system immediately. In general, there are three well-known mechanisms involved in human clearance systems. Glycoproteins with exposed galactose and N-acetylglucosamine, including desialylated complex N-glycans, bind to the asialoglycoprotein receptor found on hepatocytes and consequently are eliminated from the circulatory system (Weiss and Ashwell, 1989). There are also mannose receptors on the surface of liver endothelial cells and resident macrophage cells, which can potentially bind glycoproteins with high-mannose structures and eliminate them (Ezekowitz and Stahl, 1988). Finally, human proteins with molecular weights less than 70 kD are continuously removed from the circulation through the kidney. Protein tertiary structure and molecular weight as well as presence of surface charge can all have a major impact on the protein filtration rate through the kidney glomerular tubules.

2.3 Factors influencing protein glycosylation

The presence and structures of oligosaccharide are subjected to many factors which can influence protein glycosylation. Three major determinants of

glycosylation patterns will be discussed here: the polypeptide, the host-cell phenotype and the environment in which the cell is maintained.

2.3.1 Influence of protein

The primary, tertiary and quaternary structures of the polypeptide play significant roles in the occurrence and conformation of glycosylation due to protein-carbohydrate interactions. As a result, oligosaccharides for different proteins derived from the same cell line can be dramatically and distinctively different. For example, N-linked glycosylation for interferon-β from CHO cell culture consists mainly of complex biantennary structures. However, for EPO derived from the same cell line, only 6% of the total N-glycosylation is complex biantennary structure while the majority of the oligosaccharides are complex tetraantennary structures (Kagawa *et al.*, 1988) (Takeuchi *et al.*, 1988).

Oligosaccharides derived from different glycosylation sites on the same protein can also be dramatically different. Although N-glycosylation can occur exclusively at the tripeptide sequence Asn-X-Ser/Thr, the presence of the consensus sequence does not necessarily result in the glycosylation of an available glycosylation site. For example, Thr at postion 3 leads to an increased chance of glycosylation compared to Ser at this position, and a proline residue within or near this sequence reduces the likelihood of glycosylation (Gravel and von Heijne, 1990). Furthermore, perspective glycosylation sites near the N-terminus are more likely to be glycosylated (Gravel and von Heijne, 1990), which suggests temporal competition between protein folding and the initiation of glycosylation. The study of t-PA glycosylation is a good example of site-specific

glycosylation heterogeneity (Parekh *et al.*, 1989). There are four potential glycosylation sites for t-PA: Asn-117, Asn-184, Asn-218 and Asn-448. Asn-218 with the amino acid sequence of Asn-Pro-Ser is never glycosylated. For the t-PA derived from several mammalian cell types, Asn-184 is subjected to variable site occupancy. With respect to microheterogeneity, the oligosaccharide structures at Asn-117 are high-mannose, and the structures at both Asn-184 and Asn-448 are complex type. This site-associated glycosylation heterogeneity of t-PA clearly demonstrates the impact of local protein environment on product glycosylation pattern.

2.3.2 Influence of expression system

The influence of expression system on product glycosylation is related primarily to the presence, concentration, kinetic characteristics and compartmentalization of the individual glycosyltransferases and glycosidases Common bacteria systems are known to be incapable to glycosylate proteins, whereas yeast, insect, plant and mammalian cells share the features of N-linked oligosaccharide processing in the ER, including the attachment of the precursor $Glc_2Man_9GlcNAc_2$-P-P-Dol and subsequent truncation to a $Man_8GlcNAc_2$ structure. However, oligaccharide processing inside the Golgi apparatus varies in different cell types. For example, plant-derived glycoproteins are generally not sialylated and frequently contain xylose, a monosaccharide not normally found in mammalian N-linked oligosaccharides. For yeast cells, oligosaccharide chains are elongated in the Golgi through stepwise addition of mannose, leading to elaborate high mannose structures and sometimes containing more than 100

mannose monomers. The baculovirus-infected insect cell system has become popular for recombinant protein production due to both its short process development time and potentially high yields. However, the glycosylation process of insect cells is not well understood, and insect cells are believed to be unable to process complex-type oligsaccharides (Kuroda *et al.*, 1990) and are limited to producing only simple oligomannose-type oligosaccharides of $Man_{3-9}GlcNAc_2$ (Grabenhorst *et al.*, 1993)

Oligosaccharide structures derived from mammalian cell lines closer to humans have more common glycosylation machinery. However, distinctive glycosylation disparities exist for proteins derived from mouse cells, human cells and transgenic animals N-glycolylneuraminic acid (NeuGc), a derivative of the sialic acid N-acetylneuraminic acid (NeuAc), has been found to be more prevalent than NeuAc in antibodies derived from mouse or human-mouse hybridoma (Monica *et al.*, 1995). Since human glycoproteins generally do not contain NeuGc, a high level of NeuGc in the glycoprotein not only leads to a quick removal of the molecule from the circulation system but also can induce an anti-NeuGc immune response (Noguchi *et al.*, 1995). NeuAc is the dominant sialic acid present in CHO-cell derived glycoproteins (Hokke *et al.*, 1995). However, CHO cells are known to lack a functional α2,6-sialyltransferase (ST) enzyme, and, thus, they only synthesize α2,3- linked terminal sialic acid via α2,3-ST (Lee *et al.*, 1989). In contrast, human and mouse cell line have both enzymes and, therefore, express both sialic acid linkages. However, CHO cells have been shown to be capable of producing glycoproteins with both α2,3-linked and α2,6-

linked sialic acid after they are transfected by the cloned rat α2,6-ST genes (Lee *et al.*, 1989) Mouse-human hybridomas have been found to perform the glycosylation characteristics of the mouse parental line (Tandai *et al.*, 1991). For the glycoproteins derived from the milk of transgenic animals, low percentages of complex-type glycans have been observed. For example, a greater proportion of truncated and high-mannose structures has been observed for interferon-γ expressed in transgenic mice (James *et al.*, 1995).

2.3.3 Culture Environment

There is a growing awareness that glycosylation profiles of mammalian cell culture-derived glycoproteins can be influenced by culture conditions. For example, pioneering work (Curling *et al.*, 1990) has demonstrated that the macroheteroneity of IFN-γ glycosylation changes dramatically during batch culture of recombinant CHO cells. Early work on t-PA (Spellman *et al.*, 1989) showed that culture environment can influence both the macroheterogeneity and microheterogeneity of oligosaccharide structures of glycoproteins. As a result, it is critical to fully understand the culture's environment impacts on product glycosylation for optimization of culture condition to minimize glycoprotein heterogeneity and improve product consistency.

2.3.3.1 Cell culture medium composition

The content of many intermediates involved in glycosylation precursor synthesis may have an impact on product glycosylation. Some studies have suggested that product glycosylation is affected by the glucose concentration in the culture medium. For example, the degree of glycosylation of monoclonal

antibodies produced by human hybridomas in batch culture has been reported to be influenced by the availability of monosaccharide (Tachibana *et al.*, 1994). In glucose-limited chemostat cultures, cells at low growth rates produce product with less degree of glycosylation compared to faster-growing cells (Hayter *et al.*, 1993). This change may have resulted from changes in the glucose metabolism (due to limiting the culture on glucose) or a lack of key nucleotide sugars (*e g.*, UDP-GlcNAc) essential to the assembly of oligosaccharides on glycoproteins. Pulsed additions of glucose caused a rapid improvement in the proportion of fully glycosylated IFN-γ secreted and cell growth increased, but the glycosylation deteriorated once the glucose had been depleted (Hayter *et al.*, 1992) Lipid, particularly dolichol, is a key carrier for the oligosaccharide moiety ($Glc_2Man_9GlcNAc_2$-P-P-Dol) before it is transferred to nascent protein. Lipid suppplements alone or in combination with lipoprotein carriers has been shown to improve the N-glycosylation site occupancy of IFN-γ (Castro *et al.*, 1995) (Jenkins *et al.*, 1994a). Supplementation of precursors for cytidine and uridine to rat hepatocytes has also been shown to be able to alter protein glycosylation by increasing the availability of nucleotide sugars (Rickjen *et al.*, 1995).

Proteins derived from serum-containing culture and serum-free culture have shown differences in glycosylation patterns. For example, monoclonal IgG produced by mouse hybridomas in a serum-free medium had higher levels of terminal sialic acid and galactose residues compared to that produced using serum (Patel *et al.*, 1992). However, better galactosylation was observed for antibody produced from serum-containing culture of CHO cells (Lifely *et al.*,

1995). Adaptation of BHK-21 cells producing a recombinant IL-2 mutant from serum-containing to serum-free medium results in substantial changes to its glycosylation, such as the complexity of glycan chains (number of arms and higher levels of terminal sialylation and proximal α1-6 fucosylation), and increases the overall level of glycosylation (Gawlitzek *et al.*, 1995). More consistent glycosylation has been observed for protein produced from cell culture than that made in ascites fluid (Lund *et al* , 1993).

Growth factors are often added to promote cell proliferation and increase the cell productivity; however, the expression levels of glycosyltransferase may also be influenced by the cell's growth rate. For example, the activity of GlcNAc-transferase V has been correlated with the growth rate of HepG2 cells (Hahn and Goochee, 1992). The addition of growth factor IL-6 to a myeloma cell line was reported to reduce the activity of N-acetylglucosaminiyltransferase III (GnT-III), but increase the acitivity of GnT-IV and GnT-V, leading to altered glycan structures (Nakao *et al.*, 1990).

2.3.3.2 Other intracellular events

It has been known for some time that protein is usually glycosylated during translation (Bergman, 1978). The spatial and temporal competition as well as relationship among translation and glycosylation have been proposed, and investigated by several groups. Lau *et al.*(1983) has suggested that only a brief moment in time may exist when the potential glycosylation site on a nascent polypeptide is near the region of space where the oligosaccharyltransferase active site resides. Lowering the protein synthetic rate by cycloheximide

improves the glycosylation site occupancy of recombinant prolactin produced by C127 cells (Shelikoff *et al.*, 1994). However, studies on tPA synthesis in CHO suggest that the rate of protein synthesis by itself has little influence on protein glycosylation (Bulleid *et al.*, 1992).

A competition between glycosylation and protein folding was also proposed when the normally unglycosylated potential site of ovalbumin was able to become glycosylated only after denaturation (Pless, 1977). Folding and disulfide bond formation can influence the efficiency of N-linked glycosylation in certain proteins. For example, low concentrations of reducing agent dithiothreitol prevent cotranslational disulfide bond formation in the endoplasmic reticulum and lead to complete glycosylation of a tPA sequon that normally undergoes variable glycosylation (Allen *et al.*, 1995). On the other hand, the partial glycosylation site occupancy of a non-standard Asn-X-Cys sequon in protein C (Miletich, 1990) was believed to result from obstruction of the site by disulfide bond formation. These results suggest that cotranslational folding events can prevent oligosaccharide transfer by burying the site within the interior of the protein.

It has also been suggested that the extent of protein glycosylation might be affected by the expression level of chaperone proteins inside the ER. Chaperones represent one major class of ER proteins identified as facilitators of protein folding, and the glucose-regulated binding proteins (BiP) are one important type of chaperone protein. It has been suggested BiP may affect the product glycosylation profile by selectively retaining non-glycosylated proteins. Studies with separate CHO cell lines producing three different proteins (tPA,

Factor VIII and von Willebrand Factor) correlated underutilization of N-linked glycosylation sites to increased extent and stability of association with BiP (Dorner *et al* , 1987). Subsequent studies indicated that when levels of BiP were decreased by co-expressing antisense BiP genes, secretion of nonglycosylated tPA increased proportionally (Dorner *et al.*, 1988). Association with BiP may reflect aggregation or inefficient folding of nonglycosylated proteins. Therefore, overexpression of BiP would be expected to increase the selective retention of unglycosylated protein.

2.3.3 3 Physical parameters of culture

The effects of changing the physical parameters of cell culture have also been investigated. Mild or even severe hypoxia has minimal effects on the glycosylation of tPA produced by recombinant CHO cells (Lin *et al.*, 1993). However, the degree of sialylation of CHO-derived follicle stimulating hormone (FSH) was influenced by hypoxia (Chotigeat *et al.*, 1994). Similarly, pH changes within the range 6.9-8.2 in the cell culture medium do not have a dramatic effect on the glycosylation profile of recombinant placental lactogen expressed in CHO cells. However, there was some evidence for underglycosylation outside this range (Borys *et al.*, 1993). Increases in the concentration of ammonium ion in the culture medium above 2mM may compromise sialyltransferases present in the Golgi, resulting in reduced sialylation degree of G-CSF produced by recombinant CHO cells (Anderson *et al.*, 1994).

2.3.3.4 Degradation of product glycosylation

Several reports have suggested that culture time can play a critical role in defining product sialylation. Sliwkowski *et al.* (1992) have reported the qualitative loss of sialic acid from CHO-derived human deoxyribonuclease I over the course of a batch culture. Several types of glycosidase activity have been measured in CHO cell lysate and culture supernatant, and sialidase has been reported to be of the greatest activity (Gramer and Goochee, 1993). Extracellular sialidase activity arising from cell lysis (Gramer and Goochee, 1993) has been reported to be capable of desialylating exogenously-added glycoproteins (Gramer *et al.*, 1995, Warner *et al.*, 1995) in CHO cell culture. However, quantitative analysis of the sialylation profile of a recombinant glycoprotein product throughout the course of a CHO culture process has not been previously reported. Although sialidase, β-galactosidase, β-hexosaminidase, and fucosidase can be detected at low levels in supernatants from mouse 293, NS0, and hybridoma cells, the sialidase activity in these cell lines is much lower than that found in CHO cells (Gramer and Goochee, 1995).

2.4 Analytical techniques for protein glycosylation determination

Propelled by the great interest of producing recombinant therapeutic proteins with consistent glycosylation homogeneity to meet increasing regulatory needs for protein quality control, much advancement has been made in recent years in the development of analytical methodologies to characterize both the macro- and microheterogeneity in protein glycosylation.

The analysis of protein glycosylation generally require two steps: purification of the product protein and the determination of the carbohydrate structure. In most mammalian cell culture, the desired product represents only a small fraction of the different compounds. Highly selective and rapid protein purification from such complex mixtures can be obtained by the use immunoaffinity chromatography utilizing immobilized antibodies to the target protein. Immunoaffinity chromatography can capture the desired protein in a single step and at high purity

2.4.1 Analytical techniques for glycosylation macroheterogeneity

Basic information as to the presence and type of glycans can be obtained by SDS-PAGE and Western blots, at times combined with endo- and exoglycosidase treatment. However, there are some drawbacks associated with these techniques. Preparation of gels are time-consuming, and at times relatively unreliable since the migration of a glycoprotein in SDS-PAGE is influenced by the negative charges on the glycans and other functional groups, as well as the shape of the molecule. In additon, no site-specific information on product glycosylation can be obtained by these techniques. Isoelectric focusing gels, which share similar features with SDS-PAGE, are another technique and have been extensively used for assessing gross heterogeneity in product glycosylation, primarily the degree of sialylation.

An emerging technique for profiling glycoprotein macroheterogeneity is capillary electrophoresis (CE), a separation procedure facilitated by high voltage-induced migration inside narrow-bore capillaries. CE has become a favorable

technique for profiling glycoprotein heterogeneity due to its low cost, minimal sample requirement and high degree of product resolution. Various modes of CE (*e. g.*, zone electrophoresis, isoelectric focusing, isotachophoresis and micellar electrokinetic chromatography), and combined with the selection of separation buffers, have demonstrated the capacity to characterize the glycosylation of various recombinant proteins, including EPO (Watson *et al* , 1993) and interferon-γ (James *et al.*, 1995)

2.4.2 Analytical techniques for detailed glycan analysis

In order to characterize the detailed oligosaccharide structures present on a glycoprotein, two appoaches are generally taken. The glycoprotein can be proteolytically digested to yield glycosylated and non-glycosylated fragments, or the oligosaccharide moieties can be enzymatically cleaved from the intact peptide backbone and sequential analysis are then performed.

2.4.2.1 Analysis of free glycans

The cleavage of carbohydrate from the protein can be achieved by using the enzyme peptide N-glycosidase F (PNGase F), which cleaves most common mammalian N-linked oligosaccharides at the N-glycosidic linkage or, alternatively, by hydrazinolysis. Due to the poor UV absorbance of carbohydrates, isolated glycans need to be derivatized and profiled by high pH anion exchange chromatography (HPAE) or gel permeation chromatography (Spellman *et al.*, 1989) (Hermetin *et al.*, 1992). Alternatively, HPLC with pulsed amperometric detector is able to profile glycan structures directly without derivatization. However, since these glycans are separated from the

glycosprotein as a pool, site-specific glycosylation information is generally lost by this approach for glycoprotein containing more than one glycosylation site.

2.4.2.2 Analysis of glycopeptides

Generating glycopeptides has the advantage that site-specific glycan information can be produced, and this is becoming increasingly important as more products are shown to exhibit glycan differences between individual glycosylation sites on the same protein (Parekh *et al.*, 1989) (Hiyama *et al.*, 1992). In order to identify the sites of glycosylation, peptide maps obtained by proteolytic digestion (*e.g.* trypsin) of the intact glycoprotein are compared to those observed when the protein has been previously treated with an endoglycosidase to remove the oligosaccharide moieties (Carr *et al.*, 1990). PNGase F is frequently used for this purpose due to its broad substrate specificity for the hydrolysis of all of the commonly encountered N-linked oligosaccharides. For glycan structure determination from specific attachment sites, the corresponding glycopeptide is typically analyzed by mass spectrometry to provide composition, molecular heterogeneity and limited sequence information (Carr *et al.*, 1990).

Mass spectrometric (MS) techniques have begun to play an important role in the determination of the structures of carbohydrates in glycoproteins. The ionization method is critical to the applicability of mass spectrometry. Three common ionization methods for the analysis of glycoproteins are fast atom bombardment (FAB), electrospray (ES) and matrix-assisted laser desorption ionization (MALDI). FAB-MS offers the highest mass accuracy of these methods and has been used to deduce the glycan structures of several glycoproteins

(Jenkins and Curling, 1994b). However, the instrument is very expensive as well as requiring a relatively large amount of sample. Although ES-MS and MALDI-MS do not offer quite the mass accuracy of FAB-MS, they exhibit greater mass ranges than FAB-MS and require much smaller sample for analysis. ES-MS has the added advantage that it can be directly coupled to HPLC or CE systems. MALDI-MS is the least expensive of these methods, and it is more tolerant of buffer salts than ES-MS.

In MALDI-MS (Figure 2.4), a low concentration of analyte molecules, which exhibit only moderate absorption at the emission wavelength of the laser, is embedded in either solid or a liquid matrix consisting of a small, highly-absorbing species. The matrix (Figure 2.5) is believed to serve two major functions: absorption of energy from the laser light and isolation of the analyte molecules from each other. Ion detection is generally accomplished by a time-of-flight (TOF) detector, as demonstrated by Figure 2.6. An acceleration voltage is applied to the resulting metastable ions (i.e. stable ions that do not dissociate in flight), and the arrival time of an individual ion at the detector is proportional to $(m/z)^{1/2}$ of the particular species. If the ion beam approaches the detector in a straight line, the method is termed the linear mode. However, if an ion mirror is utilized to reflect the ion beam before it reaches the detector, the technique is referred to as the reflector mode. There is a greater chance for fragment formation in the reflector mode, and, thus more detailed structural information can be obtained in that method via post-source decay (PSD) experiments. Digestion of the peptides by mixtures of glycosidases can be used to determine the carbohydrate composition

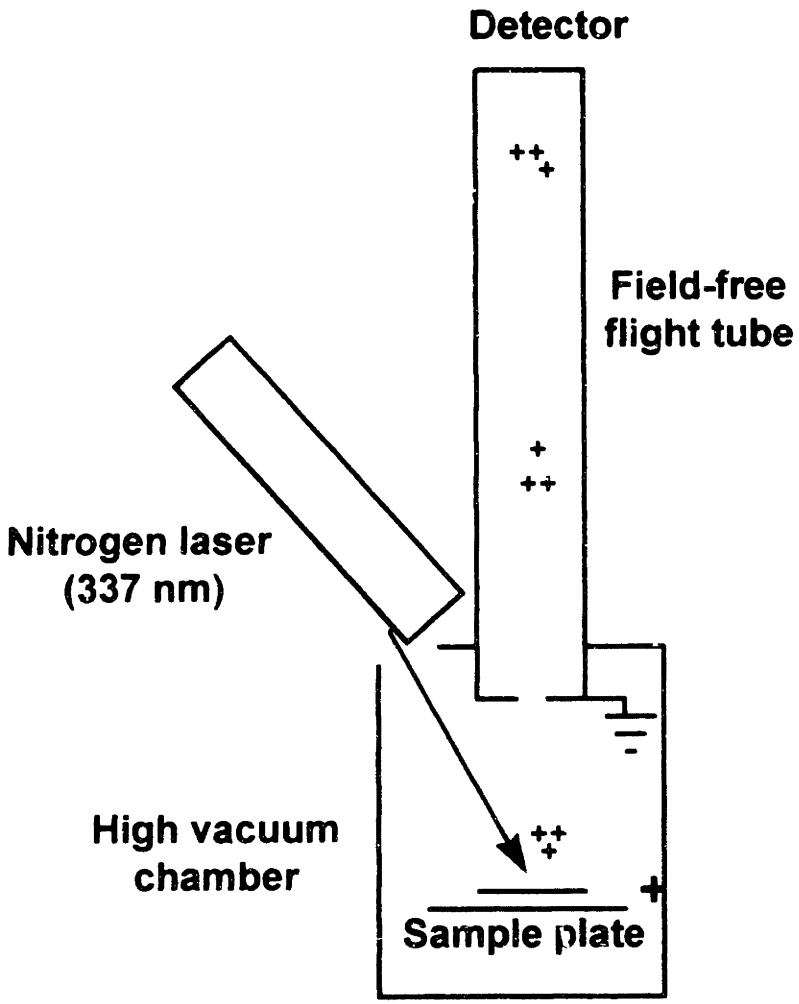

Figure 2.4: Matrix-Assisted Laser Desorption Ionization/ Time-of-Flight Mass Spectrometry (MALDI/TOF MS)

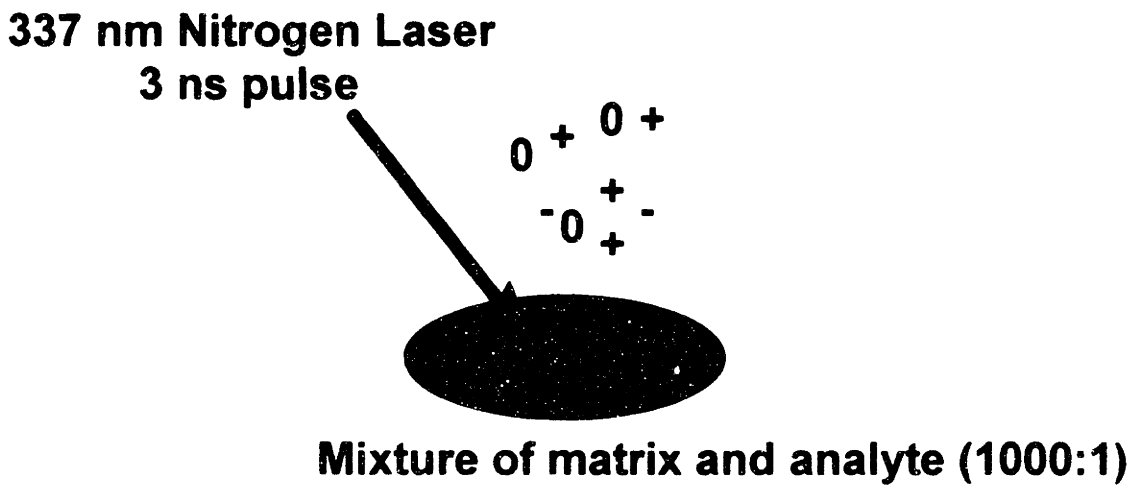

Matrix	Applications
sinapinic acid	proteins
α-cyano-4-hydroxycinnamic acid	peptides
2,5-dihydroxybenzoic acid	peptides

Figure 2.5: Matrix-assisted laser desorption ionization (MALDI)

in the linear mode while the corresponding reflector mode mass spectrum can be used to identify carbohydrate components without requiring digestion by glycosidases (Huberty *et al.*, 1993).

Site-specific glycoform microheterogeneity is best obtained by MALDI/TOF by analyzing glycopeptides resulting from proteolysis of glycoproteins (Treuheit *et al.*, 1992) (Treuheit *et al.*, 1993). If each glycosylation site can be isolated on separate proteolytic fragments, pools of microheterogeneous glycopeptides representing each glycosylation site can be fractionated by reversed-phase HPLC. Due to the capability of MALDI/TOF to analyze mixtures, the mass shift of each glycopeptide relative to the known mass of its peptide portion can be correlated to a site-specific oligosaccharide structure.

Although MALDI/TOF analysis is very rapid, sample preparation steps required for determination of site-specific glycoform microheterogeneity (*i.e.*, purification of target glycoprotein from culture supernatant, buffer exchange, proteolysis of intact glycoprotein, and isolation of pools of glycopeptides representing each potential glycosylation site) can require from one to several days when performed manually. This makes the oligosaccharide structure determination of glycoprotein not practical for routine monitoring of glycan structures of recombinant glycoproteins. Therefore, glycoform microheterogeneity is typically assessed only following termination of cell culture. Since glycosylation microheterogeneity has been reported to change during the course of cell culture, the development of rapid and sensitive analytical methods to monitor site-specific glycan structures is needed to allow glycoprotein quality to

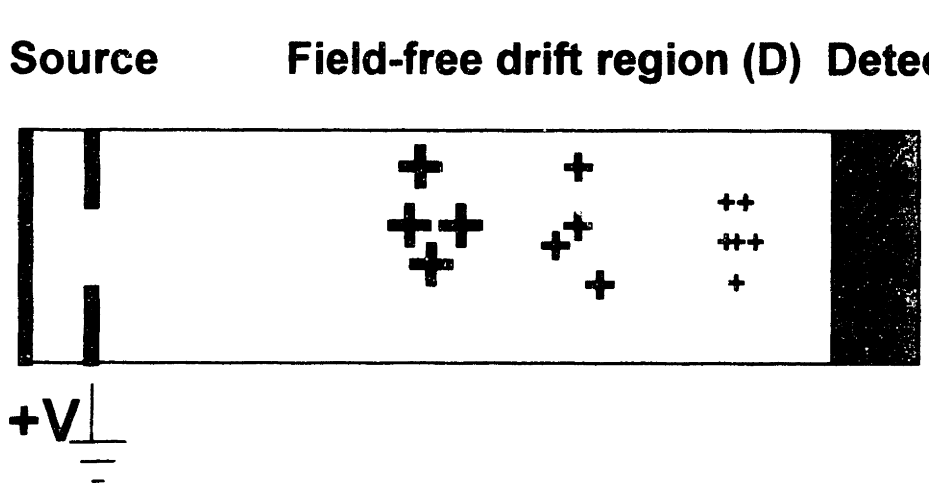

Ions are accelerated by the source electric field (E_S) and enter drift region with same kinetic energy (E_K)

$$E_K = zeE_S = \frac{1}{2}mv^2$$

Time required to reach detector is determined by mass (m) and charge (z)

$$t = \left(\frac{m}{2zeE_S} \right)^{1/2}$$

Times can be converted to mass/charge (m/z) spectrum

$$\frac{m}{z} = 2eE_S \left(\frac{t}{D} \right)^{1/2}$$

Figure 6: Time-of-flight (TOF) detector

be evaluated throughout culture. Furthermore, such techniques would provide tremendous opportunities for understanding and exploring cell culture strategies to improve product glycosylation in mammalian cell culture.

2.5 Model system: IFN-γ and γ-CHO cell culture

The model recombinant glycoprotein for this study was human interferon-γ (IFN-γ) derived from Chinese hamster ovary (CHO) cell line. There are three classes of human interferons identified based upon their biological and chemical properties as well as their antigenicities: IFN-α, IFN-β and IFN-γ. Inside the human body, IFN-γ is usually induced by T-lymphocytes by specific mitogenic stimuli (Rinderknecht *et al.*, 1984). A broad range of biological activities have been attributed this cytokine, including antiviral, antiproliferative, and immunomodulatory activities (Farrar *et al.*, 1993). Natural human IFN-γ generally exists as dimer, and its 143-amino acid sequence offers two potential N-linked glycosylation sites (*i.e.*, Asn^{25} and Asn^{97}). The natural protein is partly glycosylated as seen by SDS-PAGE, which shows three bands at molecular masses of 16, 20 and 24 kDa, presumably corresponding to the protein with zero-site, one-site and both sites glycosylated (Rinderknecht *et al.*, 1984). MALDI/TOF MS, combined with glycosidase digestion, has been employed to characterize the site-specific microheterogeneity of natural human IFN-γ (Mortz *et al.*, 1996). Mortz *et al.* (1996) have shown that the glycan structures at the two potential glycosylation sites differ in composition and heterogeneity. The glycans

at Asn^{25} consist of a mixture of hybrid structures and fucosylated complex bi-, tri- and tetra-antennary structures whereas the glycans at Asn^{97} are more heterogeneous and consists of a mixture of high mannose structures, hybrid structures and unfucosylated complex bi- and tri-antennary structures.

Human IFN-γ cDNA was cloned (Devos *et al.*, 1982) and subsequently transfected to a Chinese hamster ovary (CHO) $DHFR^-$ cell line (Scahill *et al.*, 1983). Based upon 2-D ^{1}H-NMR of oligosaccharides released by hydrazinolysis, Mutsaers and coworkers (1986) determined that glycans of recombinant human IFN-γ produced by CHO cell culture are predominantly complex biantennary structures with microheterogeneity arising from the degree of terminal sialylation as well as variable presence of a core fucose. James and coworkers (1995) have utilized MALDI/TOF analysis of tryptic glycopeptides of IFN-γ in combination with exoglycosidase array sequencing to confirm complex biantennary structures as the most abundant glycans of IFN-γ derived from CHO culture. Lesser proportions of complex triantennary and tetraantennary, high-mannose, and truncated glycans were also observed, and a site-specific difference in fucosylation was found (*i.e.*, glycans of Asn^{25} were predominantly substituted with a core fucose whereas glycans of Asn^{97} were largely nonfucosylated).

Several reports have attributed biological and pharmacokinetic significance to glycosylation of human IFN-γ. Sareneva *et al.* (1994) have observed that glycosylated human IFN-γ exhibited twice the antiviral activity of its nonglycosylated form and that glycosylation of Asn^{25} was critical to the proper folding, dimerization, and secretion of the nascent protein. Proper glycosylation

of human IFN-γ has been shown to increase its circulatory lifetime (Bocci *et al.*, 1985), and glycosylation of Asn^{25} has been reported to be essential for resistance to common cellular proteases (Sareneva *et al.*, 1995).

CHAPTER THREE: MATERIALS AND METHODS

3.1 CHO cell culture

3.1.1 CHO cell stock preparation

Recombinant human IFN-γ was originally produced by an anchorage-dependent CHO cell line (γ-CHO) cotransfected with genes for dihydrofolate reductase (DHFR) and human IFN-γ (Scahill *et al.*, 1983) and selected for growth in the presence of $2.5x10^{-7}$ M methotrexate (Sigma, St. Louis, MO). The cell line was then adapted to grow in suspension in serum-free SFM-CHO-II (Gibco, Gaithersburg, MD) medium supplemented with $2.5x10^{-7}$ M methotrexate, 10 units mL^{-1} penicillin (Sigma), and 10 μg mL^{-1} streptomycin (Sigma). One frozen vial was thawed and diluted ten-fold in a 20-mL shake flask supplemented with SFM-CHO-II medium. The shake flask was placed in a shaker with an agitation speed of 70 rpm and maintained in a 37°C incubator (10% carbon dioxide). Cells were diluted four-fold after reaching over $1.2x10^{6}$ cells mL^{-1}. The dilution was carried out every 2-3 days until a viability of 95% was maintained. For stock preparation, cells with viability over 95% were centrifuged at 800 rpm with an IEC Centra-4B (International Equipment Company) for 10 minutes and resuspended into freezing medium (50% condition medium, 50% fresh SFM-CHO-II medium with 7.5% dimethy sulfoxide (DMSO) (Sigma)) to a density of $2X10^{7}$ cellsml^{-1}. Vials containing 1 mL of the cell suspension was maintained at 4°C for one hour, and then at -20°C for 12 hours before being transferred to a liquid nitrogen cell bank

for storage as stock cultures. A new vial was taken from the cell bank for each set of experiments.

3.1.2 CHO cell batch cultures

A 150 mL suspension batch culture of CHO-γ cells growing serum-free SFM-CHO-II medium supplemented with $2.5x10^{-7}$ M methotrexate, 10 units mL^{-1} penicillin, and 10 μg mL^{-1} streptomycin was performed in a spinner flask (50 rpm) in a 37°C incubator (10% carbon dioxide). The culture was inoculated at a density of $3x10^5$ cells mL^{-1}, and a maximum viable cell density of $1.8x10^6$ cells mL^{-1} was achieved after 72 hrs. Following 48 hrs of culture, supernatants were collected for analysis at 24 hr intervals, and IFN-γ concentrations were determined by enzyme-linked immunosorbent assay (ELISA; Endogen, Cambridge, MA). Cell density and viability were determined with a Neubauer Hemacytometer (Reichert, Buffalo, NY). Prior to cell counting, samples were diluted with an equal volume of 0.4% trypan blue solution (Sigma).

A 20 mL suspension batch culture of CHO cells using the same supplemented medium was also performed in a shake-flask. The shake flask was placed in a shaker with an agitation speed of 70 rpm and maintained in a 37°C incubator (10% carbon dioxide). Culture was inoculated at a density of $3x10^5$ cells mL^{-1}, and a maximum viable cell density of $1.8x10^6$ cells mL^{-1} was achieved in 72 h. Following 48 hrs of culture, supernatant samples were collected for analysis at 24 hr intervals, and IFN-γ concentrations, cell density and viability were determined as mentioned above. Ammonia concentrations were determined using an enzymatic assay kit (Sigma Diagnostics procedure no. 171-UV).

3.1.3 CHO culture containing deoxymannojirimycin

A similar 20 mL suspension batch culture of CHO cells using the same supplemented medium was also performed in a shake-flask in the presence of 2.5 mM deoxymannojirimycin (Oxford Glycosystems, Abingdon, UK). The shake flask was placed in a shaker with an agitation speed of 70 rpm and maintained in a 37°C incubator (10% carbon dioxide). Culture was inoculated at a density of $3x10^5$ cells mL^{-1}, and a maximum viable cell density of 1 $8x10^6$ cells mL^{-1} was achieved in 72 h. Supernatant samples were collected for analysis at the end of the batch culture.

3.1.4 CHO cultures containing 2,3-dehydro-2-deoxy-N-acetylneuraminic acid

Two additional 150-ml suspension batch cultures was performed using the same supplemented medium in spinner flasks (50 rpm) in a 37°C incubator (10% CO_2) in which 1 m*M* 2,3-dehydro-2-deoxy-*N*-acetylneuraminic acid (Sigma) was introduced into the culture supernatant at the beginning and at 72 h of cultivation, respectively. Cultures were inoculated at a density of $3x10^5$ cells mL^{-1}, and a maximum viable cell density of $1.8x10^6$ cells mL^{-1} was achieved in 72 h. Each culture lasted seven days, and supernatant samples were collected for analysis at 24-h intervals.

3.1.5 CHO cultures containing Primatone RL

Four 20-ml suspension batch cultures were performed in shake flasks using the same supplemented medium in the presence of 0.02, 0 2, 2,and 20g L^{-1} Primatone RL (Sigma) . The cultures were inoculated at cell densities of $3x10^5$

cells mL^{-1}, and supernatants were collected for cell counting, ammonia and IFN-γ determination, and sialylation analysis following 96 h of culture.

3.1.6 CHO cultures containing ammonia

Four 20-ml suspension batch cultures were performed in shake flasks using the same supplemented medium in the presence of with 1, 3, 5, and 10 m*M* ammonium chloride (Mallinckrodt, Paris, KY). The cultures were inoculated at cell densities of $3x10^5$ cells mL^{-1}, and supernatants were collected for cell counting, ammonia and IFN-γ determination, and sialylation analysis following 96 h of culture.

3.1.7 CHO culture using JRH PF-CHO medium

The CHO cell line was also adapted to protein-free PF-CHO medium (JRH Bioscience, Lenexa, KS) supplemented with 2 g L^{-1} Primatone RL, $2.5x10^{-7}$ *M* methotrexate, 10 units mL^{-1} penicillin, and 10 mg mL^{-1} streptomycin, and 20-ml suspension batch cultures were performed using this medium (other conditions as described for SFM-CHO-II cultures). The cultures were inoculated at cell densities of $3x10^5$ cells mL^{-1} and supernatants were collected for cell counting, ammonia and IFN-γ determination, and sialylation analysis following 96 h of culture.

3.1.8 CHO culture containing dexamethasone

Twenty mL suspension batch cultures were performed in shake flasks using the supplemented SFM-CHO-II in the presence of 1 μM dexamethasone (Sigma). The cultures were inoculated at cell densities of $3x10^5$ cells mL^{-1}, and

supernatants were collected for cell counting, IFN-γ characterization following 96 h of culture.

3.1.9 CHO culture containing N-acetyl-mannosamine (ManNAc)

Five 20-ml suspension batch cultures were performed in shake flasks using the supplemented SFM-CHO-II in the presence of 0, 0.2, 2, 20, and 40 mM ManNAc (Sigma). The cultures were inoculated at cell densities of $3x10^5$ cells mL^{-1}, and supernatants were collected for cell counting, IFN-γ determination, and sialylation analysis after 96 h of culture. For analysis of intracellular CMP-sialic acid as well as isolation of Golgi vesicles, several additional 50-ml batch cultures containing 0, 0.2, 2, and 20 mM ManNAc were performed. From each culture, 100 million cells were collected at 96 h for extraction of nucleotide sugars and quantitation of intracellular CMP-sialic acid. To measure the incorporation of ManNAc, three additional 20-ml cultures containing 0.2, 2, and 20 mM ManNAc (Sigma) were performed with each culture supplemented with 200 mCi of N-acetyl-D-[6-^{3}H(n)]mannosamine (39 Ci $mmol^{-1}$) (NEN Research Products, Boston, MA). Supernatants were collected for determination of incorporation of radiolabeled ManNAc at 96 h. For the culture containing 2 mM ManNAc, determination of radiolabeled ManNAc incorporation was also performed at 24, 48, and 72 h.

3.1.10 Fed-batch CHO cultures

The CHO cell line was adapted to a self-designed protein-free medium supplemented with 2 mg l^{-1} insulin and 2 g l^{-1} Primatone RL (Xie, 1996). Two fed-batch cultures were initiated at 300 ml in 500-ml spinner flasks using this medium.

The flasks were placed in a 37°C incubator under a 5% CO_2 environment, and an agitation rate of 150 rpm was selected to ensure a sufficient O_2 transfer rate for high cell density growth. The two batches were fed using a stoichiometric feeding strategy previously developed for hybridoma cell culture (Xie and Wang, 1994a,b,c) to meet the nutritional demands for cell growth. As described in Table 2, the supplemental media fed to the two cultures were similar with the exception that one medium was supplemented with 25 g l^{-1} Primatone RL while the other culture was not fed any additional Primatone RL. However, based upon amino acid analysis of Primatone RL provided by the vendor, additional amino acids were added to the Primatone RL-free feeding medium to compensate for its lack of free amino acids and peptides. Feeding of the supplemental media commenced manually 24 h after inoculation and was performed every 12-24 h thereafter. A total of approximately 30 ml of supplemental feeding medium was added during each fed-batch. Supernatant samples from both fed-batches were withdrawn periodically for cell counting, ammonia and IFN-γ determinations, and sialylation analysis

3.2 IFN-γ glycosylation characterization

3.2.1 IFN-γ purification by immunoaffinity chromatography

All chromatographic steps were performed using an INTEGRAL Micro-Analytical Workstation (PerSeptive Biosystems, Framingham, MA) equipped with a high-pressure microbore flowcell (Model 9550-0150, Linear Instruments, Fremont, CA). Cell culture supernatant was filtered (0.22 μm

Millex-GS, Millipore, Bedford, MA), and a 1 mL aliquot was loaded at a flow rate of 200 μL min^{-1} onto a 0.76 X 150 mm column packed with immunoaffinity resin (Reselute-γ, Celltech Ltd., Slough, UK), which had been previously equilibrated with loading buffer, 10 mM pH 7.2 sodium phosphate (Mallinckrodt, Paris, KY) with 150 mM NaCl (Mallinckrodt). The immunoaffinity column was then washed with loading buffer and step eluted by 10 mM HCl (Mallinckrodt) with 150 mM NaCl at 30 μL min^{-1}.

3.2.2 Characterization of IFN-γ macroheterogeneity

For the IFN-γ macroheterogeneity characteriztion, the eluent of immunoaffinity column was then on-line loaded at a flow rate of 200 ml/min onto a 0.25 X 150 mm column packed with reversed-phase resin (POROS 10 R2, PerSeptive Biosystems), which had been previously equilibrated with 100% HPLC-grade water (EM Science). The reversed phase column was then washed with 100% water and step eluted by 100% acetonitrile (EM Science, Gibbstown, NJ)

The macroheterogeneity of IFN-γ after the reversed-phase concentration of the sample was determined by micellar electrokinetic chromatography. The separation was performed using an Analytical Capillary Electrophoresis System (Model 270A, Applied Biosystem, Foster City, CA) with absorbance detection at a wavelength of 200 nm. A CElect Capillary Electrophoresis Column (Supelco, Bellefonte, PA) was prepared to have a 50 cm separation distance from the inlet of the capillary to the detection window, and 20 cm between the detection window and the outlet of the capillary. The capillary was washed with washing solution

(0.1M NaOH (Sigma)) for 5 min and running buffer (20mM sodium borate (Sigma), 20mM boric acid (Sigma), 100mM SDS (Sigma), pH 8.5) for 15 min. Concentrated IFN-γ was then injected by vacuum injection for 4 seconds and a voltage of 18 kV was then applied to the capillary. The peaks for doubly-glycosylated, singly-glycosylated and non-glycosylated IFN-γ were eluted within 20 min. Data were analyzed with System Gold software supplied by Beckman Instruments (Palo Alto, CA).

To confirm the identities of each peak in the MEKC separation, 10μL of IFN-γ after reversed-phase concentration was mixed with 5 μL of 40 mM pH 7.8 ammonium bicarbonate (Sigma) containing 0.2 units of *Flavobacterium meningosepticum* PNGase F (Boehringer Mannheim, Indianapolis, IN). The digestion mixture was subjected to MEKC analysis after 10 min, 2 h, 10 h and 24 h of incubation at 37°C

3.2.3 Digestion of IFN-γ and fractionation of glycopeptides

To determine the microheterogeneity of IFN-γ, eluent from the immunoaffinity column was merged via a mixing tee with 10 μL min^{-1} of 200 mM pH 8.5 Tris (Mallinckrodt) with 40 mM $CaCl_2$ (Sigma) and 20% acetonitrile and directed to a 2.1 X 30 mm immobilized trypsin cartridge (Poroszyme, PerSeptive Biosystems) maintained at 50°C by use of an external column heater (Model CH-30, Eppendorf North America, Madison, WI). Effluent from the trypsin cartridge was directed to a 1 X 250 mm Vydac C18 (The Separations Group, Hesperia, CA) analytical reversed-phase HPLC column, which was washed for 5

min with 5% acetonitrile containing 0.1% trifluoroacetic acid (American Bioanalytical, Natick, MA) and then eluted at 50 μL min^{-1} by a 30 min linear gradient to 80% acetonitrile with 0.085% trifluoroacetic acid. Eluted peptides were monitored at 220 nm, and fractions were manually collected for MALDI/TOF analysis. Chromatographic steps were automated via the INTEGRAL's three ten-port valves and an additional switching valve.

Solution-phase tryptic digestion of IFN-γ was also performed by adding modified sequencing-grade trypsin (Boehringer Mannheim, Indianapolis, IN) reconstituted in 1 m*M* HCl to IFN-γ fraction in an approximately 1:5 (enzyme:substrate) mass ratio and allowing proteolysis to proceed at 37° C for 24 hours Reversed-phase fractionation of tryptic peptides was performed by loading the digestion mixture on a 1 X 250 mm Vydac C18 analytical reversed-phase HPLC column as mentioned above.

3 2.4 MALDI/TOF mass spectrometry

MALDI/TOF mass spectrometry was performed using a Voyager BioSpectrometry Workstation (PerSeptive Biosystems). Samples were prepared by mixing a 2 μL aliquot with 2 μL of matrix solution: a saturated solution of 3,5-dimethoxy-4-hydroxycinnamic acid (Aldrich, Milwaukee, WI) in 50% water:50% acetonitrile with 0.1% trifluoroacetic acid for analysis of intact IFN-γ, 7 mg mL^{-1} solution of 2,5-dihydroxybenzoic acid (Aldrich) in 50% water:50% acetonitrile for analysis of glycopeptides. One μL of the mixture was spotted into a well of the MALDI sample plate and allowed to air dry prior to introduction into

the mass spectrometer. Data for 10 to 50 3-ns pulses of the 337 nm nitrogen laser were averaged for each spectrum, and linear, positive-ion TOF detection was performed using an accelerating voltage of 28,125 V. Spectra were smoothed with a 19-point Savitzky-Golay filter, and external calibration was performed using a mixture of bradykinin (MW 1060.2; Sigma) and bovine insulin (MW 5733.5; Calbiochem, San Diego, CA).

3.2.5 Enzymatic digestions

Digestion with *Flavobacterium meningosepticum* PNGase F was carried out by adding 10 µL of glycopeptide fraction to 5 µL of 40 mM pH 7.8 ammonium bicarbonate (Sigma) containing 0.2 units of enzyme and incubating at 37°C for 2 hr. MALDI/TOF analysis was performed as previously described Digestion by *Arthrobacter ureafaciens* sialidase (Oxford Glycosystems) was performed by first pipeting 1 µL of glycopeptide fraction into a well of the MALDI sample plate and then adding 1 µL of 20 mM pH 5.0 sodium acetate (Fisher, Fair Lawn, NJ) containing 0.004 units of enzyme Mixing was assured by pulling the 2 µL reaction mixture back and forth through the pipet tip prior to redepositing in the sample well. The reaction was allowed to proceed at 37°C until complete evaporation One µL of matrix solution was then added and allowed to air dry prior to MALDI/TOF analysis.

3.2.6 Site- and branch-specific quantitation of sialylation

For sialic acid-based separations of glycopeptides, site-specific glycopeptide fractions were diluted in water, loaded onto a 1 X 250 mm Vydac C18 analytical reversed-phase HPLC column, and washed at 50 µl min^{-1} with

buffer A (20 m*M* pH 7 triethylamine (EM Science) and 300 mM boric acid (Mallinckrodt) in 90% HPLC-grade water:10% acetonitrile). Glycopeptides of Asn^{25} were eluted by a 60-min linear gradient from 80% buffer A:20% buffer B (20 mM pH 7 triethylamine and 300 mM boric acid in 50% HPLC-grade water:50% acetonitrile) to 100% buffer B. Glycopeptides of Asn^{97} were eluted by a 60-min linear gradient from 100% buffer A to 30% buffer A:70% buffer C (20 m*M* pH 7 triethylamine and 300 m*M* boric acid in 70% HPLC-grade water:30% acetonitrile). Eluted glycopeptides were monitored at 220 nm, and fractions were manually collected and identified by MALDI/TOF as described above.

3.2.7 Identification of monosialylated biantennary glycopeptide fractions

Digestion by *Streptococcus pneumoniae* β-galactosidase (Oxford Glycosystems, Abingdon, UK) and *Streptococcus pneumoniae* β-N-acetylhexosaminidase (Oxford Glycosystems) was performed by mixing 1.7 μl of glycopeptide fraction with 0.7 μl of digestion buffer (50 m*M* pH 5 sodium citrate (Mallinckrodt), 50 m*M* sodium phosphate, and 25 m*M* $ZnCl_2$ (Mallinckrodt)) containing 0.24 milliunits of each enzyme and allowing reaction to proceed at 37° C for 24 h. Reversed-phase separation of digested glycopeptides from enzymes was performed by loading digestion mixture onto a 1 X 250 mm Vydac C18 analytical reversed-phase HPLC column, washing with 95% HPLC-grade water:5% acetonitrile containing 0.1% TFA, and eluting by a 60-min linear gradient to 5% HPLC-grade water:95% acetonitrile with 0.085% TFA at a flow rate of 50 μl min^{-1}. Digestion by jack bean α-mannosidase (Oxford

Glycosystems) was perfomed by mixing 0.7 μl of digestion buffer containing 14 milliunits of enzyme with 1.7 μl of glycopeptide fraction and allowing reaction to proceed at 37° C for 24 h. MALDI/TOF of digested glycopeptides was performed as described above.

3.3 Nucleotide sugar extraction and quantitation of intracellular CMP-sialic acid

Cells were separated from medium by centrifugation and washed twice with ice-cold PBS (10 mM sodium phosphate (Mallinckrodt, Paris, KY), 0.154 M NaCl (Mallinckrodt) at pH 7.2). One mL of ice-cold 75% ethanol (EM Science, Gibbstown, NJ) was then added to the cells to extract the nucleotide sugars, and the soluble fraction was retained after centrifugation. The extraction procedure was repeated twice, and the soluble fractions were combined for lyophilization using a Labconco Freeze Dryer (Labconco Corp., Kansas City, MO). The dried powder was then dissolved into 4 ml of a 10:5:3 by volume mixture of chloroform (EM Science), methanol (EM Science), and water. After centrifugation, the upper-phase was retained, and the lower-phase (chloroform) was washed with a 1:1 by volume mixture of methanol and water followed by centrifugation. The original methanol/water phases and second extraction phase were combined for lyophilization. The dried powder was dissolved in 0.5 ml of water and kept frozen at -20°C prior to CMP-sialic acid quantitation.

CMP-sialic acid quantitation was performed on an HP 1090 Liquid Chromatograph (Hewlett Packard, Palo Alto, CA). Twenty-five μL of standard CMP-sialic acid solution or nucleotide extraction sample was loaded onto a 4.6 X 150 mm Supelcosil LC-18-T (Supelco, Bellefonte, PA) reversed-phase HPLC column and washed at the rate of 1 ml min^{-1} with Buffer A (0.1 M KH_2PO_4 (Mallinckrodt), 0.008 M tetrabutylammonium hydrogen sulfate (Aldrich, Miwaukee, WI) at pH 6.0). The column was then eluted 1 ml min^{-1} by the following gradient program: 100% Buffer A for 7 min, 0 to 40% Buffer B (70% Buffer A:30% methanol, at pH 6.0) over 5 min, 40 to 100% Buffer B over 6 min, and 100% Buffer B for 10 min. Eluted peaks were monitored by absorbance at 254 nm. For calculation of CHO cell volumes and intracellular CMP-sialic acid concentrations, CHO cell diameters were measured by a Coulter Channelyzer (Coulter Electronics, Inc., Hialeah, FL)

3.4 Determination of incorporation of radiolabeled ManNAc

One and half mL of supernantants collected following cell centrifugation was mixed with 1 ml of reaction buffer (50 mM Tris-HCl (Boehringer Mannheim, Indianapolis, IN), 5 mM EDTA (Mallinckrodt), 5 mM EGTA (Mallinckrodt) at pH 8.2) and 30 ml of IFN-γ immunoaffinity resin (Reselute-γ, Celltech Ltd., Slough, UK). The mixture was incubated with agitation at 4°C for 3 h and then centrifuged The supernatant was removed, and the pellet was washed twice with Wash Buffer I (0.5% Nonidet P40 (Sigma), 50 mM Tris-HCl, 500 mM NaCl, 5mM EDTA, 1 mg ml^{-1} bovine serum albumin (Sigma) at pH 8.0), twice with Wash

Buffer II (0.5% Nonidet P40 (Sigma), 50 mM Tris-HCl, 5mM EDTA at pH 8.0), and once with distilled water. Following centrifugation, the pellet was dissolved into 100 ml of 100 mM ammonium acetate (Mallinckrodt) at pH 5.0 containing 0.2 U *Arthrobacter ureafaciens* sialidase (Oxford Glycosystems, Abingdon, UK) and incubated with agitation at 37°C overnight. The incubation mixture was then centrifuged, and the pellet was washed twice with Wash Buffer I, twice with Wash Buffer II, and once with distilled water. A parallel control incubation was also performed without sialidase. The pellet was then mixed with 5 ml of Ultima Gold scintillation cocktail (Packward, Meridan, CT), and radioactivity was detected by use of an LS 6500 multi-purpose scintillation counter (Beckman, Palo Alto, CA).

3.5 Isolation of Golgi from CHO cells and study of CMP-NANA *in vitro* transport through Golgi membrane

Golgi vesicles were separated from CHO cells in the presence of 8mM $CaCl_2$ as described by Kamath and Narayan (1972). To isolate the Golgi from CHO cells, $9x10^7$ cells were centrifuged and separated from supernatant The cells were then resuspended into 1 ml of ice-cold 0.25 M sucrose (Sigma) solution and homogenized using a VirSonic homogenizer (The Virtis Company, Gardiner, NY) for 60 sec in total with 15 sec for each cycle at intensity III The homogenate was then centrifuged at 10,000 g for 10 min twice by Biofuge 15 (Heraeus Instruments, South Planifield, NJ) The collected supernatant was mixed with 1ml of a solution of 0.25 M sucrose with 16 mM $CaCl_2$. The mixture was allowed to sit at room temperature for 5 min and was then centrifuged again

for 3 min at 10,000 g. This microsome pellet was next resuspended into 0.8 ml of STM buffer (0.25M sucrose, 10mM Tris-HCL and 1mM $MgCl_2$,(Mallinckrodt) pH=7.5). The protein concentration of that microsome mixture was 7.1 mg/ml, as determined by Bradford protein assay (Bio-Rad, Hercules, CA).

To study the CMP-sialic acid transport through the Golgi membrane, a CMP-sialic acid cocktail solution was made by adding 1.5 ml of 800 mm CMP-sialic acid (Sigma) solution, 10mCi of [sialic acid-9-^{3}H]CMP-sialic acid (25.8 Ci/mmol) (NEN Research Product) into 1.5 ml STM buffer. CMP-sialic acid cocktail solution, 6mM 5'-CMP(Sigma) solution and STM buffer were then used to make the following combination as listed in Table 3.1.

Table 3.1 The incubation of Golgi vesicles with radio-labeled CMP-sialic acid with or without the presence of CMP.

Vial #	CMP-sialic acid conc. (μm)	CMP conc (μm)	Microsome solution added (μl)	Total volume(ml)
#1	10	0	100	1
#2	10	400	100	1
#3	50	0	100	1
#4	50	400	100	1
#5	100	0	100	1
#6	100	400	100	1
#7	400	0	100	1
#8	400	400	100	1

Each vial was incubated for 10 min on a rocker at 37°C and the reactions were stopped by placing the vials in ice-cold water 10 ml of 800 mM $CaCl_2$ was then added to each vial. The solutions in each vial were then centrifuged at

10,000 g for 3 min. The collected pellets were then resuspended into 0.5 ml of 75% ethanol, which was next mixed with 5ml of scintillation cocktail, followed by the detection of radioactivity by scintillation counter.

CHAPTER FOUR: CHARACTERIZATION OF IFN-γ GLYCOSYLATION

Progress will be described in this chapter on the development of a rapid and sensitive method to monitor glycosylation heterogeneity of recombinant human IFN-γ in CHO cell culture. Figure 4.1 shows schematically the analytical scheme developed to monitor the macro- and microheterogeneity of IFN-γ glycosylation. IFN-γ is initially purified from γ-CHO cell culture supernatant and quantified by immunoaffinity chromatography. In the determination of glycosylation macroheterogeneity, the immunopurified IFN-γ is concentrated by on-line solid-phase extraction using a microbore perfusion reversed-phase column, and off-line micellar electrokinetic chromatography (MEKC) separates the two-site, one-site, and unglycosylated glycoforms of IFN-γ in order to quantify the site occupancy distribution. In the assessment of glycosylation microheterogeneity, proteolysis of the immunopurified IFN-γ is perfomed by an on-line immobilized trypsin cartridge, and the resultant tryptic peptides are separated by on-line, microbore reversed-phase HPLC. The two fractions of glycopeptides corresponding to the two potential glycosylation sites are then analyzed by matrix-assisted laser-desorption ionization/time-of-flight mass spectrometry (MALDI/TOF MS) to yield site-specific glycan antennary structures. Information regarding site- and branch-specific sialylation is obtained from a neutral pH/borate complexation reversed-phase HPLC separation of the Asn^{25}- or Asn^{97}- associated glycopeptides. This analytical methodology allows the glycosylation heterogeneity of CHO-derived IFN-γ to be thoroughly assessed in a

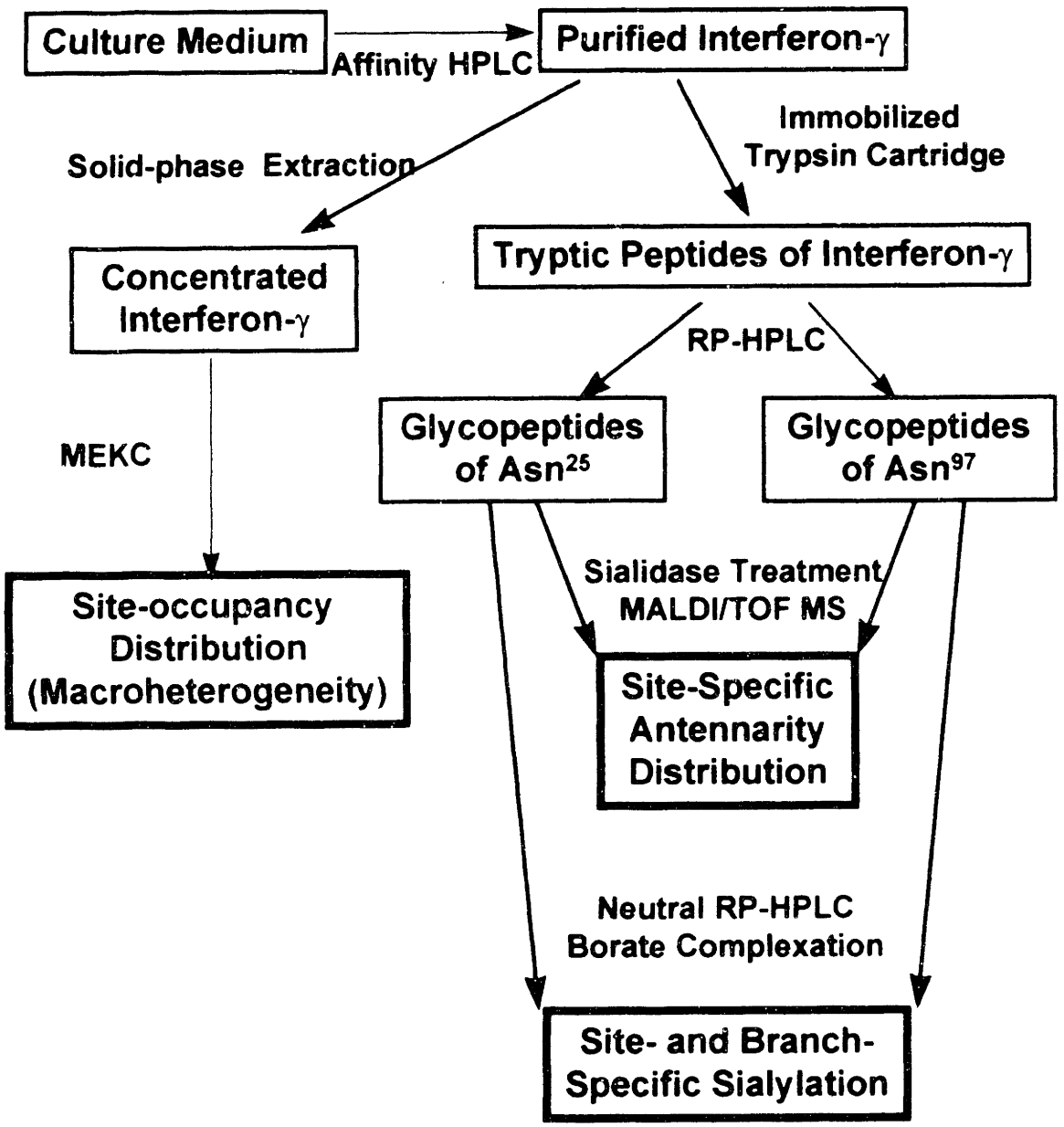

Figure 4.1: Rapid characterization of interferon-γ glycosylation macro- and microheterogeneity

time frame of approximately 4 hours using as little as 0.5 μg of the product.

4.1 Purification of IFN-γ

In most mammalian cell culture, growth factors supplemented in the culture medium for the promotion of cell proliferation, proteins secreted from cells, and molecules released during cell lysis yield a very complicated protein mixture in the culture supernatant. Therefore, the desired product represents only a small fraction of the different compounds in the culture medium. Meanwhile, the rapid and sensitive characterization of product glycosylation could only be made possible with a fast and simple step for the purification of IFN-γ from the culture supernatant. As a result, immunoaffinity chromatography was chosen in this study for the highly-selective and rapid purification of the target protein from the culture supernatant γ-Reselute, sepharose beads with cyanogen bromide-immobilized, monoclonal anti-human-IFN-γ antibody, was utilized for the purification of IFN-γ from CHO culture supernatant. Figure 4.2 shows the chromatogram of one IFN-γ purification cycle from 1 mL of CHO culture supernatant. γ-CHO cell culture supernatant was first loaded onto the immunoaffinity column, where only IFN-γ in the supernatant was retained due to specific antigen-antibody binding at neutral pH. Meanwhile, other impurities passed through the column and this is seen as the large loading peak in Figure 4.2 The affinity column was then washed with loading buffer and eluted at acidic pH in order to disrupt the antigen-antibody interaction. In this manner, purified IFN-γ was obtained as a single peak shown in Figure 4.2.

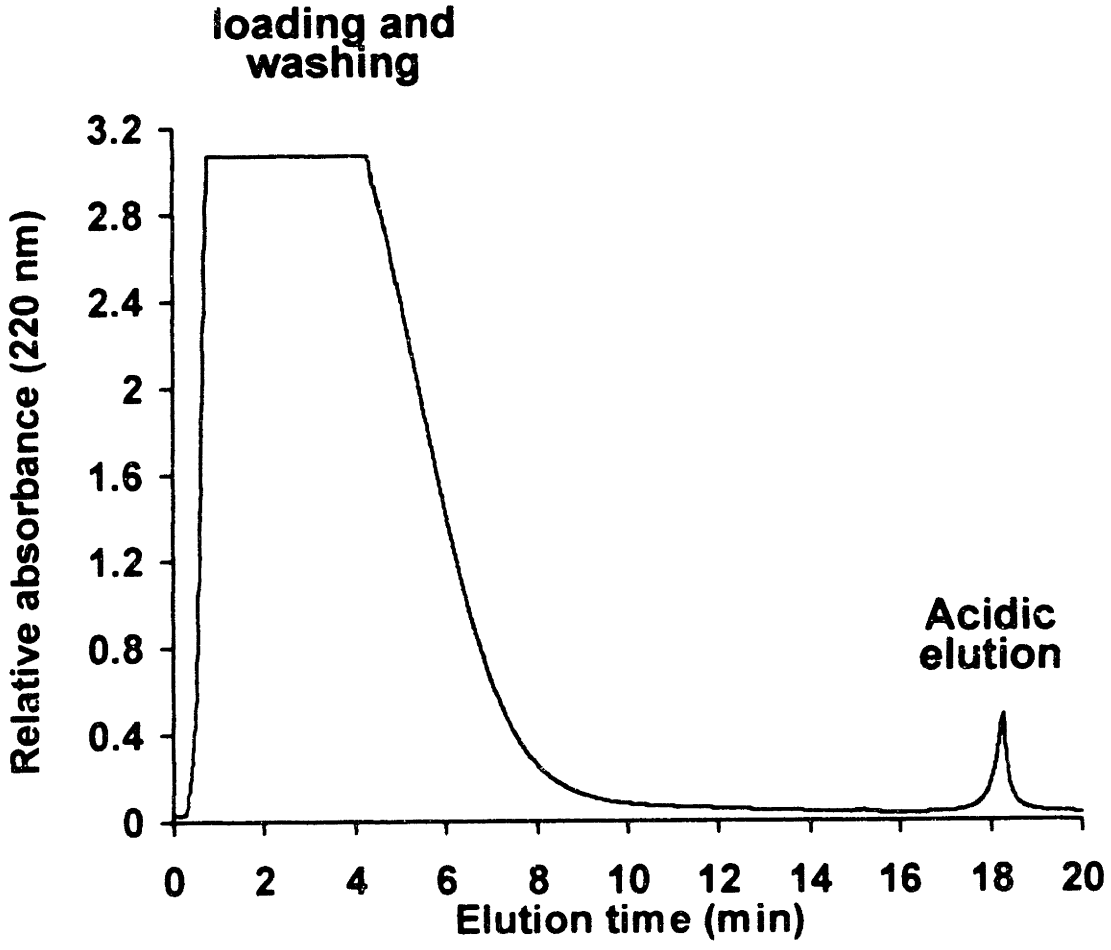

Figure 4.2: Immunoaffinity Chromatography of Interferon-γ from CHO Supernatant

Detection was achieved by UV absorbance at 220 nm. This method yielded highly pure IFN-γ (>98% by densitometry of silver-stained SDS-PAGE) with excellent reproducibility (RSD of 2.6% for peak area of eluted IFN-γ from 10 replicate supernatant samples) and recovery (>95% by absorbance using standard nonglycosylated IFN-γ). In order to quantitate IFN-γ, the elution peak areas were calibrated by comparison to ELISA standards. A typical calibration curve (R^2=0.9998) is presented in Figure 4.3. The limit of detection was approximately 0.05 μg/mL for a 1-mL supernatant loading. However, since immunoaffinity chromatography is a concentrating technique, more dilute samples could be analyzed by simply increasing the loading volume.

4.2 Determination of IFN-γ glycosylation macroheterogeneity

After immunopurification of IFN-γ from the culture supernatant, the glycosylation site occupancy was profiled by micellar electrokinetic chromatography (MEKC); a form of capillary eletrophoresis utilizing a micellar pseudostationary phase for hydrophobicity-based separations. However, the detection limit for capillary electrophoresis of proteins with on-column UV absorbance detection is about 1-5 μg/mL while the concentration of IFN-γ in γ-CHO supernatant is typically less than 3.5 μg/mL with the nonglycosylated form accounting for as little as 5% of the total product. Therefore, in order to quantitate all three macroheterogeneous glycoforms of IFN-γ with the constraint on the detection limit of capillary electrophoresis, the immunopurified IFN-γ was further concentrated using on-line, reversed-phase extraction prior to MEKC.

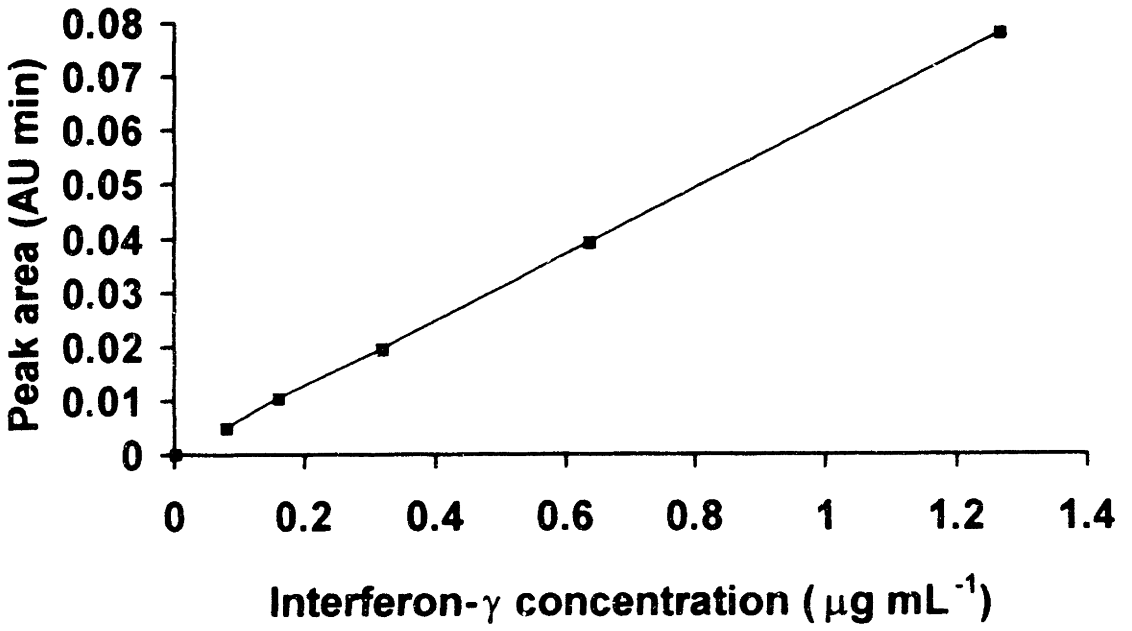

Figure 4.3: Calibration curve for quantitation of interferon-γ by immunoaffinity chromatography

In this concentrating step, acidic aqueous eluent from the immunaffinity column was directly loaded onto a microbore perfusion reversed-phase column, where eluted IFN-γ is bound due to its hydrophobicity. The reversed-phase column was then step-eluted with a hydrophobic eluent, acetonitrile, and IFN-γ was obtained in a small elution volume. Since elution volume is generally proportional to the cross-sectional area of a chromatographic column, both the immunoaffinity purification and reversed-phase concentration steps were performed using microbore columns in order to minimize the dilution of the sample and maximize sensitivity. With an inner diameter of 0.76 mm and a flow rate of 50 μL/min, the elution peak of the immunoaffinity column was approximately 2 min in width, as seen in Figure 4.4, which corresponded to an elution volume of 100 μl. Thus, a 10-fold concentration enhancement was obtained for a 1-mL supernatant loading volume. With an inner diameter of 0.25 mm and a flow rate of 20 μL/min, the reversed-phase column yielded a peak width of approximately 0.5 min, as seen in Figure 4.4. Therefore, the elution volume of the reversed-phase column was only about 10 μL, one-tenth that of the immunoaffinity column. Therefore, for a 1-mL sample of supernatant, a 100-fold concentration enhancement was obtained during the purification and concentration steps. In this manner, sufficient sensitivity was obtained for the use of MEKC to profile macroheterogeneity. MEKC was then used to determine the site occupancy distribution of the immunopurified and concentrated IFN-γ, as shown in Figure 4.5. Due to the negatively-charged silica inner surface of a CE capillary, the bulk fluid inside the capillary moves toward the cathode under the

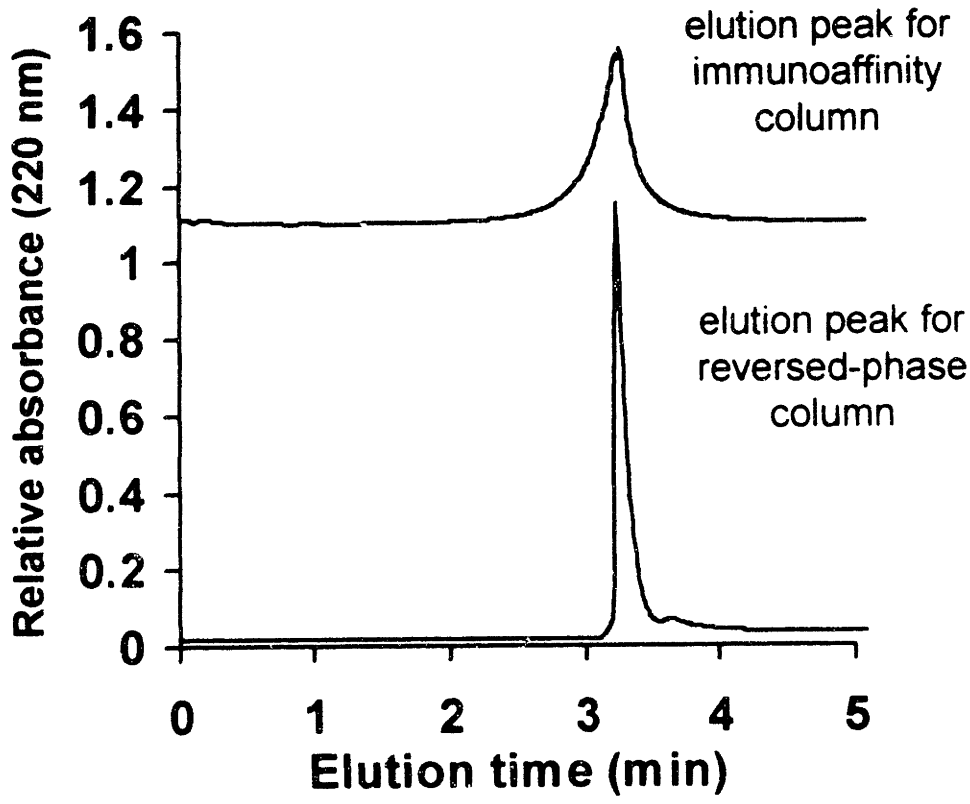

Figure 4.4: On-line concentration enhancement of interferon-γ by solid-phase extraction using perfusion reversed-phase chromatography.

influence of an applied potential. This motion is termed electroosmotic flow (EOF), as represented by the arrow to the right in Figure 4.5. However, in MEKC, a concentration of surfactant above its CMC (*i.e.*, 100 mM SDS) is utilized to form a hydrophobic phase. Due to their negatively-charged outer surfaces, the micellar phase electrophores against the EOF and, thus, migrates more slowly than the bulk flow under the influence of an applied potential. As a result, analytes are separated by their ability to partition between the hydrophilic bulk phase and the hydrophobic micellar phase. Meanwhile, the running buffer also includes 40 mM borate, which is known to form borate-diol complexes with glycans, and therefore increase the hydrophilicity of glycosylated molecules. Since the presence of oligosaccharides increases the hydrophilicity of IFN-γ, and the two-site, one-site and nonglycosylated IFN-γ were separated based upon partitioning between the two phases. A typical MEKC determination of IFN-γ macroheterogeneity is presented in Figure 4.6 Three peaks, with relative proportions of 78 5%, 18.0% and 3.5% by integration of peak areas obtained by monitoring UV absorbance at 200 nm, were observed in the separation of IFN-γ by MEKC. This separation yields good reproducibility (RSD of 0.9%, 0.7% and 0.5% respectively for the relative proportions of these three peaks from 10 replicate IFN-γ samples) Since glycosylation increases the hydrophilicity of the protein, which would cause IFN-γ to partition more strongly into the faster-moving aqueous phase, the three peaks in Figure 4.6 were believed to be two-site, one-site, and nonglycoslyated IFN-γ. Moreover, the distribution of these glycoforms was also consistent with the glycoform percentages obtained from an

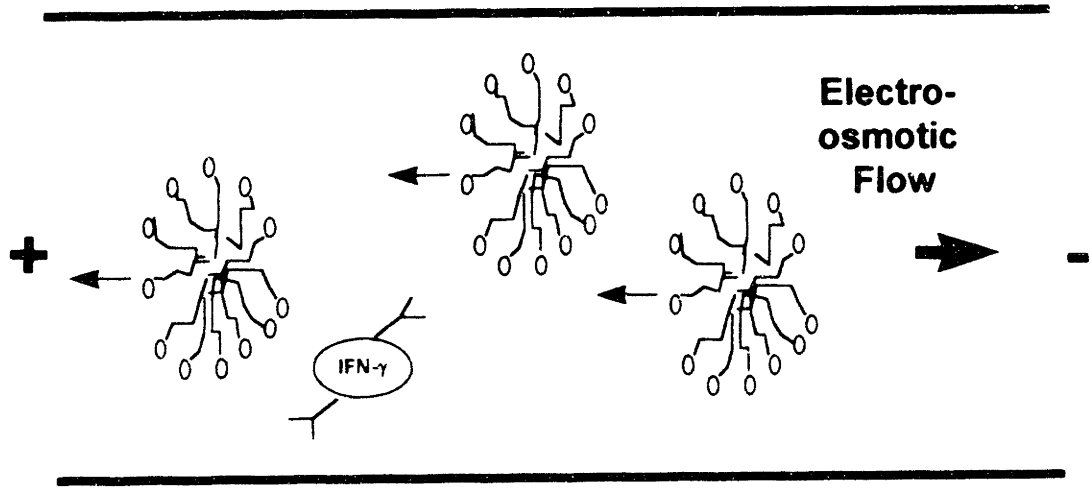

Figure 4.5: Mechanism of interferon-γ separation by micellar electrokinetic chromatography (MEKC)

SDS-PAGE assay of IFN-γ from the same culture supernatant followed by silver staining and densitometry.

In order to conclusively confirm the identities of these three peaks, IFN-γ was subjected to PNGase F digestion, an enzyme which cleaves most common mammalian N-linked oligosaccharides at the N-glycosidic bond, and the digestion process was monitored over time using MEKC. If the substrate and enzyme were prepared in the appropriate ratio, there should be a shift in the glycoform distribution from two-site glycosylated to one-site and eventually to nonglycosylated throughout the digestion process. Figure 4.7 shows a few snapshots of the IFN-γ digestion process. Before being exposed to PNGase F digestion, two-site glycosylated IFN-γ represented the majority of the glycoforms with small proportions of one-site and zero-site glycosylated. However, after a 2-h exposure to PNGase F, sufficient two-site glycosylated forms had lost one of their glycans that the proportion of the one-site glycosylated form was equivalent to that of the two-site glycosylated form. Meanwhile, the proportion of the nonglycosylated form also increased. After 10 h of digestion, one-site glycosylated IFN-γ had become the dominant glycoform. Eventually, after 24 h of digestion, the cleavage of glycans had reached completion, and the IFN-γ had been completely converted to the nonglycosylated form. IFN-γ was also subjected to sialidase treatment prior to MEKC. No changes in relative peak areas were observed relative non-sialidase-treated IFN-γ, which confirms that this separation was not due simply to the degree of sialylation of the glycans. These results confirmed the identities of the three peaks observed in the MEKC

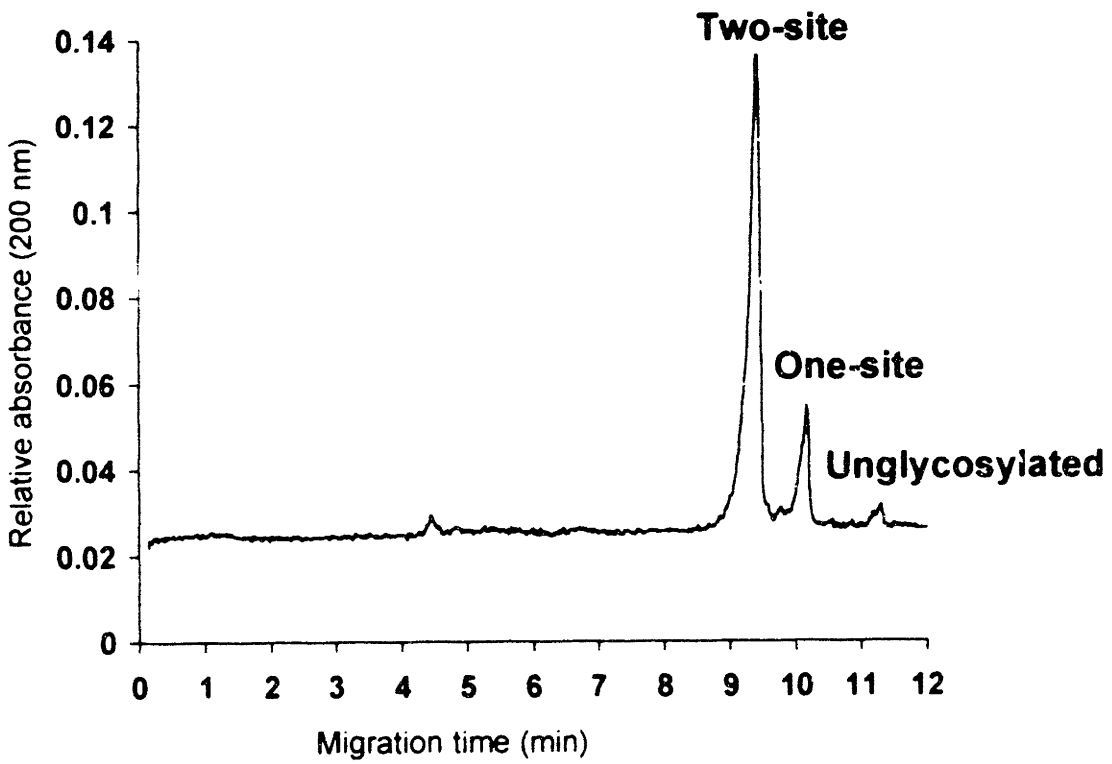

Figure 4.6: Determination of interferon-γ macroheterogeneity by micellar electrokinetic chromatography (MEKC)

separation to be the two-site, one-site, and nonglycosylated forms of IFN-γ.

In order to determine whether the use of UV absorbance detection at 200 nm in MEKC discriminated between the macroheterogeneous glycoforms of IFN-γ, the total peak areas of the three glycoforms of IFN-γ were determined before and after treatment with PNGase F. The total peak areas (corrected for migration velocity) remained identical, which indicated that MEKC with UV absorbance detection at 200 nm did not discriminate among the macroheterogeneous glycoforms and, thus, could be utilized to quantitate site-occupancy of IFN-γ.

With 30 min for immunoaffinity chromatography, 5 min for concentration enhancement of IFN-γ by reversed-phase chromatography, and 15 min for MEKC, the quantification and determination of the macroheterogeneity of IFN-γ was achieved within an hour using as little as 0 5 μg of product. Compared to traditional methods (*e g.*, SDS-PAGE followed by silver staining or western blotting), which typically require more than a day and often require milligrams amount of sample, this methodology for monitoring protein macroheterogeneity was both fast and sensitive, which provided a great opportunity to study protein glycosylation in mammalian cell culture.

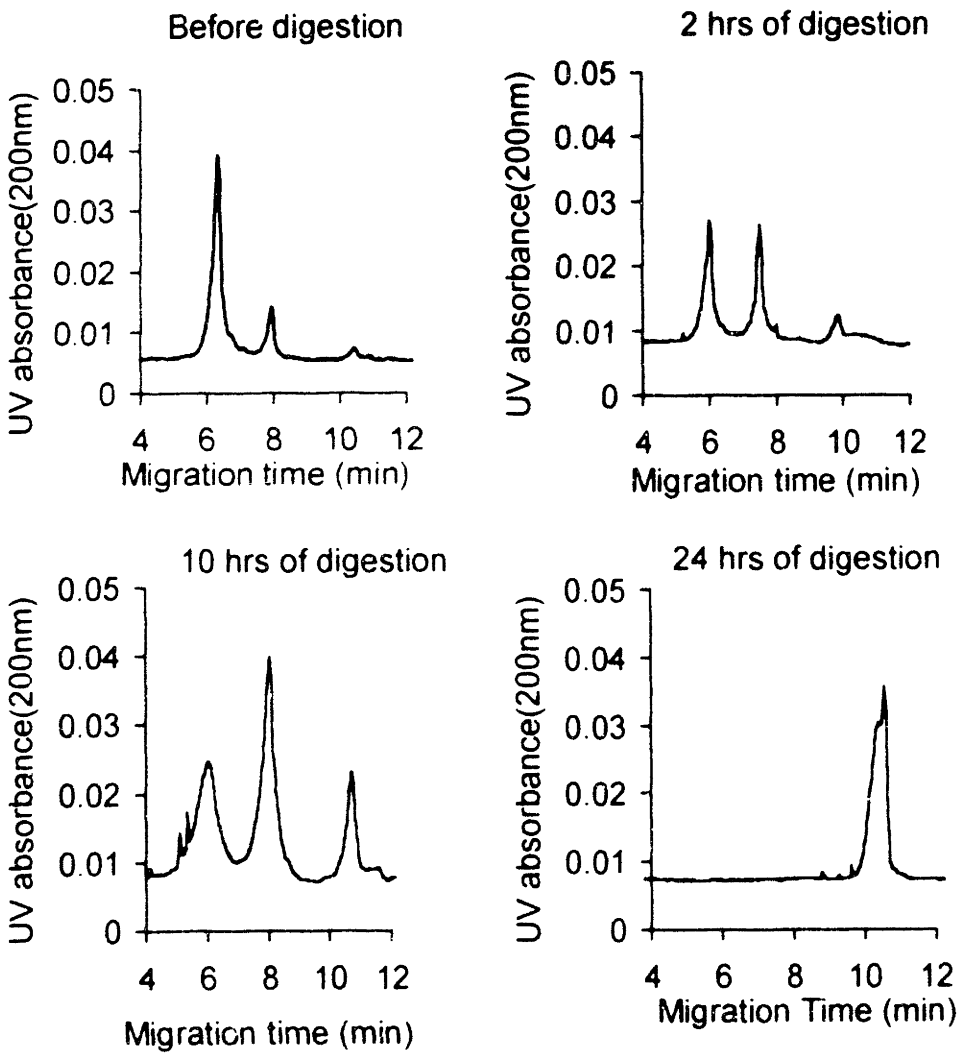

Figure 4.7: Monitoring of IFN-γ with PNGase F digestion with time

4.3 Determination of IFN-γ glycosylation microheterogeneity

As shown in Figure 4.8, MALDI/TOF analysis of intact immunopurified IFN-γ yielded mass spectra consisting of broad peaks corresponding to the three macroheterogenous glycoforms of IFN-γ, nonglycosylated (0N), one-site glycosylated (1N), and two-site glycosylated (2N). However, individual microheterogeneous glycoforms could not be well-resolved. Furthermore, even if individual glycoforms could be resolved, site-specific oligosaccharide structures cannot be unambiguously assigned based upon a single mass of the intact molecule, and interpretation is often complicated by mass shifts resulting from other post-translational modifications. Alternatively, resolution could be improved by analyzing free glycans cleaved either chemically or enzymatically from intact IFN-γ. However, site-specific information cannot be obtained by this approach for glycoproteins exhibiting more than one glycosylation site, such as IFN-γ. Site-specific glycosylation is best achieved with MALDI/TOF by the analysis of site-specific pools of glycopeptides obtained by proteolysis and site-specific fractionation, such as reversed-phase HPLC. This approach improves both the resolution and provides site-specific glycosylation information. As shown in Table 4.1, which lists the expected tryptic fragments for human IFN-γ based from the published amino acid sequence (Rinderknecht et al., 1984), the two potential glycosylation sites are isolated on separate tryptic fragments (*i.e.*, T4 and T19 for Asn^{25} and Asn^{97}, respectively). Furthermore, trypsinization secludes both glycosylation sites from heterogeneity arising from C-terminal cleavages commonly observed for IFN-γ (Rinderknecht *et al.*, 1984). However,

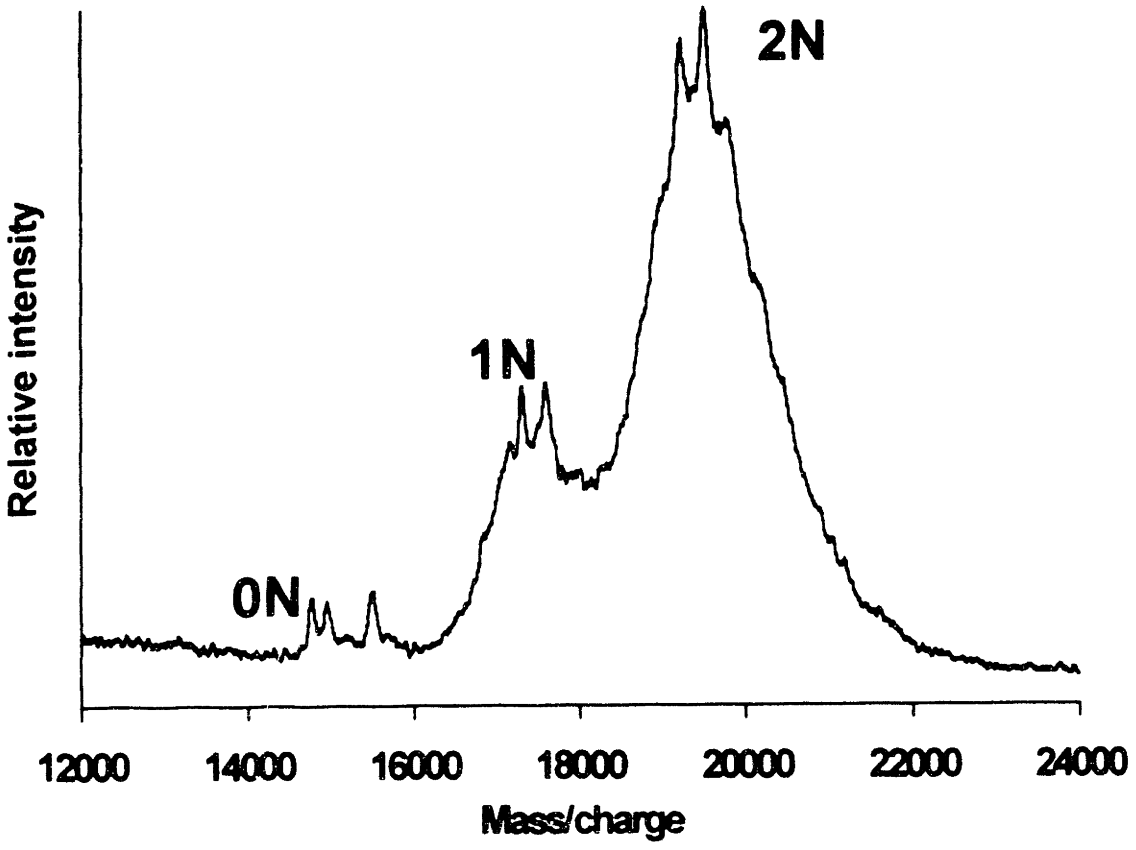

Figure 4.8: MALDI/TOF mass spectrum of intact immunopurified IFN-γ

Table 4.1 Amino acid sequence and expected tryptic peptides of human IFN-γ

peptide	position	amino acid sequence	average mass (Da)
T1	1-6	QDPYVK	748.8
T2	7-12	EAENLK	702.8
T3	13	K	146.2
T4	14-34	YFNAGHSDVADNGTLFLGILK	2252.5
T5	35-37	NWK	446.5
T6	38-42	EESDR	634.6
T7	43	K	146.2
T8	44-55	IMQSQIVSFYFK	1490.8
T9	56-58	LFK	406.5
T10	59-61	NFK	407.5
T11	62-68	DDQSIQK	832.9
T12	69-74	SVETIK	675.8
T13	75-80	EDMNVK	734.8
T14	81-86	FFNSNK	755.8
T15	87	K	146.2
T16	88	K	146.2
T17	89	R	174 2
T18	90-94	DDFEK	652.7
T19	95-107	LTNYSVTDLNVQR	1522 7
T20	108	K	146.2
T21	109-125	AIHELIQVMAELSPAAK	1821.2
T22	126-128	TGK	304.4
T23	129	R	174.2
T24	130	K	146.2
T25	131	R	174.2
T26	132-137	SQMLFR	780.9
T27	138	G	75 1

solution-phase tryptic digestion is generally carried out over a 16 to 24 hr period due to low enzyme:substrate ratios utilized (typically 1:20 to 1:100). In order to minimize time required for proteolysis, trypsinization was performed by use of an on-line immobilized enzyme column. The use of an automated chromatographic format, which is schematically depicted in Figure 4.9, allowed purification of IFN-γ, neutralization, proteolysis, and reversed-phase glycopeptide fractionation required for site-specific assessment of glycoform microheterogeneity to be performed on-line prior to off-line MALDI/TOF analysis. However, the pH 2 eluent from the immunoaffinity column was not compatible with trypsinization as activity of the enzyme was minimal at acidic pH (*i.e.*, when immunopurified IFN-γ was directed to the immobilized trypsin cartridge without neutralization, proteolysis was not observed). The pH was rapidly elevated to optimal conditions for trypsinization (*i.e.*, 50 mM pH 8.2 Tris with 10 mM $CaCl_2$ and 5% acetonitrile) by on-line mixing of the 30 μL min^{-1} effluent from the immunoaffinity column with a 10 μL min^{-1} flow of 200 mM pH 8.5 Tris with 40 mM $CaCl_2$ and 20% acetonitrile by use of a mixing tee located between the immunoaffinity and immobilized trypsin columns. A low percentage of acetonitrile was utilized in order to assure peptide recovery from the immobilized trypsin cartridge without compromising the ability of peptides to bind to the ensuing reversed-phase column. Since IFN-γ does not contain disulfide bonds, reduction and alkylation were not required prior to proteolysis.

The use of an on-line immobilized trypsin cartridge allowed proteolysis to be performed in less than 20 min. The enhanced rate of digestion could be

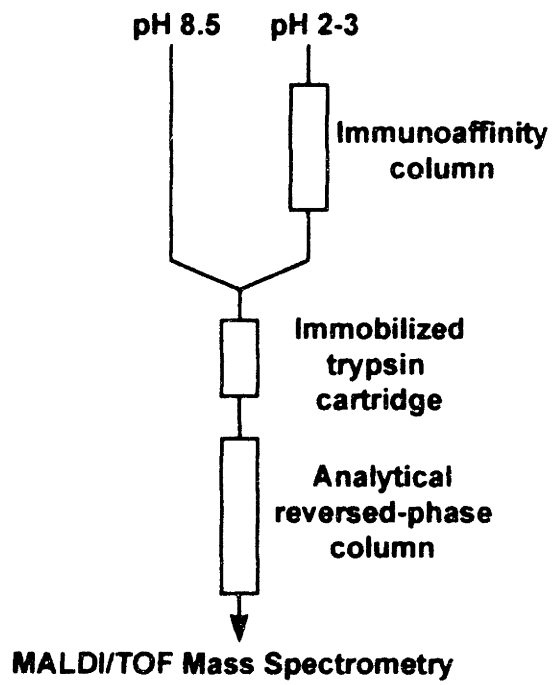

Figure 4.9: On-line proteolysis of immunopurified interferon-γ by immobilized trypsin cartridge

attributed to the high effective concentration of enzyme in the immobilized trypsin cartridge, approximately 10 mg mL^{-1} (Hsieh *et al.*, 1996). After merging with the neutralizing buffer, the volume of immunopurified IFN-γ entering the immobilized trypsin cartridge was approximately 200 µL. Based upon a 1-mL loading volume of supernatant containing 3.5 µg IFN-γ mL^{-1} (the maximum concentration obtained during a suspension γ-CHO batch culture), the concentration of IFN-γ undergoing digestion was typically less than 20 µg mL^{-1}. Thus, the enzyme:substrate ratio obtained by use of the immobilized trypsin cartridge was on the order of 500:1, a 10^5 to 10^6 increase in trypsin concentration relative to typical solution-phase digestion conditions. MALDI/TOF spectra of IFN-γ glycopeptides obtained via the immobilized trypsin cartridge were indistinguishable from those resulting from solution-phase digestion. Although no attempt was made to determine the lifetime of immobilized trypsin cartridges in this study, Hsieh and coworkers (1996) have reported the use of an immobilized trypsin cartridge for greater than 1000 digestions with no loss in performance.

In order to isolate the two pools of glycopeptides representing the potential glycosylation sites, the effluent from the immobilized trypsin cartridge was directed to an on-line, analytical reversed-phase HPLC column, which was washed at 50 µL min^{-1} with water containing 0.1% trifluoroacetic acid for 5 min and eluted by a 30 min linear gradient to 80% acetonitrile with 0.085% trifluoroacetic acid. Figure 4.10 shows the reversed-phase chromatogram resulting from the analysis of a 1-mL aliquot of supernatant collected following 168 h of cell culture (2.9 µg IFN-γ mL^{-1}). As indicated by the expected masses

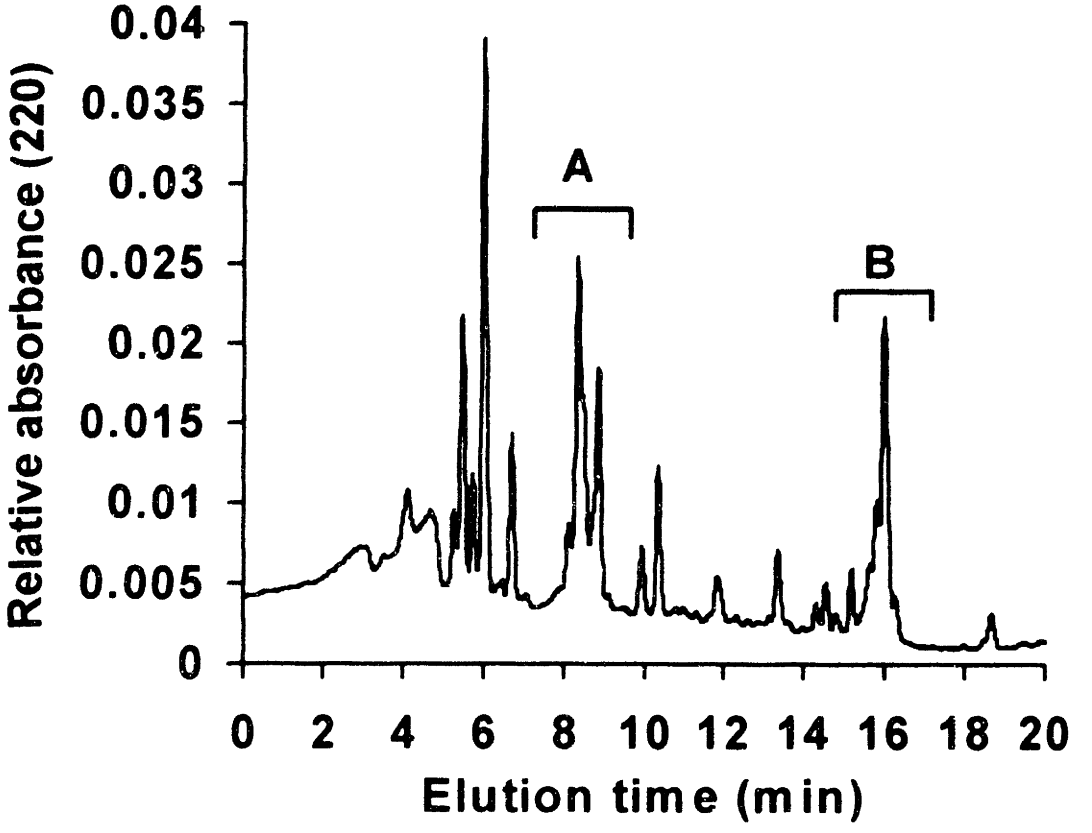

Figure 4.10: Reversed-Phase HPLC Fractionation of Tryptic Glycopeptides

listed in Table 4.1, tryptic peptides of IFN-γ not containing glycosylation sites displayed masses significantly below those observed for the glycopeptides (*i.e.*, 2500 to 6000 Da) Therefore, any nonglycosylated tryptic peptides which may have coeluted with either of the two site-specific pools of glycopeptides could be distinguished by the mass spectrometer, and the further optimization for the reversed-phase resolution was not required.

These automated chromatographic steps prepared site-specific pools of glycopeptides from MALDI/TOF analysis in less than 90 min, compared to approximately 2 days when performed manually with solution-phase trypsinization Furthermore, automation minimized the chance of sample loss or contamination inherent in manual transfers of sample

As shown in Figure 4 11, fractions A and B from Figure 4.10 yielded MALDI/TOF spectra which exhibited clusters of masses greater than those predicted for any of the nonglycosylated tryptic peptides of IFN-γ which were shown in Table 4 1 and which exhibited mass differences characteristic of sugar residues, *i e* , 146 Da for fucose (Fuc), 162 Da for galactose (Gal), mannose (Man), or glucose (Glc), 203 Da for N-acetylglucosamine (GlcNAc), and 291 Da for N-acetylneuraminic acid (sialic acid, NeuAc) In order to confirm that the observed masses were glycopeptides of IFN-γ, rather than partial digestion products or impurities, and to identify the specific glycosylation sites, these fractions were treated with PNGase F As shown in Figure 4 12, all of the glycopeptide masses collapsed into a single peak corresponding to the mass of its respective peptide portion By comparison of observed masses of the

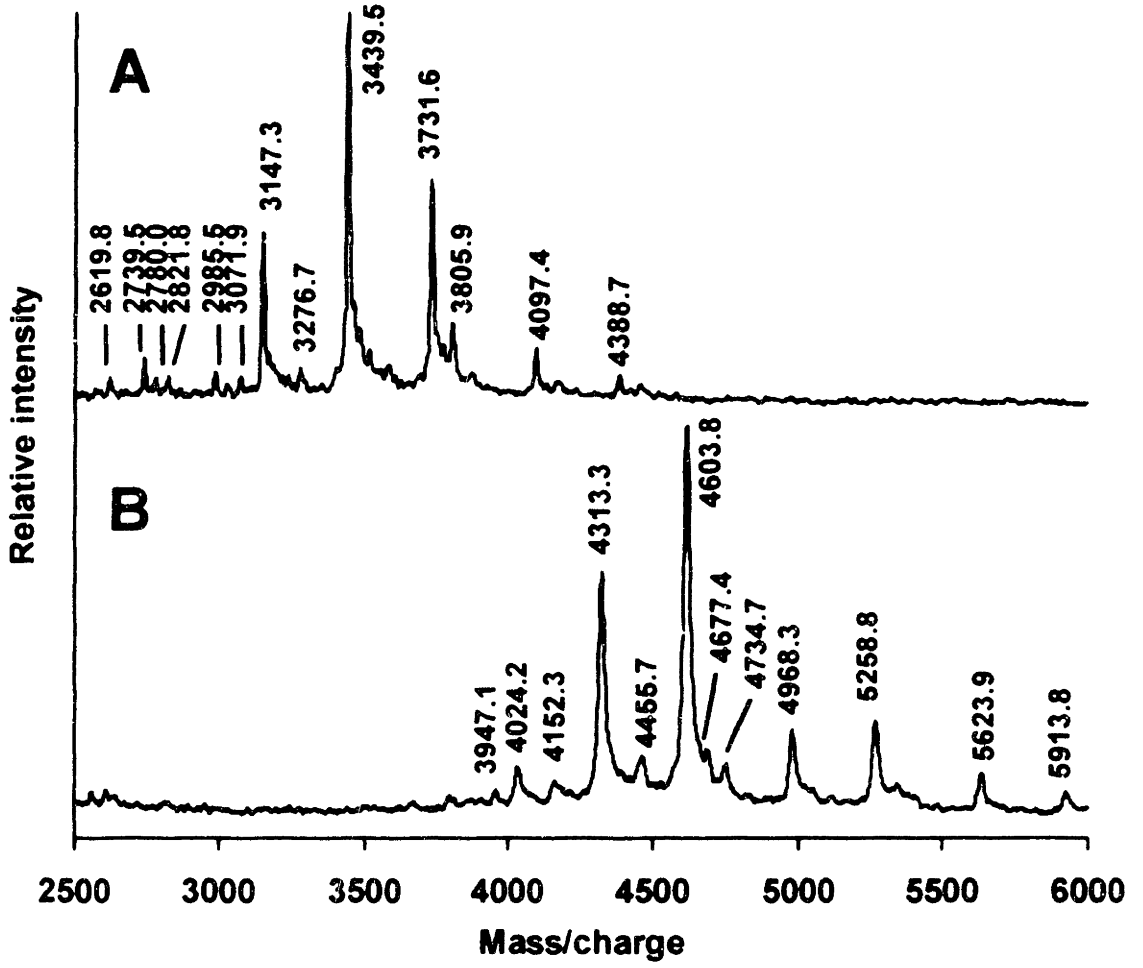

Figure 4.11 MALDI/TOF mass spectra of tryptic glycopeptides of (A) Asn^{97} (fraction A of Figure 4.10) and (B) Asn^{25} (fraction B of Figure 4.10) glycosylation sites of recombinant human IFN-γ from day 7 of suspension γ-CHO batch culture. Corresponding structures are identified in Tables II and III, respectively.

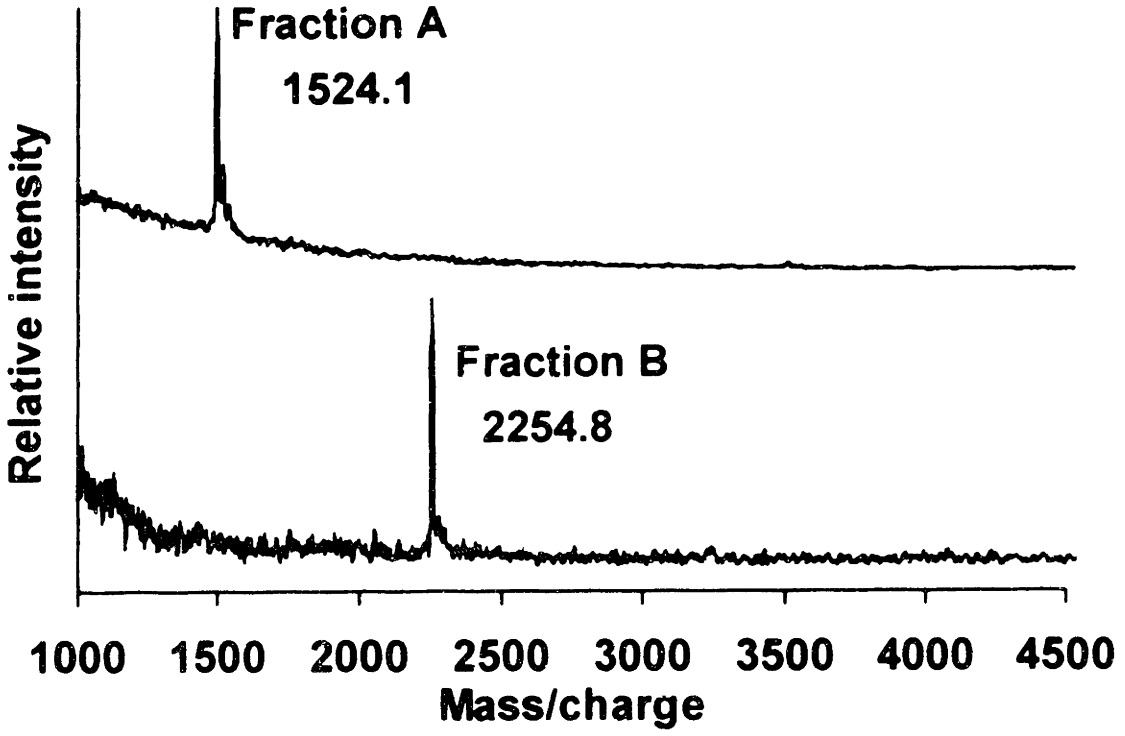

Figure 4.12: MALDI/TOF mass spectra of pNGase F-treated tryptic glycopeptides of interferon-γ

PNGase F-treated fractions to the expected masses for T4 and T19 listed in Table 4.1, the glycopeptides of fractions A and B in Figure 4.10 were identified as those of Asn^{97} and Asn^{25}, respectively. Since reversed-phase retention was dominated by their amino acid portions, the microheterogeneous glycopeptides of each glycosylation site were collected in single fractions, and no other fractions displayed evidence of glycosylation

The assigned oligosaccharide structures for glycans of Asn^{97} and Asn^{25} listed in Tables 4 2 and 4 3, respectively, were deduced by comparing the mass difference between the observed mass of a glycopeptide in Figure 4 11 and the known mass of its amino acid portion to the expected mass shifts for glycan structures previously reported for glycoproteins derived from CHO cell culture As seen in Tables 4 2 and 4 3, mass errors were typically less than 4 Da using external calibration Since the expected mass differences of common CHO-derived structures resulting from addition, loss, or substitution of a common sugar residue (*i e* , minimum difference of 16 Da for Fuc-containing structure compared to Gal or Man) were significantly greater, the mass accuracy of MALDI/TOF was generally sufficient for unambiguous assignment of CHO-derived oligosaccharide structures However, isobaric glycans (*e g*., the two nonequivalent, monosialylated, complex biantennary structures) could not be distinguished based upon glycopeptide mass At each glycosylation site, the predominant signals (*i e* , 3147 3, 3439 5, and 3731 6 Da for $(M+H)^+$ glycopeptides of Asn^{97} and 4024 2, 4313 3, and 4603 8 Da for $(M+H)^+$ glycopeptides of Asn^{25} in Figure 4 12) corresponded to complex biantennary

structures containing 0, 1, and 2 terminal sialic acids, respectively, in agreement with previous reports (James *et al.*, 1995; Mutsaers *et al.*, 1986). Upon initial observation, these proposed structures were subsequently further confirmed by MALDI/TOF analysis of sequential exoglycosidase digestions. In these subsequent analyses, structures corresponding to previously observed mass shifts were not reaffirmed. Less intense signals corresponding to truncated biantennary and complex triantennary and tetraantennary structures differing in the degree of sialylation were also identified, as previously observed by James and coworkers (1995). Oligosaccharides of Asn^{25} predominantly displayed an additional mass shift of approximately 146 Da relative to those of Asn^{97}, thus confirming the site-specific fucosylation of Asn^{25} reported by James and coworkers (1995).

Due to the lability of glycosidic linkages, metastable loss of sialic acid and, to a lesser extent, other sugar residues has been reported in MALDI/TOF analyses (Huberty *et al.*, 1993). The use of linear TOF detection, such as in this study, minimizes the observation for such fragmented species since post-source decay (PSD) does not affect observed masses (*i.e.*, fragment and parent ions travel at same velocity). However, source fragmentation, predominantly loss of sialic acid, was apparent at elevated laser intensity or when α-cyano-4-hydroxycinnamic acid was employed as sample matrix. Thus, to minimize source fragmentation, minimal (*i.e.*, ionization threshold) laser intensity, 2,5-dihydroxybenzoic acid sample matrix were utilized. The positive-ion TOF detection mode was employed as negative-ion detection displayed significantly

Table 4 2 Tryptic glycopeptides of Asn^{97} glycosylation site of recombinant human IFN-γ from γ-CHO batch culture observed by MALDI/TOF mass spectrometry (Figure 17A)

glycopeptide structure	expected $(M+H)^+$ mass (Da)	observed $(M+H)^+$ mass (Da)	% mass error
T_{19}-GlcNAc-GlcNAc-Man(Man-GlcNAc)(Man)	2619 6	2619 8	0 008%
T_{19}-GlcNAc-GlcNAc-Man(Man(Man)(Man))(Man)	2740 6	2739 5	0 040%
T_{19}-GlcNAc-GlcNAc-Man(Man-GlcNAc-Gal)(Man)	2781 7	2780 0	0 061%
T_{19}-GlcNAc-GlcNAc-Man(Man-GlcNAc)(Man-GlcNAc)	2822 8	2821 8	0 035%
T_{19}-GlcNAc-GlcNAc-Man(Man-GlcNAc-Gal)(Man-GlcNAc)	2984 9	2985 5	0 020%
T_{19}-GlcNAc-GlcNAc-Man(Man-GlcNAc-Gal-NeuAc)(Man)	3073 0	3071 9	0 036%
T_{19}-GlcNAc-GlcNAc-Man(Man-GlcNAc-Gal)(Man-GlcNAc-Gal)	3147 0	3147 3	0 010%
T_{19}-GlcNAc-GlcNAc-Man(Man-GlcNAc-Gal-NeuAc)(Man-GlcNAc)	3276 2	3276 7	0 015%
T_{19}-GlcNAc-GlcNAc-Man(Man-GlcNAc-Gal-NeuAc)(Man-GlcNAc-Gal)	3438 3	3439 5	0 035%
T_{19}-GlcNAc-GlcNAc-Man(Man-GlcNAc-Gal-NeuAc)(Man-GlcNAc-Gal-NeuAc)	3729 6	3731 6	0 054%
T_{19}-GlcNAc-GlcNAc-Man(Man(GlcNAc-Gal)(GlcNAc-Gal))(Man-GlcNAc-Gal) NeuAc	3803 6	3805 9	0 060%
T_{19}-GlcNAc-GlcNAc-Man(Man(GlcNAc-Gal)(GlcNAc-Gal))(Man-GlcNAc-Gal) 2 NeuAc	4094 9	4097 4	0 061%
T_{19}-GlcNAc-GlcNAc-Man(Man(GlcNAc-Gal-NeuAc)(GlcNAc-Gal-NeuAc))(Man-GlcNAc-Gal-NeuAc)	4386 2	4388 7	0 057%

Table 4 3 Tryptic glycopeptides of Asn^{25} glycosylation site of recombinant human IFN-γ from γ-CHO batch culture observed by MALDI/TOF mass spectrometry (Figure 17B)

glycopeptide structure	expected (M+H)⁺ mass (Da)	observed (M+H)⁺ mass (Da)	% mass error
T_4-GlcNAc-GlcNAc-Man(Man-GlcNAc-Gal-NeuAc; Man); Fuc	3948 9	3947 1	0 046%
T_4-GlcNAc-GlcNAc-Man(Man-GlcNAc-Gal; Man-GlcNAc-Gal); Fuc	4022 9	4024 2	0 032%
T_4-GlcNAc-GlcNAc-Man(Man-GlcNAc-Gal-NeuAc; Man-GlcNAc); Fuc	4152 1	4152 3	0 005%
T_4-GlcNAc-GlcNAc-Man(Man-GlcNAc-Gal-NeuAc; Man-GlcNAc-Gal); Fuc	4314 2	4313 3	0 021%
T_4-GlcNAc-GlcNAc-Man(Man-GlcNAc-Gal-NeuAc; Man-GlcNAc-Gal-NeuAc)	4459 4	4455 7	0 083%
T_4-GlcNAc-GlcNAc-Man(Man-GlcNAc-Gal-NeuAc; Man-GlcNAc-Gal-NeuAc); Fuc	4605 5	4603 8	0 037%
T_4-GlcNAc-GlcNAc-Man(Man(GlcNAc-Gal; GlcNAc-Gal); Man-GlcNAc-Gal) NeuAc; Fuc	4679 5	4677 4	0 045%
T_4-GlcNAc-GlcNAc-Man(Man(GlcNAc-Gal; GlcNAc-Gal); Man-GlcNAc-Gal) 2 NeuAc; Fuc	4970 8	4968 3	0 050%
T_4-GlcNAc-GlcNAc-Man(Man(GlcNAc-Gal-NeuAc; GlcNAc-Gal-NeuAc); Man-GlcNAc-Gal-NeuAc); Fuc	5262 1	5258 8	0 063%
T_4-GlcNAc-GlcNAc-Man(Man(GlcNAc-Gal-NeuAc; GlcNAc-Gal-NeuAc); Man(GlcNAc-Gal-NeuAc; GlcNAc-Gal)); Fuc	5627 4	5623 9	0 062%
T_4-GlcNAc-GlcNAc-Man(Man(GlcNAc-Gal-NeuAc; GlcNAc-Gal-NeuAc); Man(GlcNAc-Gal-NeuAc; GlcNAc-Gal-NeuAc)); Fuc	5918 7	5913 8	0 083%

poorer sensitivity for each pool of glycopeptides and revealed no additional structural information

To assess the reproducibility of the method five replicate supernatant samples were analyzed Good reproducibility was obtained both for the assignment of site-specific oligosaccharide structures (*i.e.*, each of the glycopeptide structures listed in Tables 4.2 and 4 3 could be observed for each of the replicate analyses) and the relative signal intensities The glycopeptides displayed an average R S.D of 0 045% for the determination of mass and an average mass error of 0 056% Da using external calibration The reproducibility of the MALDI/TOF spectra resulting from the five replicate samples was not distinguishable from five replicate MALDI/TOF analyses of a single sample, thus showing that the automated sample preparation steps did not introduce additional uncertainty

Since the labile glycosidic linkage of sialic acid is susceptible to source fragmentation, and the variable presence of charged residues, such as sialic acid, affects the relative ionization efficiencies of glycopeptides (Sutton *et al* , 1994), integrated MALDI/TOF peak areas of sialylated glycopeptides could not be related directly to concentrations. Thus, the MALDI/TOF spectra of sialylated glycopeptides served as qualitative "fingerprints" of microheterogeneous glycosylation patterns The inability to quantitate sialic acid content is an inherent limitation of MALDI/TOF-based methodologies as sialylation is frequently a primary determinant of glycoprotein clearance rate. However, Sutton and coworkers (1994) have observed that neutral oligosaccharides have minimal

effect upon ionization efficiencies of glycopeptides, and, consequently, integration of MALDI/TOF signals of several desialylated glycopeptides yielded excellent quantitative correlation with published data obtained by the established techniques of high-performance anion exchange chromatography, fast-atom bombardment mass spectrometry, and reversed-phase HPLC Thus, the two site-specific glycopeptide fractions of IFN-γ were desialylated in order to quantitate asialoglycan structures Desialylation was performed by sialidase digestion on the MALDI sample plate in a manner similar to that described by Patterson and coworkers (1995) for the generation of carboxypeptidase Y C-terminal ladders One-μL aliquots of glycopeptide fraction and enzyme solution were pipetted into a well of the MALDI sample plate and mixed with the pipet tip prior to redepositing the digestion mixture into the sample well The digestion was allowed to proceed for approximately 5 to 10 min at 37°C until solvent evaporation terminated the reaction Due to the tolerance of MALDI to buffer salts, clean-up of digestion mixtures was not required, and the asialoglycopeptides were simply resuspended in matrix and allowed to dry prior to MALDI/TOF analysis As seen in Figure 4 13, single peaks were observed for intact biantennary, triantennary, and tetraantennary structures (3151 0, 3516 3, and 3882 8 Da in Figure 4 13A correspond to asialoglycopeptides of Asn^{97} containing nonfucosylated complex biantennary, triantennary, and tetraantennary glycans, respectively, while 4020 2, 4384 6, and 4750 6 Da in Figure 4 13B represent fucosylated complex biantennary, triantennary, and tetraantennary asialoglycopeptides of Asn^{25}, respectively) No masses representing structures

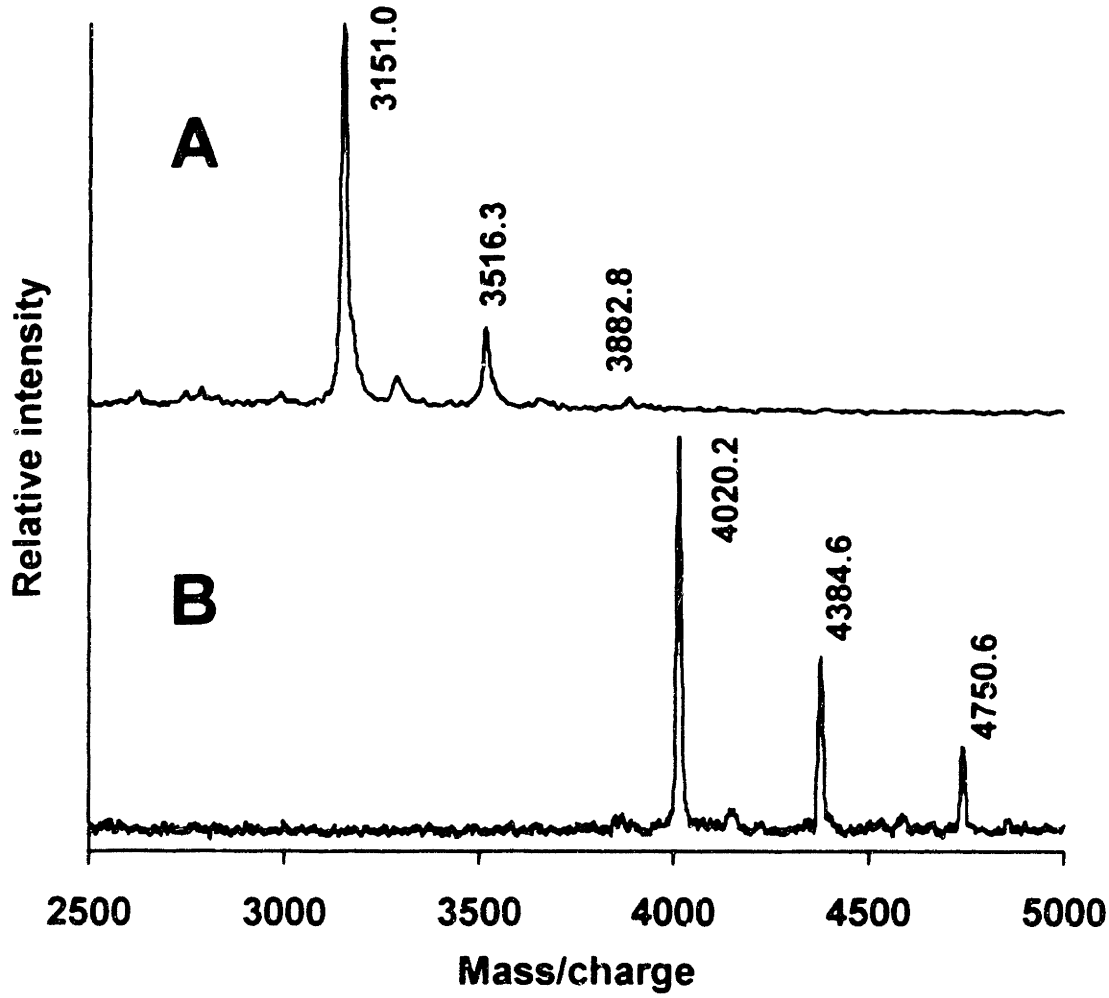

Figure 4.13 MALDI/TOF mass spectra of sialidase-treated tryptic glycopeptides of (A) Asn^{97} and (B) Asn^{25} glycosylation sites of recombinant human IFN-γ from day 7 of suspension γ-CHO batch culture.

containing sialic acid were identified, thus indicating that complete desialylation was achieved by this on-plate digestion strategy. Based upon integrated MALDI/TOF signals for the five replicate supernatant aliquots, biantennary, triantennary, and tetraantennary glycans accounted for (average ± standard deviation) (77 5±2 1)%, (18 4±2 1)%, and (4 1±1 3)%, respectively, of Asn^{97}-linked glycans, and (63 4±2 7)%, (24 8±1 7)%, and (11 8±1 0)%, respectively, of Asn^{25}-linked oligosaccharides

In order to illustrate use of this methodology to rapidly assess the effects of altering cell culture conditions, γ-CHO cell culture was performed in which deoxymannojirimycin, an inhibitor of glycoprotein processing, was added to the culture medium As shown in Figure 4 14, following transfer of the "core" $(GlcNAc)_2Man_9Glc_3$ oligosaccharide from its dolichol-P carrier to the nascent polypeptide chain, the glycan is modified by a series of processing reactions in the endoplasmic reticulum and Golgi (Elbein, 1991) Following initial removal of the α(1→2)-linked glucose and two α(1→3)-linked glucose units by glucosidase I and II, respectively, to produce a high-mannose $(GlcNAc)_2Man_9$ structure, all four α(1→2)-linked mannose residues are removed by mannosidase I to yield $(GlcNAc)_2Man_5$ A series of exoglycosidase and glycosyltransferase reactions then generate complex structures, such as those previously observed for IFN-γ Deoxymannojirimycin is an inhibitor of mannosidase I (Fuhrmann *et al*., 1984) and, thus, results in accumulation of high-mannose structures when added to culture medium Figure 4 15 depicts MALDI/TOF spectra obtained for glycopeptides of Asn^{97} and Asn^{25} from a γ-CHO culture containing 2 5 mM

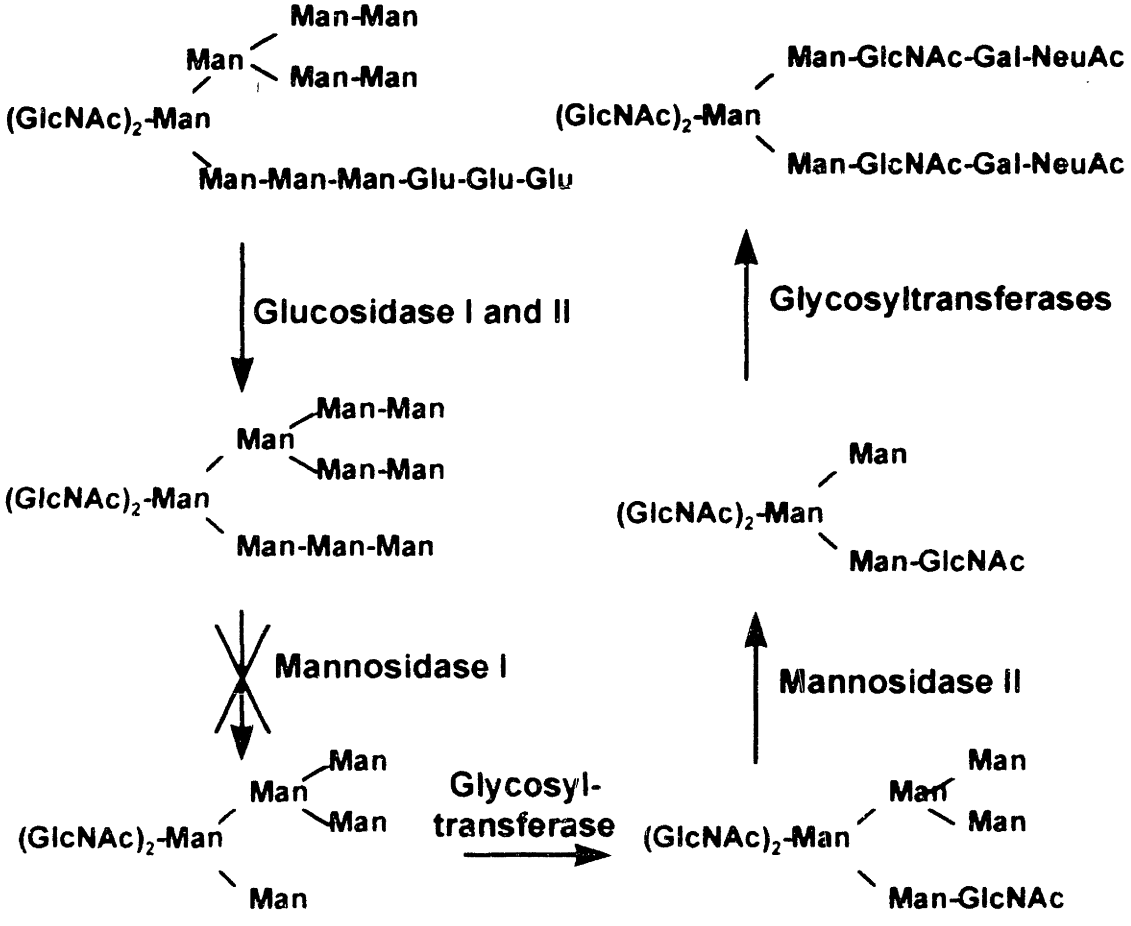

Figure 4.14: Inhibition of glycoprotein processing by deoxymannojirimycin

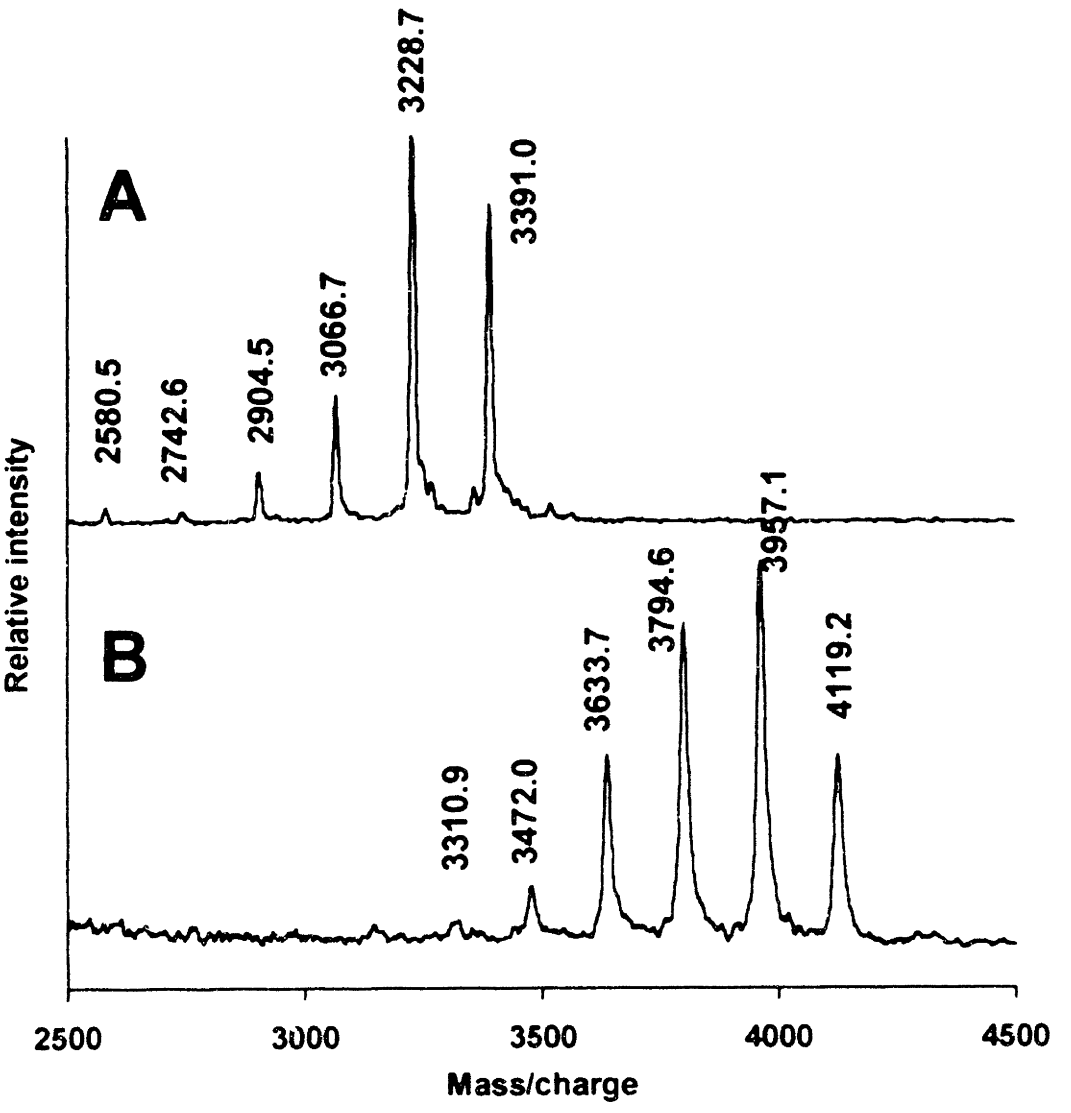

Figure 4.15. MALDI/TOF mass spectra of tryptic glycopeptides of (A) Asn^{97} and (B) Asn^{25} glycosylation sites of recombinant human IFN-γ from γ-CHO culture in presence of 2.5 mM deoxymannojirimycin. Corresponding structures are identified in Table 4.4.

deoxymannojirimycin The highest indicated mass in each spectra corresponds to the expected mass shift of the $(GlcNAc)_2Man_9$ glycan. Each spectrum also displays a series of peaks each differing by approximately 162 Da (the characteristic mass shift of Man) corresponding to $(GlcNAc)_2Man_{4-8}$ structures, thus indicating inhibition of mannosidase I was not complete As noted previously, it was not possible to distinguish mass degenerate structures (*e.g.*, the three isomers of $(GlcNAc)_2Man_8$) based upon mass shifts of intact glycopeptides The mass differences between the peak clusters of Asn^{25} and Asn^{97} corresponded precisely to the mass difference between the amino acid portions of the Asn^{25} and Asn^{97} glycopeptides, thus indicating that inhibition of the glycoprotein processing pathway at the mannosidase I step prevented the site-specific fucosylation of Asn^{25} Since each high-mannose glycopeptide observed in Figure 4 15 was not sialylated, a quantitative estimation of the relative proportions of each microheterogeneous glycoform could be made without sialidase treatment and is included in Table 4 4

4.4 Determination of IFN-γ sialylation

Due to the recognized biological significance of sialic acid, sialylation is often a desirable feature of recombinant glycoproteins intended for therapeutic use Consequently, the characterization and monitoring of sialylation patterns of such products are essential to ensure their efficacy, homogeneity, and consistency Although qualitative trends in sialylation could be identified by MALDI/TOF of the site-specific pools of glycopeptides described in the previous

Table 4.4. Tryptic glycopeptides of Asn^{97} and Asn^{25} glycosylation sites of recombinant human IFN-γ from γ-CHO batch culture containing 2.5 mM deoxymannojirimycin observed by MALDI/TOF mass spectrometry

	Asn^{97} glycopeptides (T_{19})			Asn^{25} glycopeptides (T_4)		
glycan structure	expected $(M+H)^+$ mass (Da)	observed $(M+H)^+$ mass (Da)	% of total signal	expected $(M+H)^+$ mass (Da)	observed $(M+H)^+$ mass (Da)	% of total signal
GlcNAc-GlcNAc-Man(Man-Man, Man)	2578 5	2580 5	1%	3308.3	3310 9	1%
GlcNAc-GlcNAc-Man(Man(Man, Man), Man)	2740 6	2742 6	1%	3470 4	3472 0	3%
GlcNAc-GlcNAc-Man(Man(Man, Man), Man) + Man	2902 7	2904 5	3%	3632.5	3633 7	16%
GlcNAc-GlcNAc-Man(Man(Man, Man), Man) + 2 Man	3064 8	3066 7	11%	3794.6	3794 6	28%
GlcNAc-GlcNAc-Man(Man(Man, Man), Man) + 3 Man	3226.9	3228.7	47%	3956 7	3957 1	36%
GlcNAc-GlcNAc-Man(Man(Man-Man, Man-Man), Man-Man-Man)	3389 0	3391 0	37%	4118 8	4119 2	16%

section (*i.e.*, Figure 4.11 indicates the glycans of Asn^{25} are more highly sialylated than those of Asn^{97}), MALDI/TOF did not adequately quantify the sialylated glycopeptides of IFN-γ due to the lability of the glycosidic linkage of sialic acid leading to source fragmentation (Huberty *et* al., 1993) and the variable presence of negatively-charged sialic acid residues affecting the relative ionization efficiencies of the glycopeptides (Sutton *et al.*, 1994), as shown by Table 4.5, which compares the quantification of the sialylation of the Asn^{97}-linked glycopeptides of IFN-γ using either the positive- or negative-ion mode of MALDI-TOF to a quantitative HPLC method (*i.e.*, a neutral pH/borate complexation reversed-phase HPLC method described below). Although minimal source fragmentation loss of sialic acid was observed in the positive-ion mode of MALDI/TOF when threshold laser intensity and 2,5-dihydroxybenzoic acid sample matrix were employed, this method underestimated sialylation due to lower ionization efficiency of sialylated species. Although the negative-ion mode would be expected to over estimate sialylation due to preferential ionization of sialylated species, sialylation was also underestimated due to the poorer sensitivity of this method for the glycopeptides of both Asn^{25} and Asn^{97}. Consequently, much higher laser intensity had to be employed resulting in significant source fragmentation loss of sialic acid.

Furthermore, MALDI/TOF could not distinguish between mass degenerate structures (*e.g.*, the two isomers of the monosialo complex biantennary structure differing in the branch of sialylation, Man(α1-3) or Man(α1-6)) based on the masses of the intact glycopeptides. The determination of branching by

MALDI/TOF requires the interpretation of post-source decay fragmentation patterns obtained with reflectron TOF detection and is highly qualitative.

Table 4.5. Comparison of methods to quantify Asn^{97}-associated sialylation of IFN-γ derived from CHO cell culture.

Method	Observed Sialylation Percentage
HPLC Method	79±1
Positive-ion MALDI/TOF	70±2
Negative-ion MALDI/TOF	74±1

Several analytical methods have been routinely employed to quantify sialylation of glycoproteins. Charge-based separations of intact glycoproteins, such as isoelectric focusing (Righetti, 1983) or capillary electrophoresis (Watson *et al.*, 1993), as well as colorimetric or chromatographic analysis of sialic acids chemically or enzymatically released from glycoproteins (Reuter and Schauer, 1994) can be utilized to estimate total sialic acid content. However, site- or branch-specific information is not obtainable by such techniques. Furthermore, these analyses cannot detect differences in the number of available sialylation sites due to variability in the site occupancy or variability in the antennarity of glycans. Quantitation of sialic acid content by high-pH anion-exchange chromatography (Townsend *et* al., 1989) of free glycans released by chemical or enzymatic methods can reveal antennarity and branch-specificity. However, if the glycans are cleaved from the intact glycoprotein, site-specific information is lost.

Site-specific sialylation is best obtained by the analysis of glycopeptides obtained by proteolysis of the glycoprotein so that the potential glycosylation sites are isolated on separate fragments.

In this study, site- and branch-specific quantitation of sialylation of CHO-derived IFN-γ was obtained by introducing an additional analytical step to the previously-describe analytical scheme, sialic acid-based separations of the site-specific pools of glycopeptides using a neutral pH/borate complexation reversed-phase HPLC method previously reported by Rice *et al.* (1990). To illustrate the sialic acid-based separations obtained by this methodology, Figure 4.16 shows the separation of the Asn^{97}-linked tryptic glycopeptides of IFN-γ after 168 h of suspension batch CHO cell culture. Following MALDI/TOF analysis of each fraction, oligosaccharide structures were assigned based upon the observed masses of the glycopeptides relative to the known masses of their respective amino acid sequences (*i.e.*, 1523 and 2253 Da for the glycopeptides of Asn^{97} and Asn^{25}, respectively). As listed in Table 4.6, the observed masses of fractions C_0, C_{1a}, C_{1b}, and C_2 in Figure 4 16 corresponded to glycopeptides containing complex biantennary oligosaccharide structures with zero, one, one, and two sialic acids, respectively. Fractions B_2 and B_3 were identified as complex triantennary glycans containing two and three sialic acids, respectively, and fractions A_3 and A_4 were classified as complex tetraantennary glycans with three and four sialic acids, respectively.

As show by Figure 4.17, there were two mass-degenerate forms, fractions C_{1a} and C_{1b}, which corresponded to monosialo biantennary structures. Since the

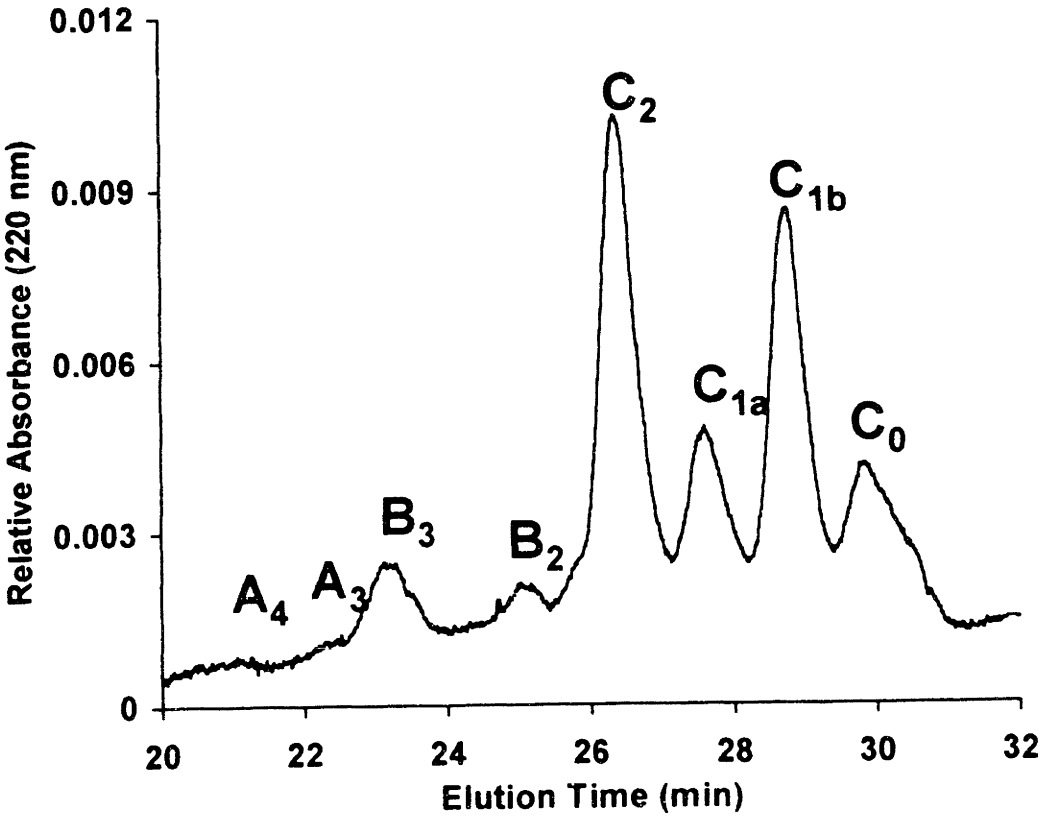

Figure 4.16: Neutral pH/borate complexation reversed-phase HPLC separation of Asn^{97}-linked IFN-γ tryptic glycopeptides following 168 h of suspension batch CHO cell culture. A_3 and A_4 represent nonfucosylated complex tetraantennary glycans with 3 and 4 sialic acids, respectively; B_2 and B_3 indicate nonfucosylated complex triantennary glycans with 2 and 3 sialic acids, respectively; and C_0, C_{1a}, C_{1b}, and C_2 correspond to nonfucosylated complex biantennary glycans with 0, 1 (on α1-6 branch), 1 (on α1-3 branch), and 2 sialic acids, respectively.

Table 4.6 Oligosaccharide structures for Asn^{97}-linked glycopeptide fractions (Figure 4.16) identified by MALDI-TOF mass spectrometry.

Symbol	Glycan structure	(M+ H)$^+$ mass (Da) Observed	Expected
A_3	-GlcNAc-GlcNAc-Man(Man(GlcNAc-Gal)(GlcNAc-Gal))(Man(GlcNAc-Gal)(GlcNAc-Gal)) 3 NeuAc	4754	4752
A_4	-GlcNAc-GlcNAc-Man(Man(GlcNAc-Gal-NeuAc)(GlcNAc-Gal-NeuAc))(Man(GlcNAc-Gal-NeuAc)(GlcNAc-Gal-NeuAc))	5045	5043
B_2	-GlcNAc-GlcNAc-Man(Man(GlcNAc-Gal)(GlcNAc-Gal))(Man-GlcNAc-Gal) 2 NeuAc	4097	4095
B_3	-GlcNAc-GlcNAc-Man(Man(GlcNAc-Gal-NeuAc)(GlcNAc-Gal-NeuAc))(Man-GlcNAc-Gal-NeuAc)	4388	4386
C_0	-GlcNAc-GlcNAc-Man(Man-GlcNAc-Gal)(Man-GlcNAc-Gal)	3148	3147
C_{1a}	-GlcNAc-GlcNAc-Man(3(1 Man-GlcNAc-Gal)(6(1 Man-GlcNAc-Gal-NeuAc)))	3439	3438
C_{1b}	-GlcNAc-GlcNAc-Man(3(1 Man-GlcNAc-Gal -NeuAc)(6(1 Man-GlcNAc-Gal)))	3439	3438
C_2	-GlcNAc-GlcNAc-Man(Man-GlcNAc-Gal-NeuAc)(Man-GlcNAc-Gal-NeuAc)	3730	3730

two common forms of sialic acid observed in mammalian cell culture (NeuAc and N-glycolylneuraminic acid, NeuGc) differ in mass by 16 Da, and C_{1a} and C_{1b} displayed identical masses of 3438 Da (corresponding to the presence of a single NeuAc), this separation could not have been due to variability in the form of sialic acid incorporated.

The presence of two mass-degenerate reversed-phase peaks for the monosialo complex biantennary structure indicated that a branch-specific separation might have taken place. The single terminal sialic acid might have been either on the Man(α3-1) branch or the Man(α1-6) branch, consequently creating the two mass-degenerate isomers depicted below:

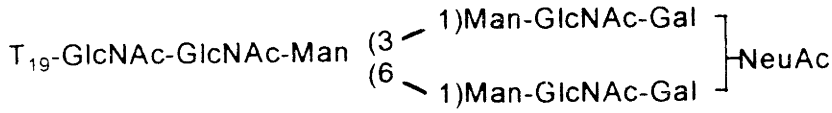

Since insufficient material was available for ^{1}H-NMR analysis for conclusive confirmation of the branch of sialylation of these two mass-degenerate structures, the specificity of exoglycosidase digestion and sensivity of MALDI/TOF were employed to identify C_{1a} and C_{1b} α-Mannosidase from jack bean, at a concentration of 6 units ml^{-1} cleaves a mannose which is α1-3 linked to the core β-mannose, but does not remove a mannose which is α1-6 linked to the core β-mannose (Yamashita, 1980). Although the presence of sialic acid would block digestion of the sialylated branches, galactose and N-acetylglucosamine would be sequentially removed by β-galactosidase and β-N-acetylhexosaminidase,

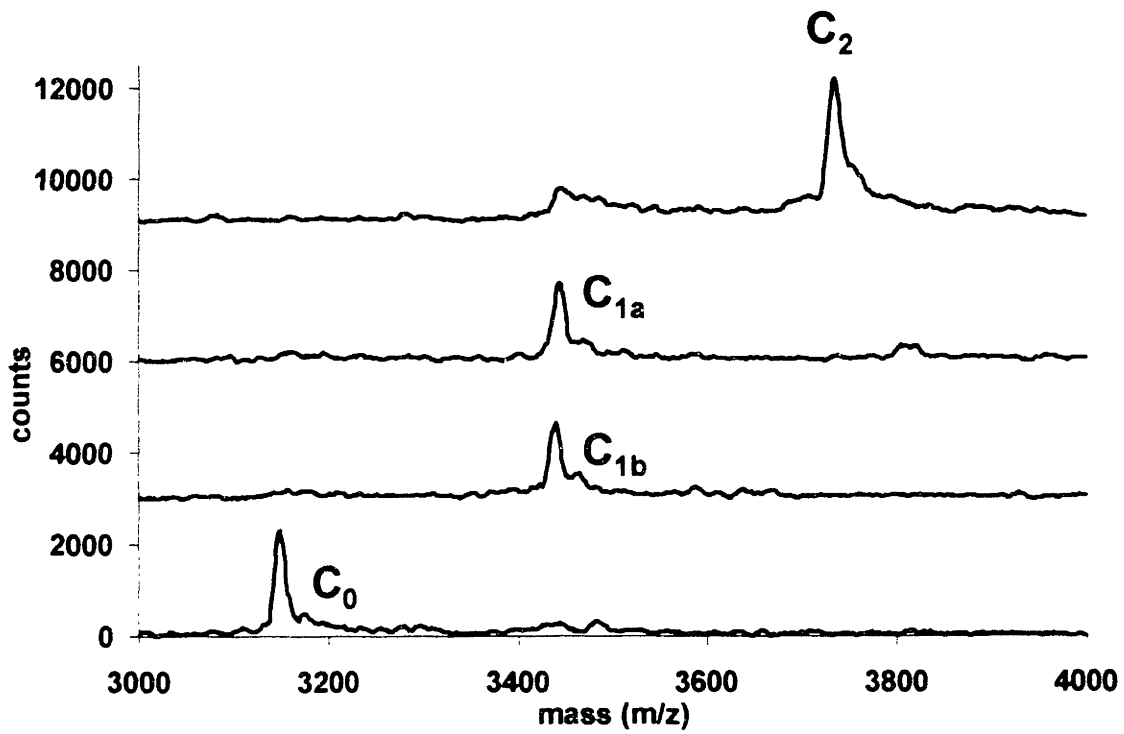

Figure 4.17:MALDI-TOF mass spectra of complex biantennary peaks of Asn^{97}-linked tryptic glycopeptides of IFN-γ eluted from neutral pH/borate complexation reversed-phase HPLC chromatography. C_0 and C_2 correspond to the asialo and biasialo complex biantennary structures, respectively . Both C_{1a} and C_{1b} depicts mass-degenerate monosialo complex biantennary structures.

respectively, from the unsialylated branches. Upon α-mannosidase treatment, if the exposed mannose was α1-3 linked to core β-mannose, it would be cleaved by α-mannosidase treatment. However, the bare mannose α1-6 linked to core β-mannose would remain intact. These two corresponding structures would create a mass difference of 162, the mass of mannose, which could be disclosed by MALDI-TOF analysis. Using this methodology, the two pools of mass-degenerate glycopeptides were treated by exoglycosidase digestions of β-galactosidase, β-N-acetylhexosaminidase and jack bean α-mannosidase, and the resultant mass shifts were observed by MALDI-TOF. Figure 4.18 shows the MALDI-TOF mass spectra of C_{1a} and C_{1b} following simultaneous β-galactosidase and β-N-acetylhexosaminidase treatment and separation from the digestion mixture by reversed-phase HPLC, indicated as C_{1a}-I and C_{1b} -I, respectively. Both C_{1a}-I and C_{1b} -I displayed masses of 3073 Da, corresponding to the loss of one galactose and one N-acetylglucosamine.

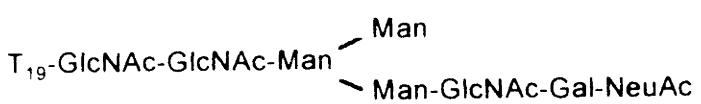

Therefore, branch-specific sialylation could not yet be confirmed. Subsequently, C_{1a}-I and C_{1b} -I were subjected to treatment with jack bean α-mannosidase and analyzed by MALDI/TOF, yielding structures C_{1a}-II and C_{1b}-II, respectively, in Figure 4.19. The poorer resolution seen in Figure 4.19 relative to Figure 4.18 can be explained by the high salt concentration of the α-mannosidase digestion

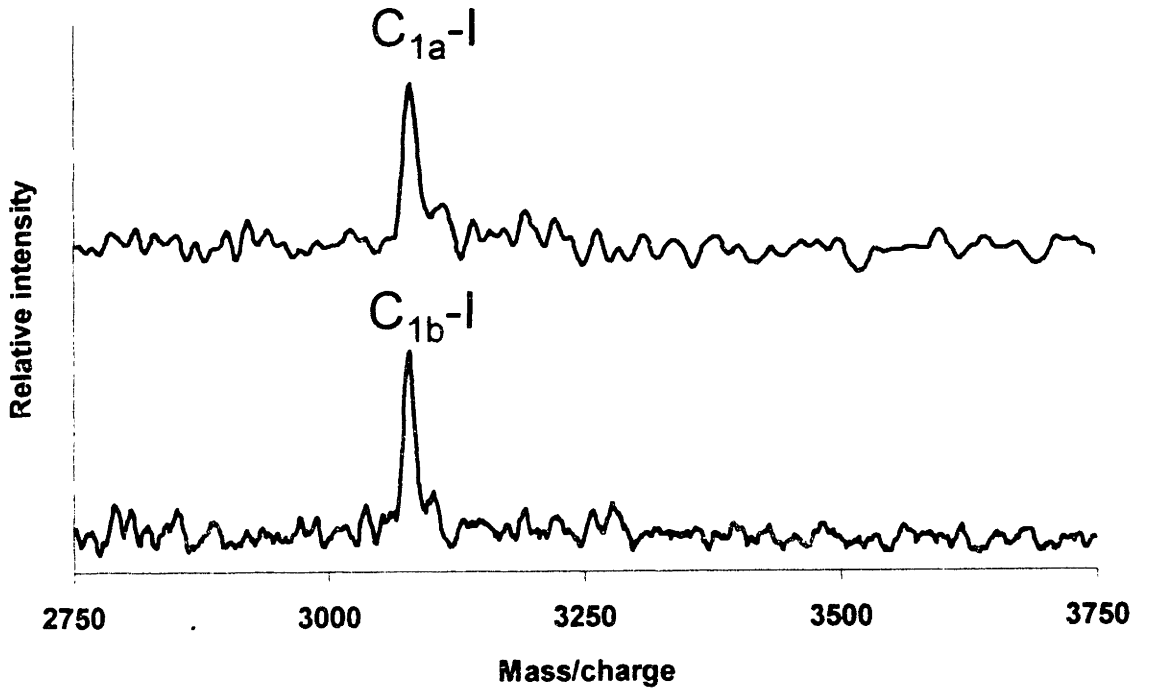

Figure 4.18: Monosialo isomers treated with galactosidase and N-acetylhexoaminidase

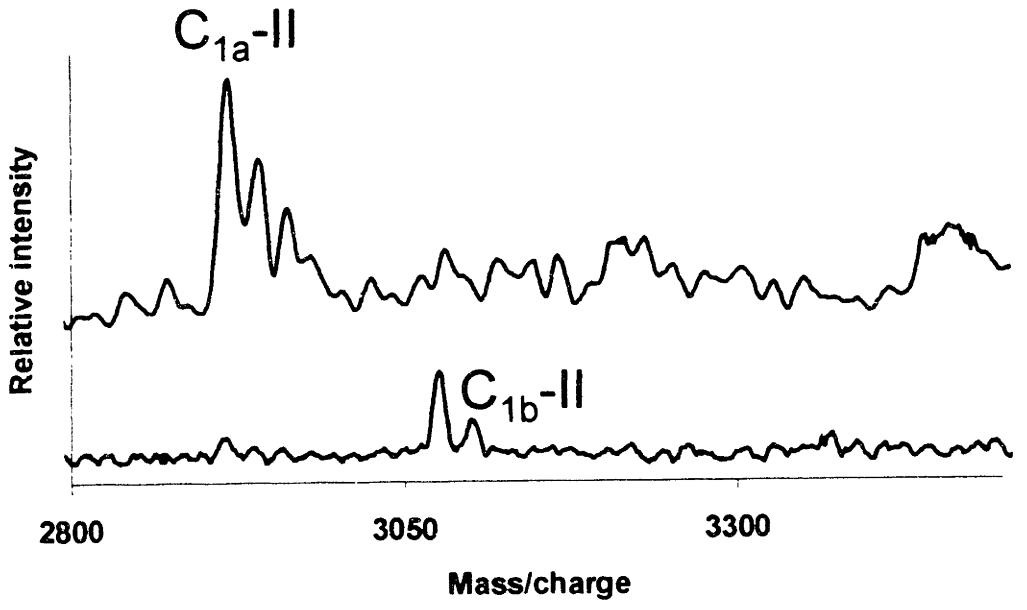

Figure 4.19: Monosialo isomers treated with galactosidase, N-acetylhexoaminidase and mannosidase.

mixture while the β-galactosidase/β-N-acetylhexosaminidase digestion mixture was desalted by reversed-phase HPLC prior to MALDI/TOF analysis. Compared with C_{1b}-II, C_{1a}-II demonstrated a mass shift of 162 Da corresponding to the loss of mannose, as shown in Table 4.7.

Table 4.7: Results of exoglycosidase treatment of mass-degenerate glycopeptides of IFN-γ

Name	Structure	$(M+H)^+$ Mass (Da)
C_{1a}-II	T_{1g}-GlcNAc-GlcNAc-Man (3 1) (6 1)Man-GlcNAc-Gal-NeuAc	2911
C_{1b}-II	T_{1g}-GlcNAc-GlcNAc-Man (3 1)Man-GlcNAc-Gal-NeuAc (6 1)Man	3073

Since the Man cleaved from C_{1a} by branch-specific jack bean α-mannosidase was on the Man(α1-3) branch, the sialic acid must have been present on the Man(α1-6) branch. Furthermore, the lack of cleavage of the α1-3-linked Man of C_{1b}-II indicated that this branch was protected by a sialic acid. As a result, C_{1a} and C_{1b} were identified as the monosialo complex biantennary structures sialylated on the Man(α1-6) and Man(α1-3) branches, as shown in Table 4.8.

Table 4.8: Structures of mass-degenerate glycopeptides of IFN-γ

Name	Structure	$(M+H)^+$ Mass (Da)
C_{1a}	T_{19}-GlcNAc-GlcNAc-Man (3 1)Man-GlcNAc-Gal; (6 1)Man-GlcNAc-Gal-NeuAc	3438
C_{1b}	T_{19}-GlcNAc-GlcNAc-Man (3 1)Man-GlcNAc-Gal-NeuAc; (6 1)Man-GlcNAc-Gal	3438

Since complex biantennary structures represented the majority of oligosaccharides at each glycosylation site, sialylation percentage was calculated for each glycosylation site based upon the occupancy of the available sialylation sites of biantennary glycans:

$$\text{sialylation percentage} = \frac{2A_{C2} + A_{C1a} + A_{C1b}}{2(A_{C2} + A_{C1a} + A_{C1b} + A_{C0})} \times 100\%$$

where A_n is the integrated peak area of fraction n from the neutral pH/borate complexation reversed-phase HPLC chromatogram. Using this definition, the complex biantennary glycans of Asn^{25} were calculated to be 80% sialylated while those of Asn^{97} were 70% sialylated following 168 h of cultivation. Since each glycosylation site would be expected to have similar availability of nucleotide sugar precursors, this site-specific difference in sialylation was most likely the result of differences in sialyltransferase activity due to local environmental effects. This finding is consistent with other previously-reported site-specific differences in the glycosylation of CHO-derived IFN-γ, including greater site occupancy of the Asn^{25} site (Rinderknecht *et al.*, 1984), higher average antennarity of Asn^{25}-linked

oligosaccharides than those of Asn^{97} (James *et al.*, 1995; Harmon *et al.*, 1996), and site-specific fucosylation of the glycans of Asn^{25} (James *et al.*, 1995). Each of these observations suggest that the Asn^{25} site offers a greater accessibility to the various enzymatic processes involved in glycosylation. This greater accessibility of the Asn^{25} site could be explained by the NMR data of Grzesiek and coworkers (1992) for *E. coli*-derived human IFN-γ, which indicated that Asn^{25} is contained within a loop region of high flexibility while Asn^{97} is the final residue of an α-helical region. Such site-specific differences in sialylation have been observed for other glycoproteins. For example, Sasaki *et al.* (1988) have reported that the Asn^{24}-linked oligosaccharides of recombinant human erythropoietin are much less sialylated than those at Asn^{38} despite their proximity.

The ability to separate the isomeric monosialo biantennary structures allowed the sialylation percentage of each branch to be calculated separately:

$$\text{sialylation percentage of Man}(\alpha 1\text{-}3)\text{ branch} = \frac{A_{C2} + A_{C1b}}{A_{C2} + A_{C1a} + A_{C1b} + A_{C0}} \times 100\%$$

$$\text{sialylation percentage of Man}(\alpha 1\text{-}6)\text{ branch} = \frac{A_{C2} + A_{C1a}}{A_{C2} + A_{C1a} + A_{C1b} + A_{C0}} \times 100\%$$

At each glycosylation site, the Man(α1-3) branch was more favorably sialylated than the Man(α1-6) arm. Approximately 85% and 78% of Man(α1-3) branches were sialylated at the Asn^{25} and Asn^{97} sites, respectively, while 74% and 61% of Man(α1-6) arms contained sialic acid at the Asn^{25} and Asn^{97} sites, respectively,

at 168 h of cultivation. This finding was in agreement with the ^{1}H-NMR data of Mutsaers *et al.* (1986), which indicated that the Man(α1-3) branch of CHO-derived IFN-γ was more heavily sialylated than the Man(α1-6) arm. Although α2-3-sialyltransferase from CHO cells has not been studied extensively, preferential sialylation of the Man(α1-3) arm has been previously reported for α2-6-sialyltransferases (Grabenhorst *et al.*, 1995; Joziasse *et al.*, 1985; van den Eijnden *et al.*, 1980). Since the Man(α1-3) branch exhibits a rigid exposed orientation with respect to the Man(β1-4)GlcNAc(β1-4)GlcNAc portion of the core while the Man(α1-6) arm possesses greater flexibility with a most stable conformation in which it folds back to the core, Joziasse *et al.* (1985) have suggested that this branch specificity could be related to a lower accessibility of Gal on the Man(α1-6) branch sterically hindering sialyltransferase activity.

Due to the approximately 1-h exposure of the acid-labile glycosidic linkages of sialic acid to low pH during the initial reversed-phase HPLC fractionations of the tryptic peptides, the potential loss of sialic acid during this step was examined. The glycopeptides were incubated in 0.1% TFA for an additional 4 hours prior to neutralization and analysis by the neutral pH/borate complexation reversed-phase HPLC method. Less than 2% losses in sialylation for each site and branch were observed relative to glycopeptide fractions that did not undergo extended acidic exposure. This finding was similar to the report by Rohrer *et al.* (1993) of less than 3% loss of sialic acid from fetuin tryptic digests during 1 h exposures to 0.1% TFA. Thus, the incomplete sialylation and site- and branch-specific sialylation differences observed for IFN-γ were not artifacts of the

analytical method. A limitation of the neutral pH/borate complexation reversed-phase HPLC method was the inability to distinguish the sialic acid linkages. Two distinct sialic acid linkages, NeuAc(α2-3)Gal and NeuAc(α2-6)Gal, have been identified in N-linked glycoproteins purified from cultured human cell lines (Takeuchi *et al.*, 1988). Since only NeuAc(α2-3)Gal linkages have been observed in N-linked oligosaccharides of glycoproteins derived from CHO culture (Takeuchi *et al.*, 1988; Parekh, *et al.* 1989), this limitation was not of significance for the analysis of CHO-derived IFN-γ.

Based upon data obtained prior to loss of cell viability, both site- and branch-specific differences in intracellular sialylation of CHO-derived human IFN-γ have been observed. The glycans of Asn^{25} were found to be more heavily sialylated than those of Asn^{97}, and Man(α1-3) branches of the predominant complex biantennary glycans were more favorably sialylated than Man(α1-6) arms at each site. The wide variability in sialylation of the sites and branches indicated that intracellular sialylation was highly dependent upon local environments. As a result, in attempting to optimize sialic acid content of recombinant glycoprotein products (*e.g.*, by increasing the availability of nucleotide sugar precursors or sialyltransferase activities), such physical constraints inherent in the conformations of specific glycoproteins may limit the maximal sialylation which can be achieved.

The analytical scheme presented allows for rapid (~3 h) and sensitive (~0.5 μg of product) determinations of glycosylation macroheterogeneity and site-specific microheterogeneity of recombinant human IFN-γ derived from CHO

cell culture. As a result, this methodology can be utilized to assess glycosylation patterns throughout cell culture as well as to rapidly evaluate effects of altering cell culture conditions. Although the MEKC methodology for determination of site occupancy is likely specific to IFN-γ, the general strategy described for determination of glycosylation microheterogeneity should be applicable to monitoring of other recombinant glycoproteins provided that an appropriate antibody is available for immunoaffinity chromatography and potential glycosylation sites can be isolated by proteolysis. This developed analytical scheme will be utilized throughout this thesis to understand and improve IFN-γ glycosylation in CHO cell culture.

CHAPTER FIVE: THE INFLUENCE OF CELL CULTURE CONDITIONS ON IFN-γ GLYCOSYLATION

The glycosylation pattern of recombinant protein can be dependent upon cell culture conditions, including the culture medium composition, physical parameters during cultivation and the degradation of the glycoprotein resulted from cell lysis. This part of the literature was reviewed in Chapter Two. In this chapter, only two aspects of the culture conditions would be reported using the analytical methodology developed in Chapter Four. These are changes of product glycosylation pattern throughout the culture process and the negative impact of Primatone RL on product sialylation.

5.1 Changes of glycosylation pattern throughout culture process

An advantage of the analytical methodology presented in Chapter Four was its sensitivity. Product glycosylation pattern could be obtained from as little as 0.5 μg of IFN-γ. Due to these small sample requirements, glycosylation could be monitored throughout a single batch culture without introducing the additional uncertainty inherent in the use of parallel cultures for single time points. Figure 5.1 shows IFN-γ concentrations and viable cell densities for a 100-ml suspension batch CHO cell culture performed in a spinner flask using Gibco CHO-SFM-II serum-free medium. Maximum viable cell density of 1.8×10^6 cells ml^{-1} was obtained at 72 h and declined rapidly thereafter while IFN-γ concentration reached its maximum titer at about day five and subsequently remained relatively

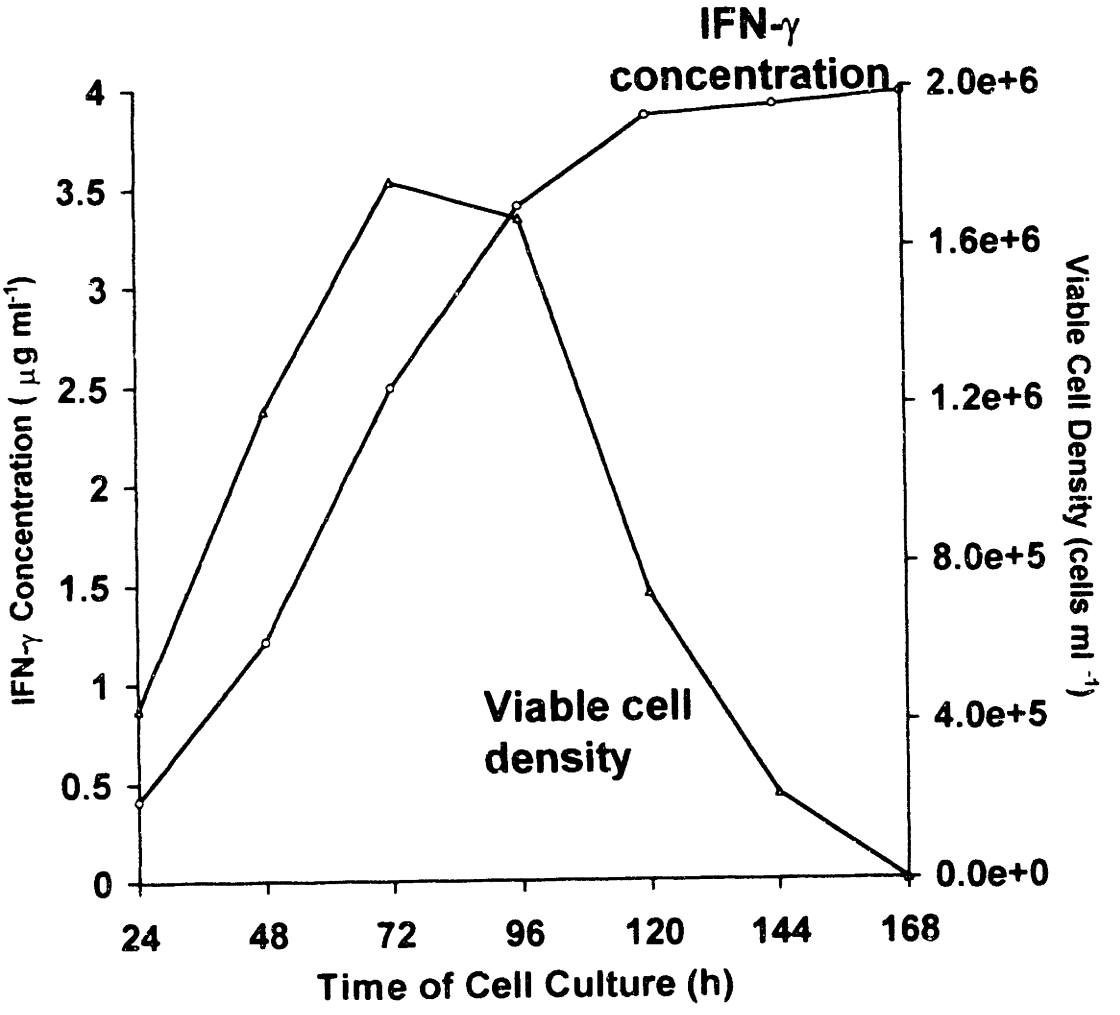

Figure 5.1: Viable cell density and IFN-γ concentration in a suspension batch CHO cell culture.

constant. One mL aliquotes of supernatant collected at 24-h intervals from this batch were analyzed using the previously described methodologies. The distribution of IFN-γ site-occupancy throughout this batch was analyzed by MEKC and presented in Figure 5.2. The macroheterogeneity remained relatively unchanged in the early stage of culture in spite of a small increase in the less glycosylated species during the first 144 hours of culture. However, during the next 24 hours, a slight increase in the proportion of two-site glycosylated IFN-γ was observed. This change appeared to be caused by a greater rate of degradation of the one-site and non-glycosylated IFN-γ compared to the two-site glycosylated. For microheterogeneity changes in IFN-γ glycosylation, the relative proportions of bi-, tri-, and tetraantennary oligosaccharide structures determined by MALDI/TOF analysis of the site-specific pools of glycopeptides following desialylation did not change significantly at either site during the course of the culture, as shown in Figure 5.3. No significant accumulations of other oligosaccharide structures were detected. This finding was in contrast to the report of Hooker and coworkers (1995), who, using similar analytical techniques, observed the accumulation of oligomannose and truncated glycans for IFN-γ during batch CHO cell cultures.

In Figure 5.4, the percentage sialylation of the complex biantennary glycans at each glycosylation site throughout the culture is presented. Sialylation was incomplete but relatively constant during the early stages of batch culture (*i.e.*, approximately 92% and 79% at Asn^{25} and Asn^{97}, respectively). However, after 96 h, a steady decrease in sialylation was observed at each glycosylation

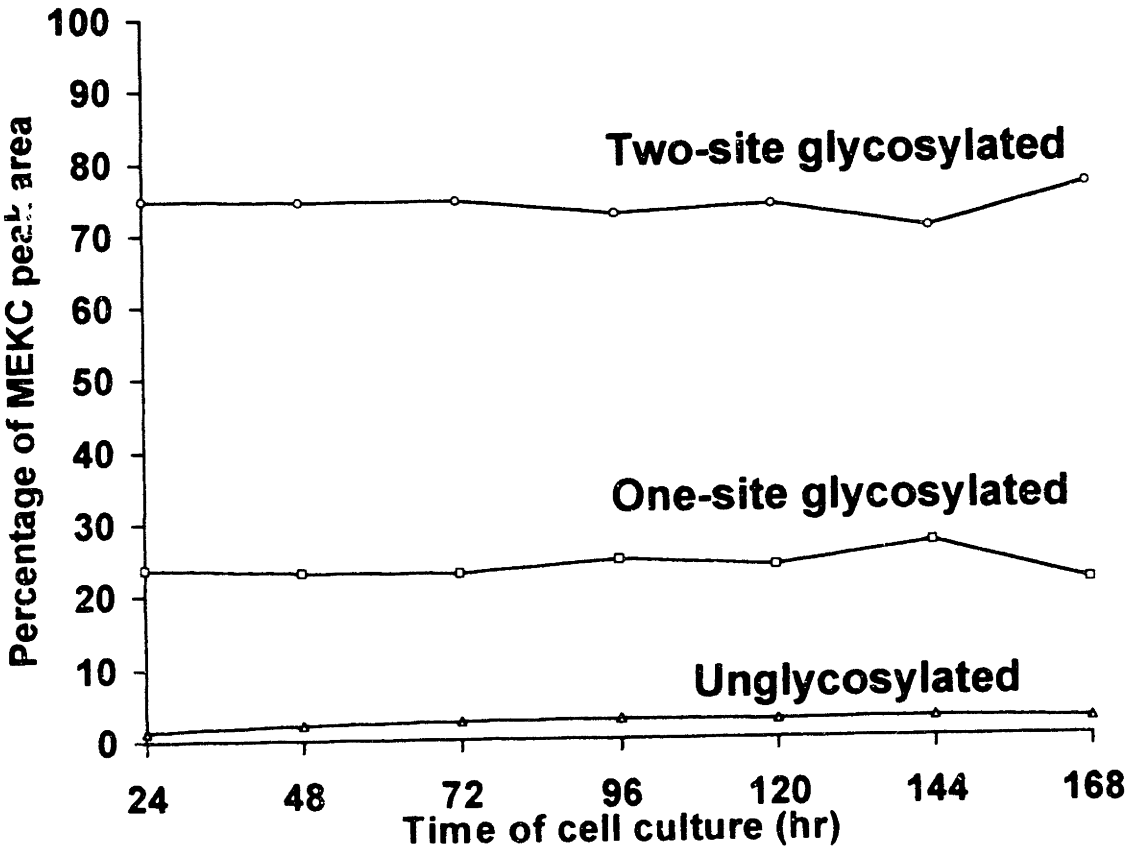

Figure 5.2: Monitoring of interferon-γ macroheterogeneity in CHO batch culture

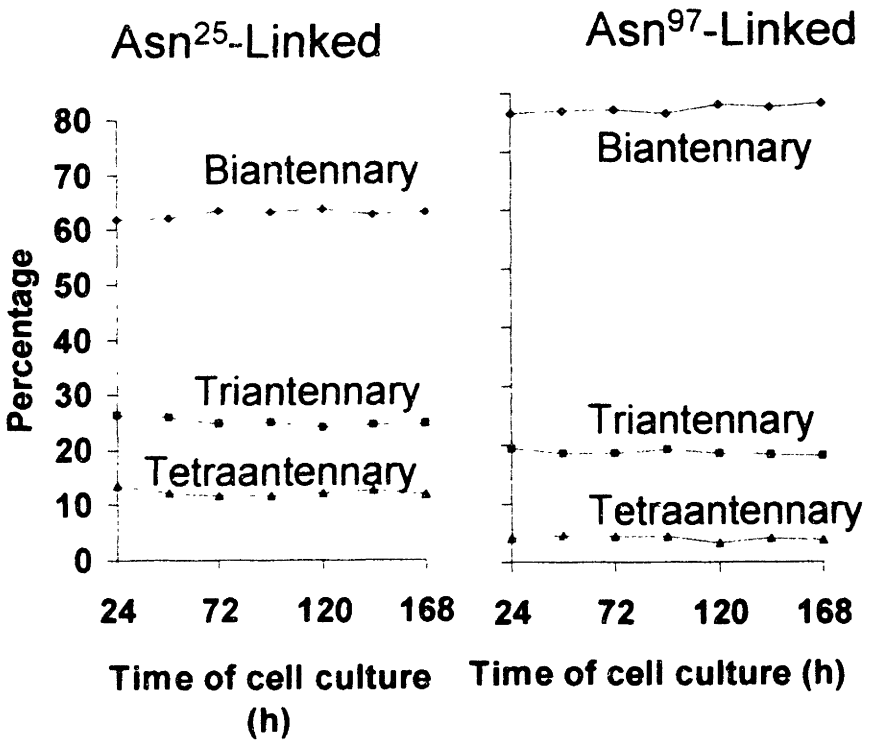

Figure 5.3: Antennarity of CHO-derived interferon-γ during batch culture

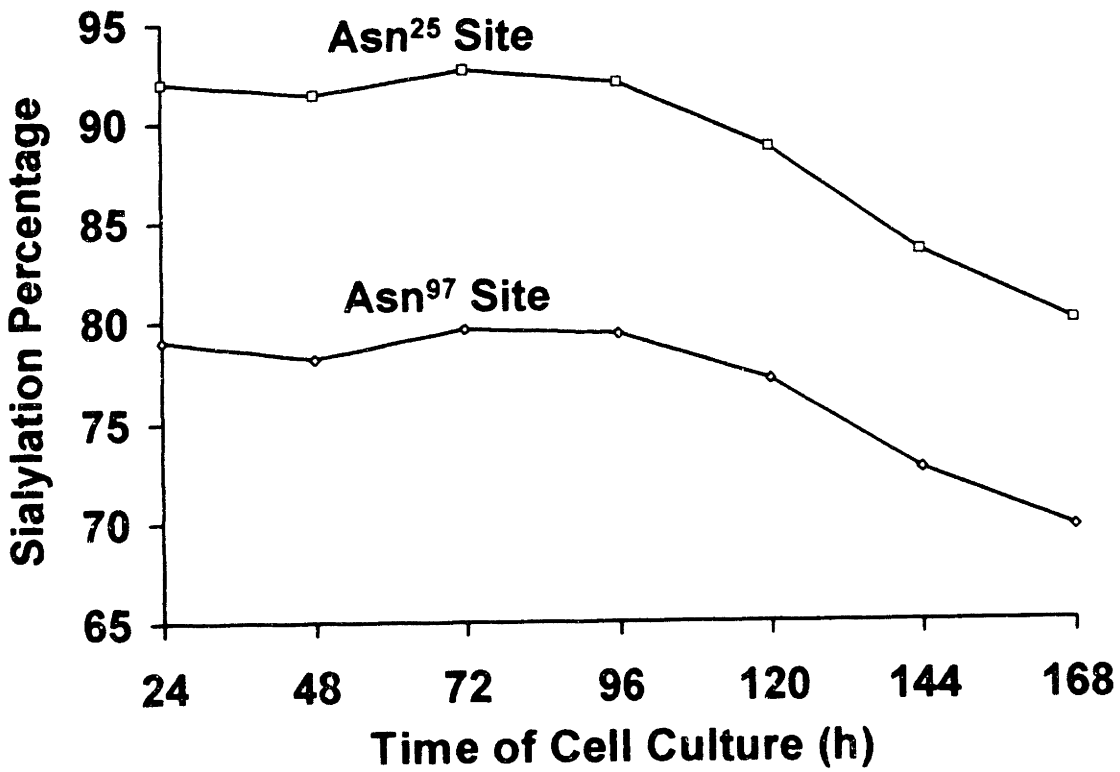

Figure 5.4: Effect of culture time on site-specific sialylation of complex biantennary glycans of IFN-γ in a suspension batch CHO cell culture.

site with sialylation percentages of 80% and 70% at Asn^{25} and Asn^{97}, respectively, observed at 168 h. The loss of sialic acid content coincided with the observed decrease in viable cell density. Warner *et al.* (1993) have previously reported the isolation of an extracellular sialidase from CHO culture capable of desialylating exogenously-added glycoproteins, and Gramer *et al.* (1995) have observed a substantial increase in extracellular sialidase activity in CHO cell culture following loss of cell viability. These reports suggested that the observed decline in sialylation of IFN-γ may have been caused by extracellular sialidase released from lysed cells following cell death. Furthermore, since there was minimal biosynthesis of IFN-γ from 120 to 168 h, the observed decline in sialylation could not be attributed to the synthesis of poorly sialylated IFN-γ.

In order to verify that the observed decrease in sialic acid content following cell death was due to extracellular sialidase activity, a similar suspension batch CHO cell culture was performed in which 1 m*M* 2,3-dehydro-2-deoxy-*N*-acetylneuraminic acid (2,3-D) was introduced into the culture supernatant on day 4. An analogue of sialic acid, 2,3-D has been shown to competitively inhibit (K_i of 0.025 m*M*) the activity of sialidase derived from CHO culture supernatant (Gramer *et al.*, 1995). Figure 5.5 shows the site-specific sialylation percentages during days 4 to 7 for the culture performed with 2,3-D. The introduction of sialidase inhibitor prevented loss of sialic acid following cell death as sialylation percentage remained essentially unchanged during the remainder of the culture. This finding confirmed that the decline in sialic acid content for the culture without 2,3-D addition was due to extracellular sialidase

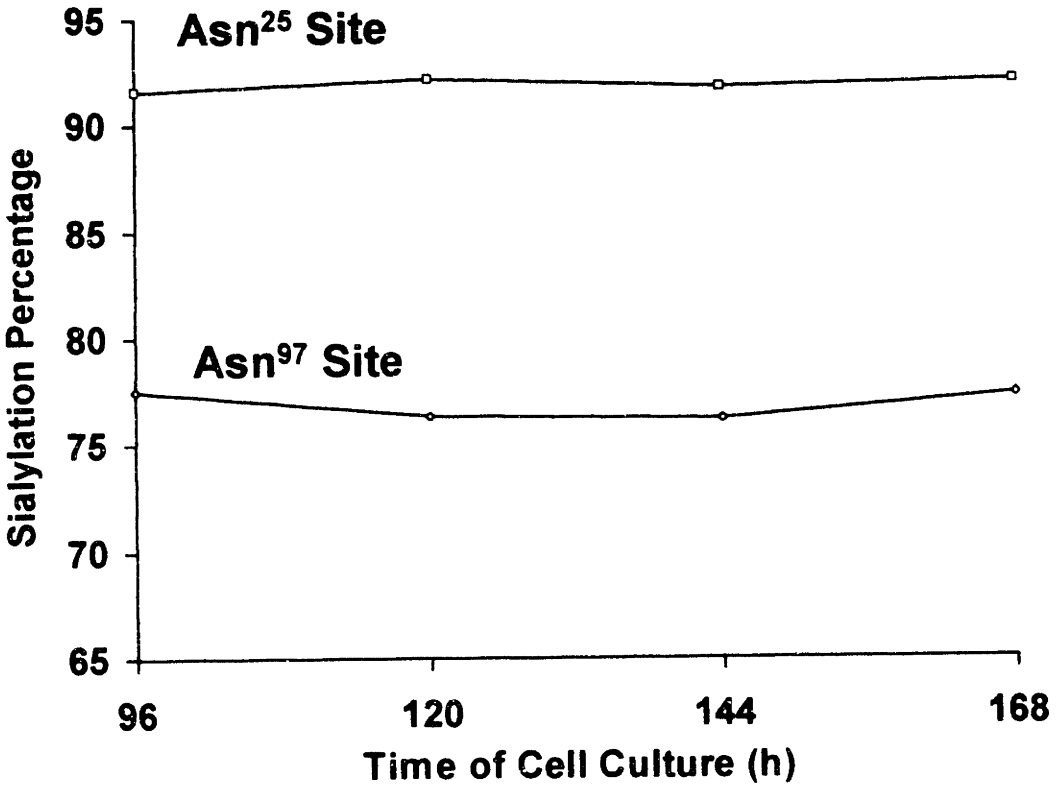

Figure 5.5: Effect of sialidase inhibitor 2,3-dehydro-2-deoxy-N-acetylneuraminic acid on site-specific sialylation of complex biantennary glycans of IFN-γ in a suspension batch CHO cell culture.

presumably released during cell lysis. An approximately 12% decrease in sialylation of both Asn^{25}- and Asn^{97}-linked biantennary glycans was observed between days 4 and 7 for the culture lacking 2,3-D, thus indicating that, although there was preferential sialylation of the glycans of Asn^{25}, extracellular desialylation did not significantly discriminate between the glycosylation sites. A similar 12% loss of sialic acid has been previously reported for a 6-day incubation of gp120 glycoprotein exogenously added to a batch CHO cell culture (Gramer *et al.*, 1995). The lack of significant accumulation of truncated oligosaccharide structures during the culture indicated that there was no significant activity of glycosidases other than sialidase.

While the loss in sialylation following cell death could be attributed to extracellular sialidase activity, incomplete sialylation was observed at each glycosylation site prior to cell lysis. Work by Gramer *et al.* (1995) has indicated that secretion of lysosomal sialidase does not contribute significantly to the accumulation of extracellular sialidase activity in CHO culture. As a result, the release of cytosolic sialidase resulting from damage to the cellular membrane is likely the predominant mechanism for extracellular sialidase activity, and lack of sialylation prior to cell lysis is expected to result from intracellular processes. To verify that incomplete sialylation observed for CHO-derived IFN-γ in the early stages of the cultivation was not due to extracellular desialylation, a culture was performed in which 2,3-D was added to the supernatant at cell inoculation. The sialylation percentages at day 4 for this culture (*i.e.*, 92% and 80% for Asn^{25}- and Asn^{97}-linked glycans, respectively) were nearly identical to those obtained without

sialidase inhibitor. This result confirmed that the incomplete sialylation observed prior to loss of cell viability was a result of incomplete intracellular sialylation rather than extracellular desialylation. Based on these results, it cannot be stated whether the observed incomplete intracellular sialylation was due to incomplete biosynthetic sialylation or intracellular degradation of more fully sialylated product. However, since intracellular IFN-γ is expected to be either in the Golgi complex or within secretory vesicles with minimal exposure to cytosolic sialidase, incomplete synthetic sialylation is suspected to be predominantly responsible for incomplete intracellular sialylation.

Figure 5.6 shows the branch-specific sialylation of the complex biantennary glycans of IFN-γ at each glycosylation site during the suspension batch CHO cell culture. Prior to loss of cell viability, the sialylation of each branch was relatively constant (*i*.e., approximately 98% and 91% sialylation of Man(α1-3) and 86% and 67% sialylation of Man(α1-6) branches at Asn^{25} and Asn^{97}, respectively). Following cell lysis, sialylation of each arm declined steadily at each glycosylation site, thus indicating that both branches were vulnerable to extracellular sialidase activity. In observing the various glycosylation sites and branches, the wide range of values for intracellular sialylation and the similar susceptibilities to extracellular desialylation suggest either that 1) the predominant cause for incomplete intracellular sialylation was incomplete biosynthetic sialylation arising from variances in steric accessibility for sialyltransferase or 2) intracellular desialylation proceeded by a different mechanism than extracellular desialylation.

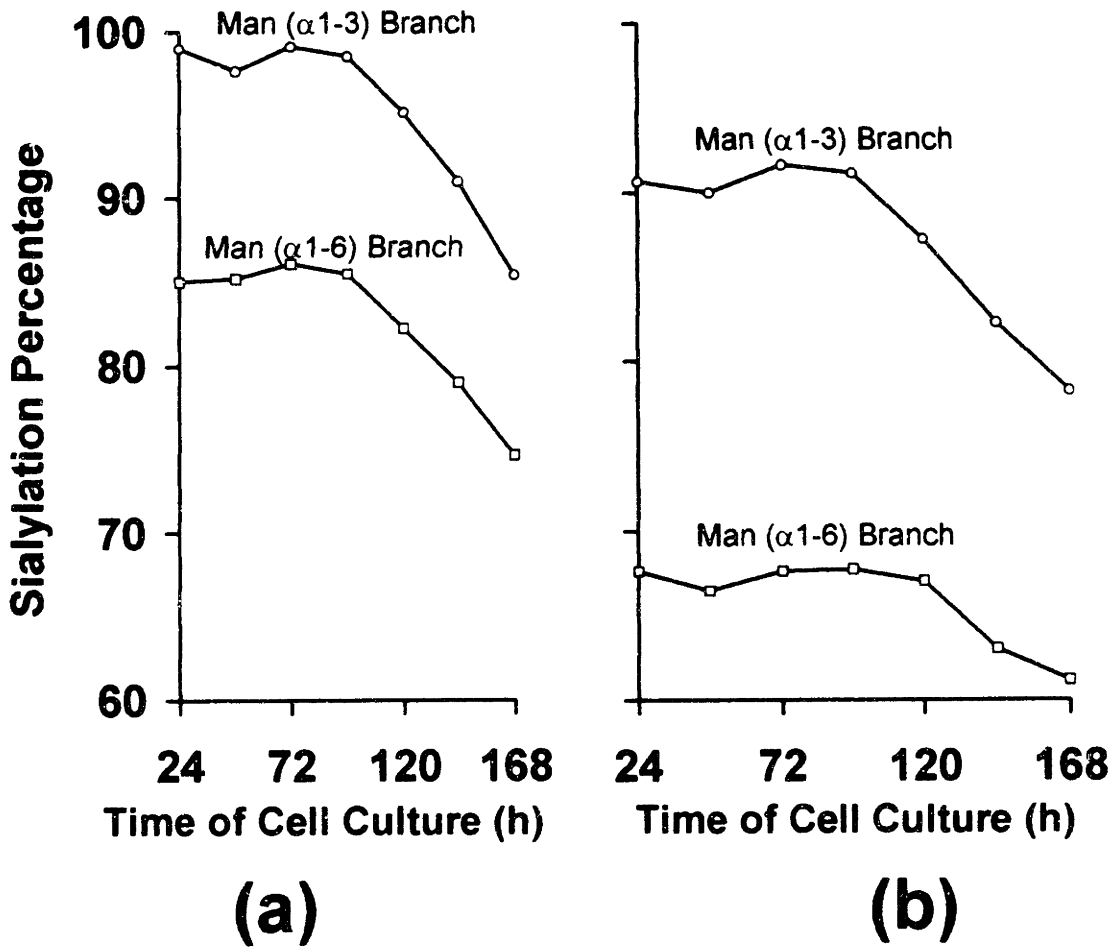

Figure 5.6: Effect of culture time on branch-specific sialylation of (a) Asn^{25}- and (b) Asn^{97}-linked complex biantennary glycans of IFN-γ in a suspension batch CHO cell culture.

During the cultivation of a suspension batch CHO cell culture, extracellular desialylation of IFN-γ was observed following cell lysis. The oligosaccharides at each glycosylation site as well as each branch of the predominant complex biantennary glycans were found to be susceptible to extracellular desialylation. As a result, both intracellular and extracellular processes defined the sialic acid content of the final product. Although most batch cultures performed in industry are terminated prior to massive cell death and its desialylating effects, significant accumulation of extracellular sialidase during the course of extended cultures (*e.g.*, fed-batch cultures) may also yield undesired desialylation of glycoprotein products.

5.2 Influence of medium composition on sialylation of recombinant human interferon-γ in Chinese hamster ovary cell culture

Serum has been extensively used as a supplement to chemically-defined media for mammalian cell culture due to its multiple functions. In addition to providing many nutritional ingredients such as amino acids, enzymes, hormones, vitamins, and cofactors required for cell proliferation and growth as well as cell attachment and spreading, serum provides buffering capacity and protects cells from physical stress (Taylor, 1974). However, there are many negative aspects associated with the use of serum in the production of therapeutic proteins. The biological activity of serum varies greatly from lot to lot; and the high cost of serum makes it often impractical for scale-up. Furthermore, serum often contains many contaminant compounds that make downstream purification processes

difficult, and serum is susceptible to contamination by mycoplasma and adventitious viruses. As a result, much effort has been made in the past several years in the identification of serum-substitutes for the development of serum-free media.

Many serum substitutes have been investigated for their biological adequate equivalences. Fractions containing growth factors and other biological active components have been isolated from serum and supplemented the chemically defined medium. Likewise, synthetic polymers such as dextran and Pluronic F68 are also commonly added in serum-free medium as protective agents. Furthermore, peptone, which is derived from acid and enzymatic hydrolysates of animal tissue and contains undefined mixture of low-molecular components, including amino acids, peptides, vitamins and trace elements, has been found to contain mitotic-stimulating components and have a tremendous impact on cell proliferation. Consequently peptone has frequently been added to mammalian cell cultures. For instance, bacto-peptone, a heat stable enzymatic digest of animal tissue, has been widely used as serum substitute in mammalian culture medium (Pumper *et al.*, 1965) for various cell lines. Primatone RL, a protein-free enzymatic meat hydrolysate mainly consisting of amino acids and peptides, has also shown a significant growth promoting effect (Mizrahi, 1977; Schlaeger and Schumpp, 1992). The studies on chemical nature of peptone was derived from a low-molecular-weight peptide(s). However, while in recent years a great deal attention has been given to the cell growth and titer expression in serum-free medium, the impact of serum substitute on the quality of the

recombinant proteins and in the case of glycoproteins, the homogeneity in glycosylation of protein, has not been intensively investigated. Teige *et al.* (1994) reported that antithrombin III (AT-III) produced by recombinant BHK-21 cell line cultivated in serum-free medium had a higher level of proteolytic-digested forms as well as non-glycosylated forms compared with those from serum-containing cultivation.

However, for the production of therapeutic proteins, the effects of serum-substitutes on product quality is a major factor which should be investigated. For therapeutic glycoproteins, a critical quality criterion is sialylation because the presence of sialic acid can often play an important role in the biological and physical properties of a glycoprotein

5.2.1 Sialylation of IFN-γ from batch CHO culture using different serum-free media

To assess the effects of various serum-free media on the sialylation of IFN-γ derived from batch CHO culture, the cell line was first adapted to two different commercial serum-free media, SFM-CHO-II (Gibco) and PF-CHO (JRH Bioscience). Both media were supplemented with 2.5×10^{-7} *M* methotrexate (selection agent), 10 units ml^{-1} penicillin, and 10 mg ml^{-1} streptomycin. The CHO-SFM-II medium supported cell growth without further supplementation, but 2 g l^{-1} Primatone RL was added to the protein-free PF-CHO medium in order to promote cell growth. As seen in Table 5.1, which lists the viable cell densities, cell viabilities, and IFN-γ concentrations at 96 h for three replicate batch cultures utilizing SFM-CHO-II and two replicate batch cultures employing PF-CHO, the

Table 5.1- Effect of two serum-free media on cell growth, product titer, and product sialylation (96-h batch CHO culture)

Serum-Free Medium	Cell Density (cells ml^{-1})	Cell Viability (%)	IFN-γ Concentration ($\mu g\ ml^{-1}$)	Sialylation Indices	
				Glycans of Asn^{25}	Glycans of Asn^{97}
SFM-CHO-II	$2.0x10^6$	97	3.7	7.0	2.7
SFM-CHO-II	$2.2x10^6$	98	4.0	7.1	2.7
SFM-CGO-II	$1.9x10^6$	95	3.6	7.0	2.6
PF-CHO	$1.8x10^6$	97	3.2	4.5	1.4
PF-CHO	$2.1x10^6$	97	3.5	4.4	1.4

two serum-free media yielded similar cell growth and product titers. The sialylation of the IFN-γ from each culture was assessed using an analytical methodology for the determination of site- and branch-specific sialylation of IFN-γ described in Chapter Four. Briefly, IFN-γ was purified from culture supernatant by immunoaffinity chromatography and subjected to trypsinization. The two pools of glycopeptides representing the potential glycosylation sites were then isolated by low-pH reversed-phase HPLC, and sialic acid-based separations of these site-specific populations of glycopeptides were obtained by neutral-pH/borate-complexation reversed-phase HPLC. It was observed that sialylation of IFN-γ was relatively constant during batch CHO culture prior to loss of cell viability. However, steady decreases in sialylation were observed following cell lysis due to extracellular sialidase activity (Warner *et al.*, 1993; Gramer *et al*, 1995). The introduction of a competitive inhibitor of sialidase into the culture supernant prevented the loss of sialic acid after the onset of cell death but did not affect sialylation prior to cell death. This finding indicated that incomplete sialylation

prior to loss of cell viability could be attributed to incomplete intracellular sialylation while the reduction in sialylation following loss of cell viability was due to extracellular sialidase activity resulting from cell lysis. Consequently, in order to compare intracellular sialylation of IFN-γ using the two serum-free media without introducing the effects of extracellular desialylation, the batch cultures were terminated, and IFN-γ determinations and sialylation analyses were performed at 96 h prior to significant loss of cell viability. As shown in Table 5.1, the viabilities of each of the cultures were close to 100% at the time of product harvest.

Figures 5.7 and 5.8 show the site-specific sialylation profiles (*i.e.*, neutral-pH/borate-complexation reversed-phase HPLC chromatograms of the site-specific pools of tryptic glycopeptides) for IFN-γ obtained from batch cultures employing CHO-SFM-II and PF-CHO, respectively. C_0, C_{1a}, C_{1b}, and C_2 indicate glycopeptides possessing asialo, monosialo (sialic acid on Man(α1-6) branch), monosialo (sialic acid on Man(α1-3) branch), and bisialo complex biantennary structures, respectively, as identified by matrix-assisted laser-desorption ionization/time-of-flight mass spectrometry and linkage-specific exoglycosidase digestion. Peaks B_2 and B_3 represent complex triantennary structures with two and three sialic acids, respectively, while A_3 and A_4 indicate complex tetraantennary structures containing three and four sialic acids, respectively. Each of the identified glycans of Asn^{25} were fucosylated while those of Asn^{97} were not. Since complex biantennary structures were the dominant oligosaccharides at each glycosylation site, and the distribution of bi-, tri-, and

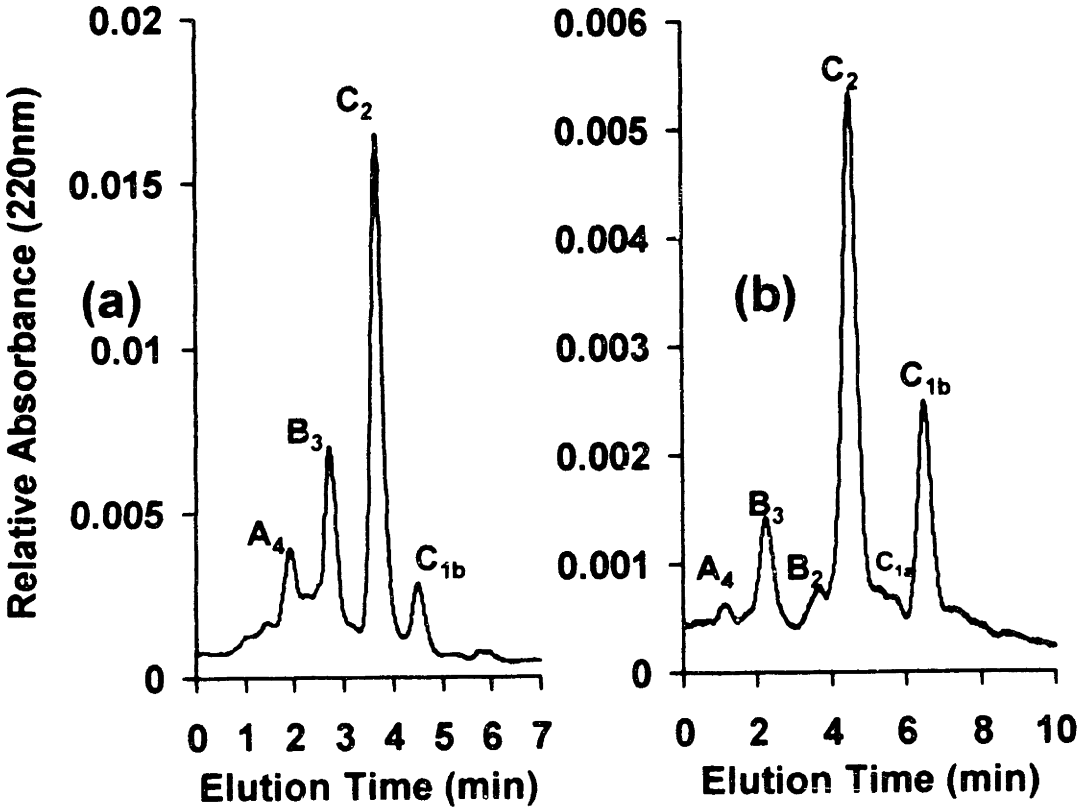

Figure 5.7: Neutral-pH/borate-complexation reversed-phase HPLC separations of (a) Asn^{25}- and (b) Asn^{97}-linked IFN-γ tryptic glycopeptides following 96 h of suspension batch CHO culture using SFM-CHO-II medium (Gibco). A_4 indicate complex tetraantennary glycans with 4 sialic acids; B_2 and B_3 represent complex triantennary glycans with 3 and 2 sialic acids, respectively; C_{1a}, C_{1b}, and C_2 correspond to complex biantennary glycans with 1 (on Man(α1-6) branch), 1 (on Man(α1-3) branch), and 2 sialic acids, respectively.

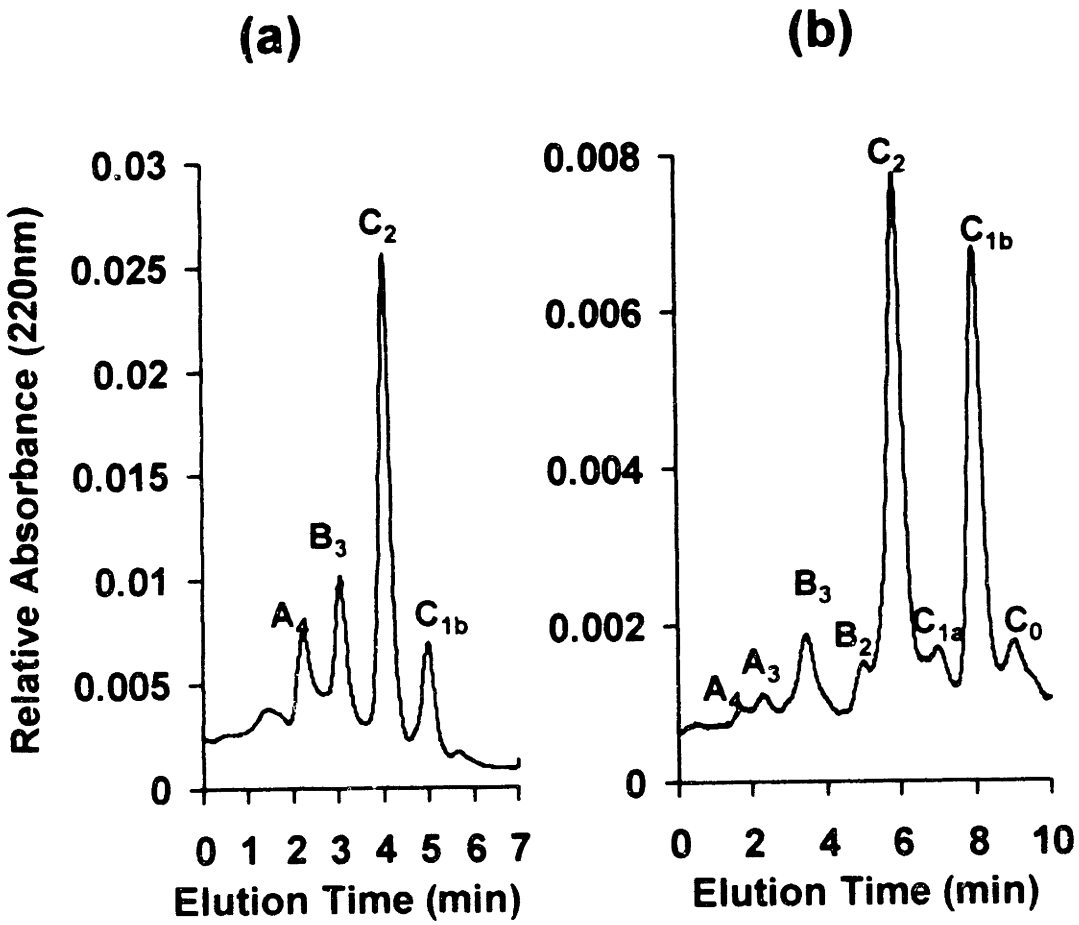

Figure 5.8: Neutral-pH/borate-complexation reversed-phase HPLC separations of (a) Asn^{25}- and (b) Asn^{97}-linked IFN-γ tryptic glycopeptides following 96 h of suspension batch CHO culture using PF-CHO medium (JRH Bioscience). A_3 and A_4 indicate complex tetraantennary glycans with 3 and 4 sialic acids, respectively; B_2 and B_3 represent complex triantennary glycans with 3 and 2 sialic acids, respectively; C_0, C_{1a}, C_{1b}, and C_2 correspond to complex biantennary glycans with 0, 1 (on Man(α1-6) branch), 1 (on Man(α1-3) branch), and 2 sialic acids, respectively.

tetraantennary structures remains relatively unchanged throughout batch CHO culture, only sialylation of the complex biantennary glycans is considered here.

Figures 5 7 and 5.8 indicate that the glycans of Asn^{25} were more heavily sialylated than those of Asn^{97} for both serum-free media. Figures 5.7 and 5.8 also show that the Man(α1-3) branches of the predominant complex biantennary glycans were more highly sialylated than the Man(α1-6) arms at each glycosylation site for both serum-free media. These findings are in agreement with our previous observation of preferential sialylation of Asn^{25}-linked glycans and the Man(α1-3) branch at each glycosylation site of CHO-derived IFN-γ. Since both serum-free batches were terminated prior to significant loss of cell viability and the resultant lack of extracellular desialylation, the contributions of Man(α1-6) branch-linked monosialo and asialo complex biantennary structures were negligible. Thus, sialylation was quantitatively evaluated by calculating the relative proportion of the two predominant structures, bisialo and Man(α1-3) branch-linked monosialo complex biantennary structures. This parameter, termed sialylation index, was calculated as the peak area ratio of C_2 to C_{1b}. As listed in Table 5.1, IFN-γ derived from the batch CHO cultures using SFM-CHO-II medium displayed sialylation indices of 7.0 to 7.1 for Asn^{25} and 2.6 to 2.7 for Asn^{97}. However, IFN-γ produced by the batch CHO cultures employing PF-CHO medium supplemented with 2 g l^{-1} Primatone RL displayed lower sialic acid content with sialylation indices of 4.4 to 4.5 for Asn^{25} and 1.4 for Asn^{97}.

Although the compositions of each of these commercial serum-free media

are proprietary, one major difference in the testing of these two media was the supplementation of PF-CHO with Primatone RL in order to support cell growth. Rather than include any animal tissue hydrolysates in its formulation, SFM-CHO-II utilizes various unspecified serum fractions to promote cell growth (Stephen F. Gorfien, Life Technologies, personal communication). The notable difference in sialylation of IFN-γ derived from the two serum-free media suggests that the use of Primatone RL might have an adverse effect on product sialylation, which could have been the result of either direct desialylation of IFN-γ by undefined components of the peptone or a secondary effect of Primatone RL upon the intracellular mechanisms of sialylation. In order to evaluate the former possibility, IFN-γ purified from batch culture employing SFM-CHO-II was further incubated for 96 h in acellular PF-CHO medium supplemented with 2 g L^{-1} Primatone RL. The IFN-γ was then purified from the incubation mixture, subjected to sialylation analysis, and compared to the sialylation profiles obtained prior to the incubation. No differences in sialylation indices before and after incubation in Primatone RL-containing medium were observed. This finding precluded the possibility of extracellular desialylation of IFN-γ by components of Primatone RL being the cause of the sialylation differences observed with the two serum-free media.

Unfortunately, the CHO cell line was not able to be adapted to PF-CHO medium without Primatone RL supplementation. As a result, this approach could not be used to confirm the role of the peptone on product sialylation. Alternatively, the effect of Primatone RL on product sialylation was further investigated by supplementing CHO-SFM-II medium with the peptone and

examining whether a concurrent reduction in IFN-γ sialylation occurred Thus, four additional batch CHO cultures containing CHO-SFM-II medium supplemented with 0 02, 0.2, 2, and 20 g l^{-1} Primatone RL were performed The batches were terminated at 96 h of cultivation prior to massive cell death, and supernatant samples were subjected to sialylation analyses as previously described. As shown in Table 5.2, cultures employing 0.02, 0.2,and 2 g l^{-1} Primatone RL each displayed increased cell growth and, consequently, improved product titers relative to the culture without Primatone RL supplementation However, the culture supplemented with 20 g l^{-1} Primatone RL demonstrated diminished cell growth and product yield. This result was in agreement with previous reports (Schlaeger and Schumpp, 1992; Zhang *et al*, 1994; Jan *et al* , 1994) of growth inhibition at peptone concentrations above an optimal concentration for cell growth, typically 2 to 5 g l^{-1}.

As indicated by the sialylation indices listed in Table 5.2 for both the Asn^{25}- and Asn^{97}-linked glycans of IFN-γ, the batch cultures supplemented with low concentrations of the peptone displayed similar sialylation to the nonsupplemented culture. However, slight decreases in sialylation were detected at both glycosylation sites with the optimal Primatone RL concentration for cell growth and product yield (2 g l^{-1}), and markedly poorer sialylation was observed at the growth-inhibiting peptone concentration of 20 g l^{-1}. As seen in Table 5.2, the viabilities of all cultures using CHO-SFM-II containing 0 to 20 g l^{-1} Primatone RL were nearly 100% after 96 h, which suggests that the presence of the peptone did not impact cell lysis, and, thus, the decreased sialylation observed with high

concentrations of Primatone RL cannot be attributed to enhanced desialylation by extracellular sialidase

Table 5.2 - Effect of Primatone RL supplementation on cell growth, product titer, ammonia accumulation, and product sialylation using SFM-CHO-II serum-free medium (96-h batch CHO culture)

Primatone RL Conc. ($g\ l^{-1}$)	Viable Cell Density ($cells\ ml^{-1}$)	Cell Viability (%)	IFN-γ Conc. ($\mu g\ ml^{-1}$)	Ammonia Conc. (*mM*)	Sialylation Indices	
					Glycans of Asn^{25}	Glycans of Asn^{97}
0	$2.0x10^6$	95	3.7	3.1	7.0	2.7
0.02	$2.2x10^6$	97	4 1	3.2	7 1	2 6
0.2	$2.6x10^6$	95	4.3	3.3	7.0	2 6
2	$4.0x10^6$	98	4.9	3 3	6.5	2.2
20	$1.4x10^6$	97	3 4	5.0	5.1	1.2

Increased ammonia levels were also observed with elevated concentrations of Primatone RL, as shown in Table 5.2. Zhang *et al* (1994) have previously reported this correlation between peptone concentration and ammonia accumulation and have suggested elevated ammonia levels as the cause of inhibition of cell growth at high peptone concentration. This accumulation of ammonia can be largely attributed to the utilization of peptone-supplied L-glutamine for cell growth. Although vendor specifications indicate that Primatone RL contains no free L-glutamine, the peptone supplies glutamine-containing peptides. Anderson and Goochee (1995) have also shown that ammonia concentrations as low as 2 m*M* are associated with reduced sialylation of O-linked glycans of granulocyte colony-stimulating factor produced by CHO These two reports suggest that the negative effect of Primatone RL upon sialylation could be the consequence of ammonia accumulation.

To assess the effects of ammonia upon the sialylation of CHO-derived IFN-γ, four additional batch cultures were performed in which 1, 2, 5, and 10 m*M* ammonium chloride were added to the non-Primatone RL-supplemented SFM-CHO-II medium. Determinations of ammonia concentration and sialylation analyses were performed after 96 h of batch culture. As seen in Table 5.3, decreases in sialylation were observed at each glycosylation site as ammonia concentration was increased, in agreement with the results of Anderson and Goochee. However, the reductions in sialylation observed with the supplementation of Primatone RL were significantly greater than those seen with the introduction of comparable levels of ammonia to peptone-free medium. Consequently, the poor sialylation observed with elevated levels of Primatone RL could not be attributed solely to the effects of ammonia accumulation.

Table 5.3 - Effect of ammonia on product sialylation using SFM-CHO-II serum-free medium (96-h batch CHO culture)

Supplemental NH_4Cl Conc. (m*M*)	Final Ammonia Concentration (m*M*)	Sialylation Indices	
		Glycans of Asn^{25}	Glycans of Asn^{97}
0	3.1	7.0	2.7
1	4.0	6.9	2.3
2	4.6	6.9	2.2
5	6.6	6.8	1.9
10	10.7	6.5	1.5

Although diminished sialylation was observed with the addition of 2 g l^{-1} Primatone RL to SFM-CHO-II relative to the nonsupplemented medium, sialylation remained much greater than that observed using PF-CHO supplemented with 2 g l^{-1} Primatone RL. Consequently, other media components

must have also been important, either constituents of PF-CHO which have a detrimental effect or components of SFM-CHO-II which offer a protective effect.

The batch cultures employing PF-CHO and SFM-CHO-II each supplemented with 2 g l^{-1} Primatone RL displayed comparable ammonia concentrations at 96 h (3.5 and 3.3 mM, respectively), and, thus, ammonia accumulation could not account for the difference in sialylation resulting from the use of the two serum-free media.

5.2.2 Sialylation of IFN-γ from fed-batch CHO culture with and without Primatone RL feeding

The impact of Primatone RL on sialylation of CHO-derived IFN-γ was further investigated in extended high cell density cultures using two parallel fed-batch cultures. Both cultures were initiated at a volume of 300 ml with a self-designed protein-free medium supplemented with 2 g l^{-1} Primatone RL (Xie, 1996). In one fed-batch, the feeding medium contained 25 g l^{-1} Primatone RL to compensate for peptone components consumed for cell growth during the course of the culture. In the other fed-batch, Primatone RL was not included in the feeding medium and, consequently, consumption of peptone components required for cell growth was expected. However, the feeding medium for the latter culture was supplemented with additional amino acids to balance the amino acids and peptides supplied by Primatone RL-feeding in the former culture. Based upon the total volumes of supplemental media added, the final Primatone RL concentrations would have been approximately 4 and 1.8 g l^{-1} in the fed-batches fed peptone-supplemental and peptone-free media, respecitively.

assuming no Primatone RL was consumed. As seen in Figure 5.9, which shows cell growth for both fed-batch cultures, no significant differences were observed in terms of growth rate and maximum viable cell density with or without peptone feeding. This observation suggests that 2 g l^{-1} Primatone RL contained in the initial medium was sufficient to achieve high cell density. As shown in Figure 5.10, product concentrations for each fed-batch were also similar prior to the onset of cell death, which indicates that the Primatone RL-feeding had no significant effect on the specific production rate of IFN-γ. However, the total amount of IFN-γ produced in the batch fed Primatone RL was slightly less due its lower viable cell density in the latter stages of culture. Both fed-batch cultures displayed no significant differences in glucose and amino acid concentrations (data not shown). The sialylation indices for the Asn^{25}- and Asn^{97}-linked glycans of IFN-γ for both fed-batches are shown in Figure 5.11. Since both fed-batch cultures had used the same initial medium containing 2 g l^{-1} Primatone RL, sialylation was nearly identical for each fed-batch in the early stages of culture (sialylation indices of approximately 4.5 and 1.25 for the glycans of Asn^{25} and Asn^{97}, respectively, after 24 h). These sialylation indices were very similar to those observed in the batch mode for the PF-CHO medium supplemented with 2 g l^{-1} Primatone RL. Since neither the initial medium for the fed-batch cultures nor PF-CHO contained serum fractions, and both displayed lower sialylation than SFM-CHO-II similarly supplemented with 2 g l^{-1} Primatone RL, it is possible that the serum fractions contained in SFM-CHO-II offer a protective effect. As seen in Figure 5.11, sialylation at both glycosylation sites improved throughout the course

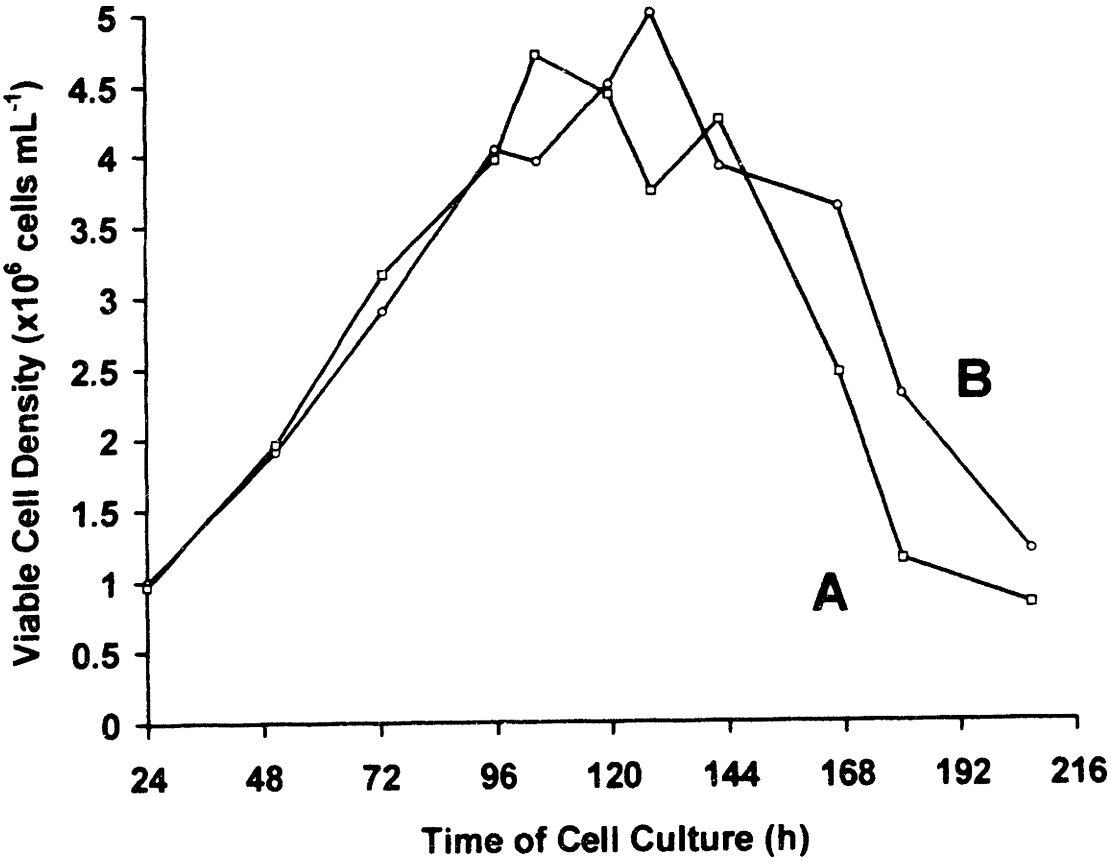

Figure 5.9: Cell growth for fed-batch CHO cultures. A and B indicate cultures utilizing Primatone RL-supplemented and Primatone RL-free feeding media, respectively.

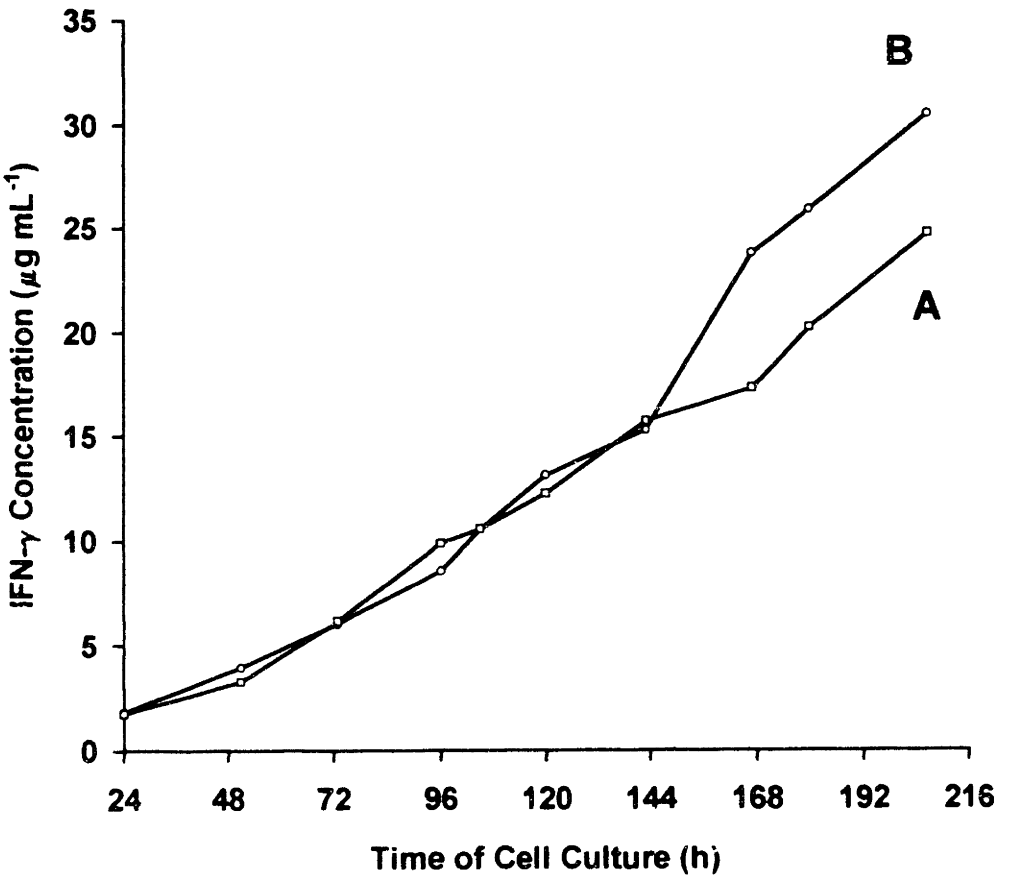

Figure 5.10: IFN-γ concentrations for fed-batch CHO cultures. A and B indicate cultures utilizing Primatone RL-supplemented and Primatone RL-free feeding media, respectively.

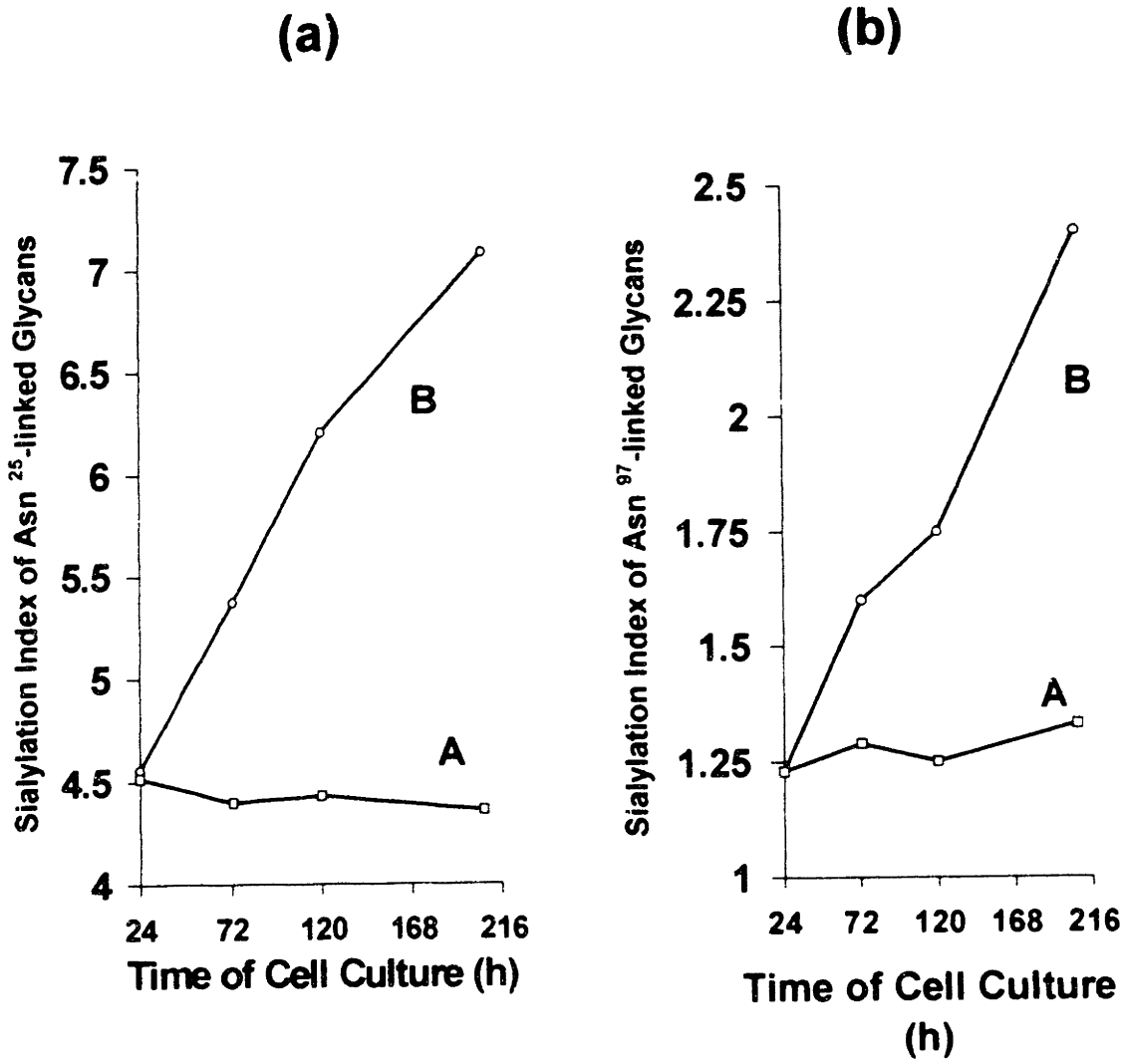

Figure 5.11: Sialylation indices of (a) Asn^{25}- and (b) Asn^{97}-linked glycans of IFN-γ produced by fed-batch CHO cultures. A and B indicate cultures utilizing Primatone RL-supplemented and Primatone RL-free feeding media, respectively.

of the culture for the fed-batch where peptone was not fed. Presumably components of Primatone RL responsible for poor sialylation were consumed during the course of the culture. Due to the fact that the majority of IFN-γ was produced after the achievement of high cell density in the latter stages of the culture, the sialylation indices of the cumulative IFN-γ reached 7.1 and 2.4 for Asn^{25}- and Asn^{97}-linked glycans, respectively, at the end of the fed-batch. Thus, sialylation of the final product was comparable to that previously obtained in the batch mode with the non-Primatone RL-supplemented CHO-SFM-II medium. Meanwhile, sialylation of IFN-γ produced by the batch utilizing the feeding medium containing Primatone RL remained poor and relatively constant throughout the course of the culture. Since both fed-batches displayed similar viability profiles, as shown in Figure 5.12, the observed difference in sialylation should be attributed to impact of the peptone on intracellular sialylation rather than extracellular desialylation. This conclusion is consistent with the poor sialylation observed in the beginning of both fed-batches when cell viability was nearly 100%. The two fed-batches offered further evidence that the poor sialylation of IFN-γ observed with supplementation of high concentrations of Primatone RL cannot be attributed solely to ammonia accumulation. The non-peptone-supplemented feeding medium was designed to contain similar concentrations of total L-glutamine as the Primatone RL-supplemented feeding medium, and, thus, the two fed-batches displayed similar accumulations of ammonia, as seen in Figure 5.13.

Much research has been invested in the search for serum-substitutes

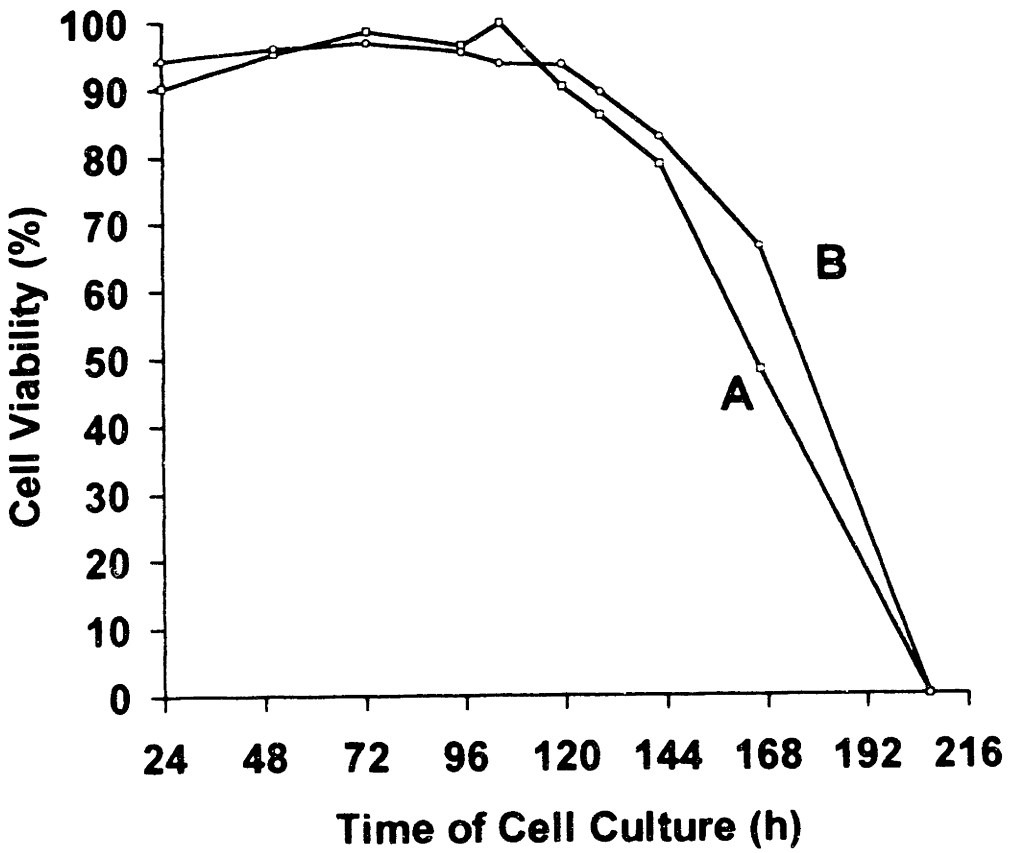

Figure 5.12: Viability profiles for fed-batch CHO cultures. A and B indicate cultures utilizing Primatone RL-supplemented and Primatone RL-free feeding media, respectively.

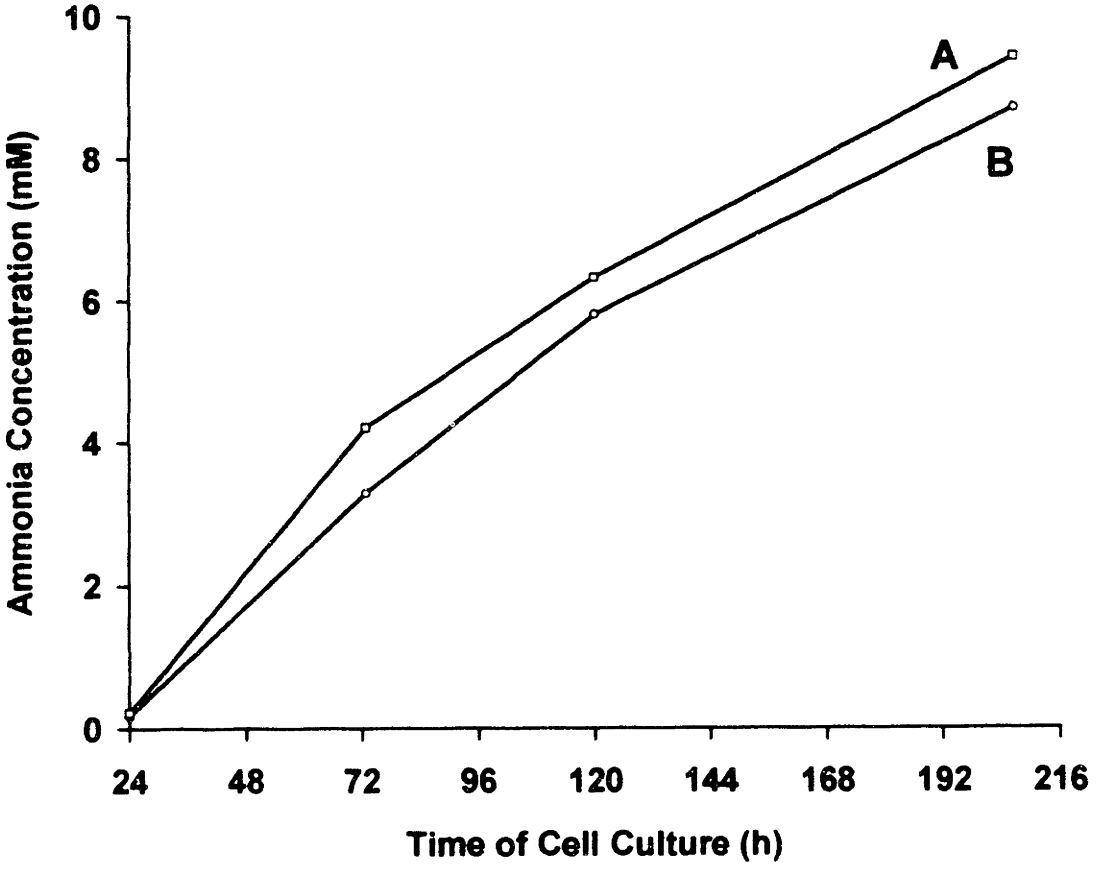

Figure 5.13: Ammonia concentrations for fed-batch CHO cultures. A and B indicate cultures utilizing Primatone RL-supplemented and Primatone RL-free feeding media, respectively.

which can promote cell growth and, thus, product yield for serum-free production of therapeutic proteins. However, the effect of such serum-substitutes on product quality also demands consideration in order to assure that product efficacy is not compromised. The results of these experiments have indicated that the use of Primatone RL can adversely affect sialylation of CHO-derived IFN-γ in both batch and fed-batch modes. The observation of diminished sialylation at the optimal concentration of peptone for cell growth and product yield in the batch mode illustrates the potential tradeoff between product quantity and quality which must be evaluated in the use of serum-substitutes.

CHAPTER SIX: IMPROVEMENT OF IFN-γ GLYCOSYLATION IN CHO CELL CULTURE

As shown in Chapter Four, IFN-γ derived from CHO cell culture generally exists as a set of microheterogeneous glycoforms. Both the antennarity distribution and sialylation percentage of the attached oligosaccharides contribute greatly to the heterogeneity of both glycosylation sites, Asn^{25} and Asn^{97}. Furthermore, the exclusive fucosylation of Asn^{25} serves as a good example of site-specific heterogeneity. The heterogeneity of oligosaccharides, which can be sensitive to cell culture conditions, as described in Chapter Five, is critical to the properties of glycoproteins, as reviewed in Chapter Two. As a result, it is desirable to improve protein glycosylation homogeneity for protein quality control as well as regulatory concerns. This chapter explores cell culture strategies for improving glycosylation homogeneity. In particularly, the effects of dexamethasone, which improves antennarity homogeneity, and N-acetylmannosamine, which increases the sialic acid content, will be discussed in detail here.

6.1 Improvement of antennarity homogeneity by dexamathasone feeding

As discussed in Chapter Four, biantennary, triantennary and tetraantennary glycans accounted for 77%, 18% and 4%, respectively, of Asn^{97}-linked glycans, and 63%, 25% and 12%, respectively, of Asn^{25}-linked oligosaccharides based upon integrated MALDI/TOF signals for desialylated glycopeptides. Although biantennary structures represented the majority of

glycans for both glycosylation sites, Asn^{25} possessed a higher proportion of highly -branched structures than Asn^{97}. When glycoproteins are removed from the circulation system by asialoglycoprotein receptors on human hepatocytes, glycoproteins with tri- and tetraantennary oligosacchrides are more easily recognized than those with biantennary glycans (Drickamer, 1991). Therefore, an increase in the proportion of biantennary structures would not only improve the product glycosylation homogeneity, but also improve the glycoprotein's capability to avoid clearance by asialoglycoprotein receptors.

All of the reactions responsible for the branching of oligosaccharides take place in Golgi vesicles, as shown in Figure 6.1. Catalyzed by N-acetylglucosaminyltransferase V (GlcNAc-Tase V), an additional GlcNAc is attached to one arm of the biantennary structure to form the triantennary structure. The activity of the same enzyme can further add an additional GlcNAc to the other arm of the triantennary structure and thus yielding the tetraantennary structure. These behaviors show that the activity of GlcNAc-Tase V appears to be the determinant factor governing the branching of N-linked glycans As an example, an increase in the activity of GlcNAc-Tase V observed in malignant cells was correlated to the higher proportion of highly-branched carbohydrate structures of glycoproteins on the surface of cancer cells (Yamashita *et al* , 1984). On the other hand, dexamethasone, a very common transcription inducer, has been shown to reduce the activity of GlcNAc-Tase V *in vitro* (Easton *et al.*, 1991). Using oligosaccharide as substrate, the activity of GlcNAc-Tase V was shown to be reduced by 40% by 1μM dexamethasone (Easton *et al.*, 1991). As a result,

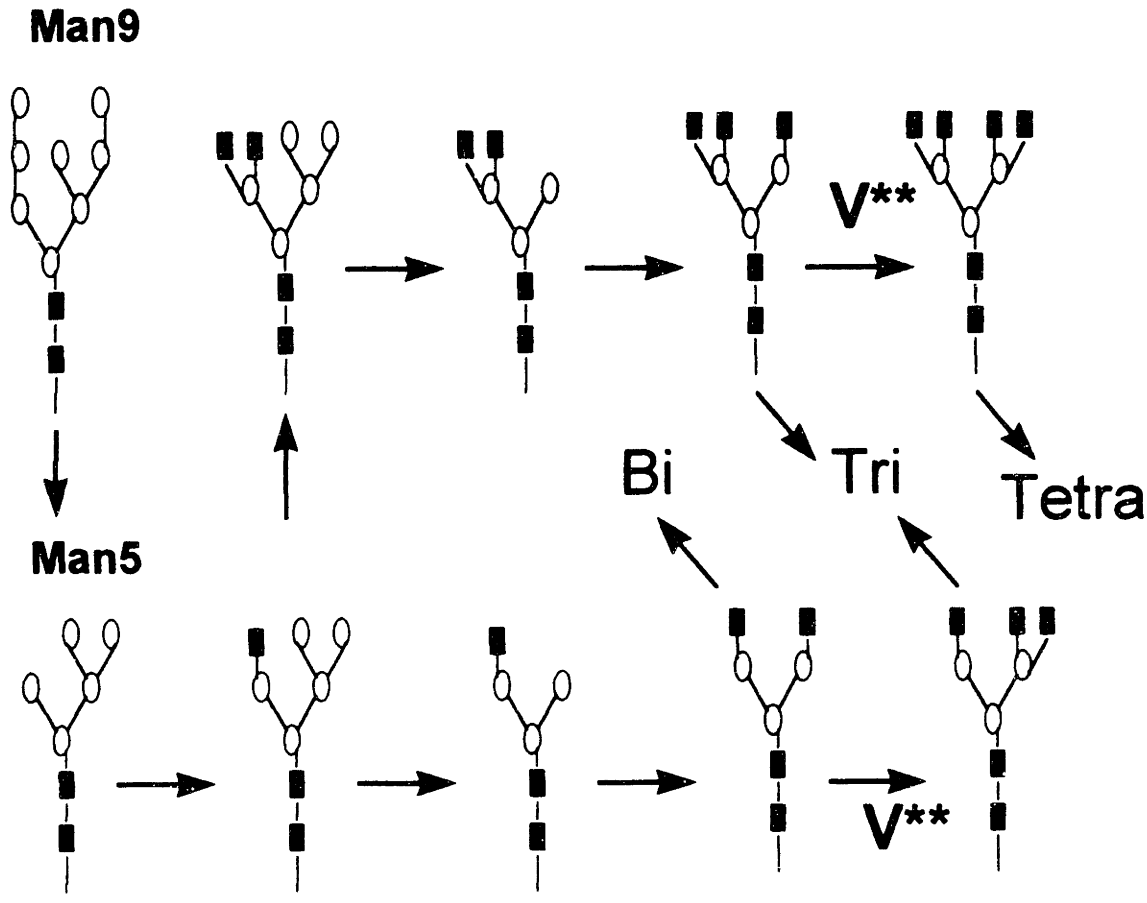

V**: N-acetylglucosaminyltransferase V (GlcNAc-Tase V), controls the branching of oligosaccharide

○ : Mannose ▮ : N-acetylglucosamine

Figure 6.1: Oligosaccharide Branching Reaction in Golgi

dexamethasone offers promise to decrease the antennarity heterogeneity of recombinant glycoproteins.

To test the potential effect of dexamethasone on IFN-γ branching in CHO cell culture, 1 μM dexamethasone was introduced at the beginning of a 20-mL shake flask batch culture of CHO cells using Gibco CHO-SFM-II. Culture supernatant was collected after 96 h with cell viability at about 100%. Maximum cell density as well as titer expression are reported in Table 6.1. Compared with the control culture which did not contain dexamethasone, the presence of 1μM dexamethasone did not have a major impact on either cell growth or product yield. The IFN-γ produced in the 96-h batch containing dexamathasone was purified, and the site-specific pools of tryptic glycopeptides were isolated, as described in Chapter Four. Desialylation and MALDI-TOF mass spectrometry were then utilized to quantify the asialo antennary structures, as depicted in Figure 6.2. The Asn^{25}- and Asn^{97}- associated distribution of bi-, tri- and tetraantennary structures of IFN-γ derived from the dexamathasone-containing batch and the control batch are summarized in Table 6.1. With 1μM dexamethasone, the proportion of biantennary structure was increased by 20% for Asn^{25} and 10% for Asn^{97}, respectively. The proportion of tri- and tetra-antennary was correspondingly decreased. Therefore, the overall antenarity homogeneity for both glycosylation sites was improved.

Table 6.1: Effect of 1μM dexamethasone on cell growth, product yield and antennary structure distribution of CHO-derived IFN-γ.

		No dexamethasone	1 μM dexamethasone
Glycans of Asn^{25}	Biantennary	63%	83%
	Triantennary	25%	13%
	Tetrantennary	12%	4%
Glycans of Asn97	Biantennary	78%	88%
	Triantennary	18%	9%
	Tetraantennary	4%	3%
Maximum cell density (x10^6 cell/ml)		2.3	2.1
Interferon-γ concentration (μg/ml)		4.53	4.57

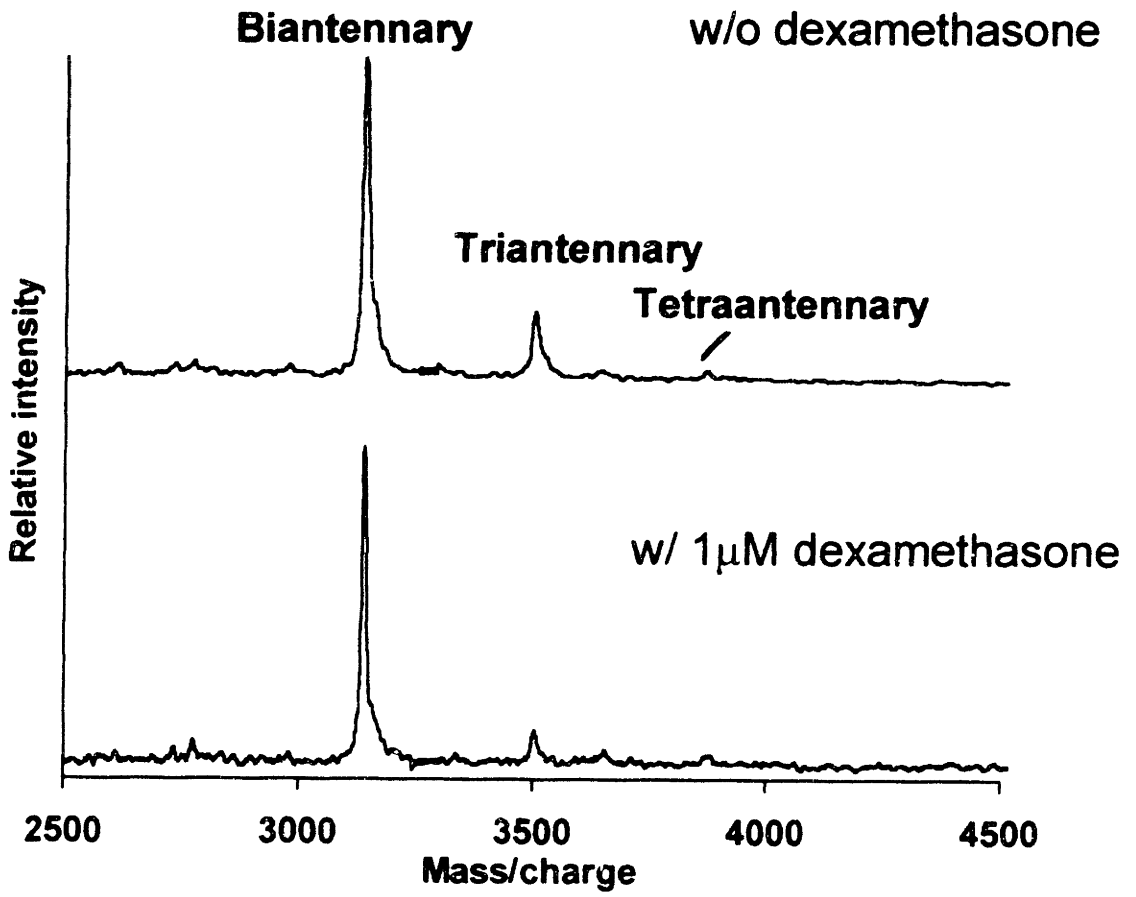

Figure 6.2: Dexamethasone can alter the Asn^{97}-associated antennary structure distribution of interferon-γ in CHO cell culture

6.2 Improvement of sialylation by feeding of N-acetylmannosamine

Sialic acid, the terminal sugar for N-linked complex glycan structures, has been found to influence the solubility (Lawson *et al.*, 1983), thermal stability (Tsuda *et al.*, 1990), resistance to protease attack (Aquino *et al.*, 1980), antigenicity (Schauer, 1988), and specific activity (Smith *et al.*, 1990) of various glycoproteins. Most generally, sialylation can play a major role in determining a glycoprotein's circulatory lifetime since the presence of sialic acid can prevent recognition of the glycoprotein by asialoglycoprotein receptors on the surface of blood hepatocytes (Weiss and Ashwell, 1989) Therefore, it is generally desired to maximize the final sialic acid content of a glycoprotein product to ensure its quality and consistency as an effective pharmaceutical.

In Chapter Five, sialylation of recombinant human interferon-γ (IFN-γ) produced during batch Chinese hamster ovary (CHO) cell was observed to be defined by both incomplete intracellular sialylation and extracellular desialylation. The latter effect was caused by the sialidase released during cell lysis similar to that found by others (Warner *et al.*, 1993; Gramer *et al.*, 1995). The extracellular desialylation can be readily prevented by terminating the culture process prior to cell lysis. However, means to improve intracellular sialylation would be of significant value scientifically and industrially.

The intracellular events of protein glycosylation are regulated by a number of factors. These include the expression and subcellular localization of glycosyltransferases and glycosidases (Paulson and Colley, 1989), the availability of intraluminal nucleotide sugar substrates (Rijcken, *et al.*, 1995), the steric

accessibility of the glycosylation site for oligosaccharide processing, as well as the transit time of the glycoform for oligosaccharide formation. In particular, sialylation, being the last event of the post-translational glycosylation modification process inside the trans-Golgi, requires the availability of sufficient amount of the nucleotide sugar precursor CMP-sialic acid as well as adequate sialyltransferase activity to transfer the sialic acid to the galactose termini of complex oligosaccharides. Deutscher *et al.* (1984) have reported decreased sialylation of glycoproteins and gangliosides resulting from deficiency in CMP-sialic acid translocation, and Rijcken *et al.* (1995) have observed that elevated cytosolic levels of UDP-N-acetylhexosamine impaired the transport of CMP-sialic acid to the Golgi and, thus, caused reduced sialylation. These findings suggest that insufficient concentration of CMP-sialic acid inside the trans-Golgi could be a cause for the incomplete intracellular protein siaylation. The goal of this study was to explore cell cultivation strategies for increasing the CMP-sialic acid pool in the trans-Golgi as a means to increase product sialylation

Figure 6.3 shows the biosynthetic pathways of the precursors of glycosylation (Schachter and Roden, 1973; Corfield and Schauer, 1983). It should be noted that the synthesis of CMP-sialic acid from sialic acid and CTP is catalyzed by CMP-sialic acid synthetase in the reaction shown below (Kean, 1972). This reaction is unlike the cytoplasm localization of the enzymes responsible for other nucleotide sugars, which occurs in the nucleus (Kean, 1972, van den Eijnden, 1973, Coates *et al.*, 1980; van Rinsum *et al.*, 1983):

$$\text{sialic acid} + \text{CTP} \rightarrow \text{CMP-sialic acid} + \text{Pp}_i$$

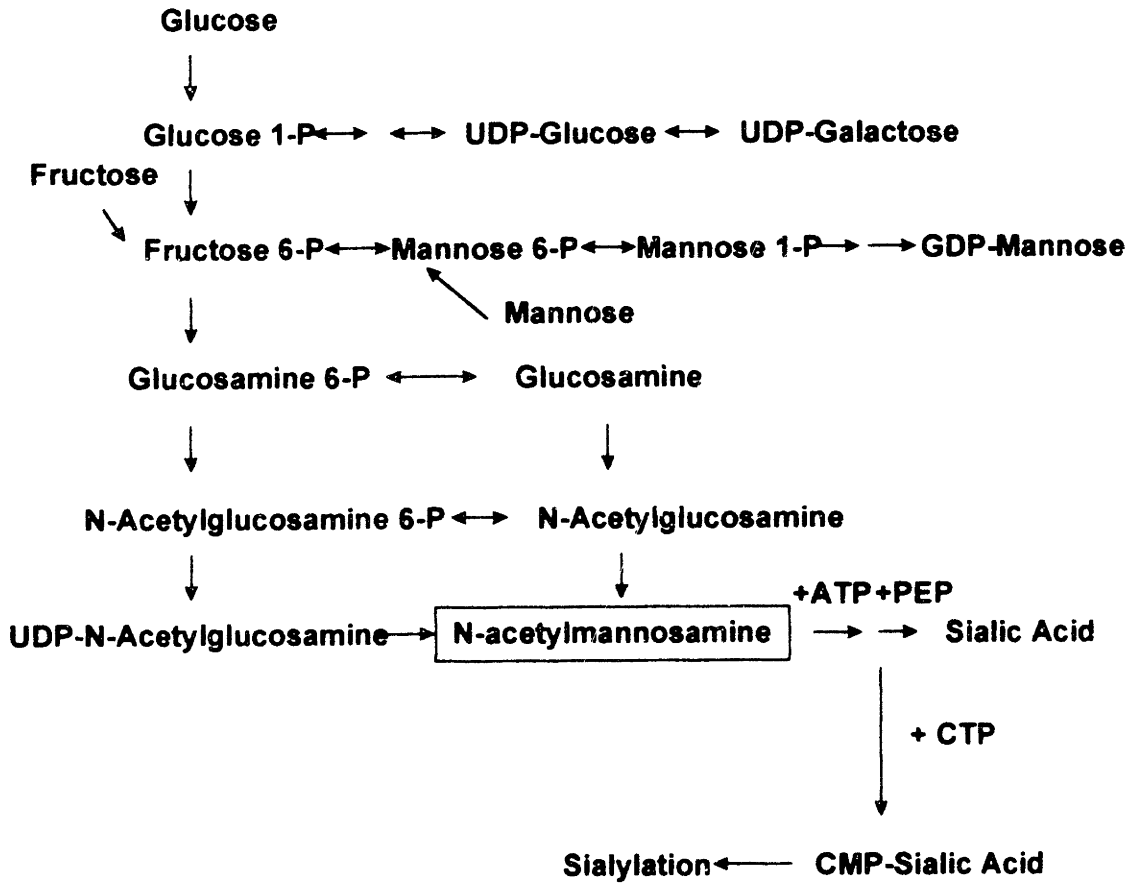

Figure 6.3: Synthetic pathway of CMP-sialic acid

However, both sialic acid and CMP-sialic acid have poor permeability to enter the cell. Thus, feeding either of these sialylation precursors will not increase the intracellular pool of CMP-sialic acid. As seen in Figure 6.3, ManNAc is an important linkage between hexosamine and sialic acid synthesis and can be regarded as the first specific precursor in the biosynthesis of sialic acid (Corfield and Schauer, 1979). Although ManNAc can be produced intrinsically by 2-epimerization from either UDP-N-acetylglucosamine or N-acetylglucosamine (Schachter and Roden, 1973), the simultaneous incorporation of externally-added ManNAc into sialic acid has been observed for animals, surviving tissue slices, and individual cells (Ferwerda, 1983; Schoop *et al.*, 1969; Yohe *et al.*, 1980) Given its role as a specific precursor for intracellular synthesis of sialic acid and its greater permeability than sialic acid or CMP-sialic acid at physiological *p*H (Harms *et al.*, 1973; Hirschberg and Yeh, 1977; Kohn *et al.*, 1962), this study thus investigated the feeding of ManNAc to CHO cell culture as a method of improving product sialylation by increasing the CMP-sialic acid pool in the trans-Golgi.

6.2.1 Effect of supplemental ManNAc on intracellular CMP-sialic acid

In order to assess the effect of ManNAc feeding on the intracellular pool of CMP-sialic acid, batch CHO cultures supplemented with 0, 0.2, 2, and 20 mM ManNAc were performed in shake flasks using serum-free Gibco SFM-CHO-II medium. As seen in Table 6.2, ManNAc feeding did not affect cell growth or product concentration. After 96 h of culture, about one million cells were collected from each culture, and the intracellular nucleotide sugars were extracted following the protocol suggested by Rijcken (1993) Ethanol (75%), rather than

Table 6.2: Effect of supplemental ManNAc on cell growth and IFN-γ production of CHO batch cultures using SFM-CHO-II serum-free medium (96 h).

Supplemental ManNAc Conc. (mM)	Viable Cell Concentration (cells ml^{-1})	Cell Viability (%)	IFN-γ Conc. ($\mu g\ ml^{-1}$)
0	$2.3x10^6$	98	4.53
0.2	$2.4x10^6$	96	4.65
2	$2.2x10^6$	95	4.45
20	$2.4x10^6$	98	4.72

perchloric acid or KOH, was selected as the nucleotide sugar extraction agent to minimize hydrolysis of CMP-sialic acid. Lipids were subsequently removed from the nucleotide sugar extracts by chloroform extraction. As shown in Figure 6.4, the nucleotide sugars were separated using a reversed-phase HPLC method described by Ryll and Wagner (1991). CMP-sialic acid, NAD^+, GDP-mannose, and UDP-N-acetylgalactosamine were identified by spiking with standards. CMP-sialic acid was quantified by comparison to a CMP-sialic acid standard curve The intracellular CMP-sialic acid concentrations shown in Table 6.3 were

Table 6 3: Effect of supplemental ManNAc on sialylation of CHO-derived IFN-γ (96 h of batch culture using SFM-CHO-II serum-free medium)

Supplemental ManNAc Conc. (mM)	Intracellular CMP-Sialic Acid Conc. (μM)	Incomplete Sialylation of Asn^{97} Glycans (%)	Product Sialylation Originating from Supplemental ManNAc (%)
0	33	35	0
0.2	31	35	0
2	73	26	60
20	900	20	100

calculated based upon CHO cell diameter (16 μm) measured by a Coulter Channelyzer Feeding of 0.2 mM ManNAc did not affect the intracellular

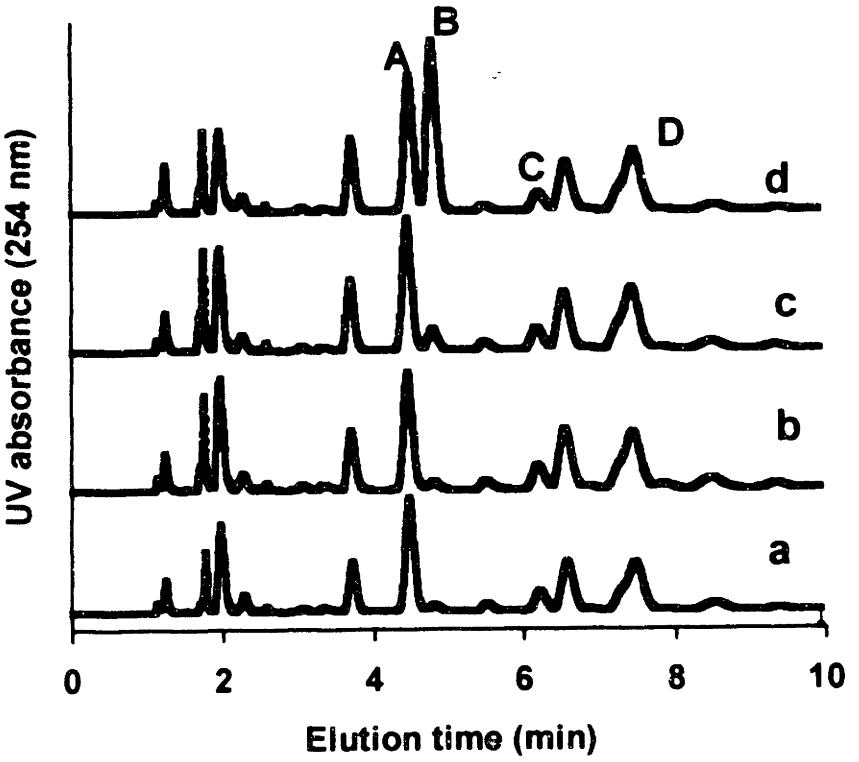

Figure 6.4: Reversed-phase HPLC separations of nucleotide sugars extracted from CHO cells cultured in medium supplemented with a) 0, b) 0.2, c) 2, and d) 20 mM ManNAc. A, B, C, and D indicate NAD+, CMP-sialic acid, GDP-mannose, and UDP-N-acetylgalactosamine, respectively.

concentration of CMP-sialic acid as compared to the control. However, 2 mM supplemental ManNAc doubled the intracellular concentration of CMP-sialic acid, and 20 mM supplemental ManNAc increased the intracellular concentration of the sialylation precursor nearly thirty-fold.

6.2.2 Incorporation of supplemental ManNAc

Following the observation of an increased intracellular concentration of CMP-sialic acid with ManNAc feeding, radiolabeled ManNAc was used to trace the incorporation of the added ManNAc into IFN-γ. After 96 h of cultivation, supernatant was collected from a culture supplemented with 2 mM ManNAc as well as 200 μCi of radiolabeled ManNAc. Following immunoprecipitation of 1.5 ml of the supernatant with Reselute-γ, an immunoaffinity resin for IFN-γ, and washing the pellet, 2343 dpm (disintegrations per minute) of radioactivity was detected. When the immunoprecipitated pellet was resuspended and treated with sialidase, the enzymatic treated sample showed a decrease in the radioactivity to 220 dpm following recentrifugation and washing. In the control experiment, the immunoprecipitated pellet was treated identically except the incubation buffer did not contain sialidase. The measured radioactivity was 2412 dpm. These results suggest that supplemental ManNAc is incorporated into IFN-γ almost exclusively as sialic acid, and, thus, ManNAc serves as a specific precursor for sialylation. This finding is in agreement with the observation by Rijcken *et al.* (1995) that the radioactivity of radiolabeled supplemental ManNAc is found in CMP-sialic acid, the direct precursor for sialylation, rather than UDP-GlcNAc.

Similar cultures supplemented with radiolabeled ManNAc were performed with supplemental ManNAc concentrations of 0.2 and 20 mM. The radioactivity of the immunoprecipitated IFN-γ provided a measure of the product sialylation from the supplemental ManNAc. The total sialic acid content of the immunoprecipitated IFN-γ was determined by reversed-phase HPLC. From these experiments, the percentage of sialic acid on the product originating from the external ManNAc was calculated for each culture. These results are summarized in Table 6.3. At 2 mM supplementation of ManNAc, approximately 60% of sialic acid on the product originated from the supplemental ManNAc. It is seen than an increase of 40 μM (*i.e.*, from 33 to 73 μM) in the intracellular CMP-sialic acid concentration when 2 μM ManNAc was fed as compared to the control This also corresponded to a 60% of the total intracellular CMP-sialic acid This result indicates that there is no intracellular discrimination between the CMP-sialic derived from the externally added ManNAc and that which is synthesized during cell metabolism. This conclusion is further supported by the data from the cultures supplemented with 0 2 and 20 mM ManNAc. Further increasing the ManNAc to 20 mM in the culture medium resulted in an increase of the intracellular CMP-sialic acid concentration to 900mM: nearly 30-fold increase. This was accompanied by 100% of the sialylated IFN-γ being from the externally-added ManNAc. However, only 10% of sialic acid content of the product originated from the external ManNAc when 0.2 mM was added. This in turn showed no significant change in the intracellular CMP-sialic acid concentration.

6.2.3 Effect of supplemental ManNAc on product sialylation

Thus far, an increased intracellular concentration of CMP-sialic acid with ManNAc feeding and the incorporation of the ManNAc into the sialylated product were observed. The effect of ManNAc feeding on the completeness of IFN-γ sialylation was evaluated using analytical methodologies for determining the site- and branch-specific sialylation. Briefly, IFN-γ was purified from culture supernatant by immunoaffinity chromatography and subjected to trypsinization The two fractions of glycopeptides representing the two potential glycosylation sites were then isolated by low-pH reversed-phase HPLC. A sialic acid-based separations of these site-specific populations of glycopeptides were obtained by neutral-pH/borate-complexation reversed-phase HPLC. In Chapter Five, it was observed that sialylation of IFN-γ was relatively constant during batch CHO culture prior to loss of cell viability However, steady decreases in sialylation were observed following cell lysis due to extracellular sialidase activity (Warner *et al.*, 1993, Gramer *et al*, 1995). The introduction of a competitive inhibitor of sialidase into the culture supernatant prevented the loss of sialic acid after the onset of cell death but did not affect sialylation prior to cell death. This finding indicated that incomplete sialylation prior to loss of cell viability could be attributed to incomplete intracellular sialylation while the reduction in sialylation following loss of cell viability was due to extracellular sialidase activity resulting from cell lysis. Consequently, in order to elucidate the role of ManNAc on intracellular sialylation of IFN-γ without having to consider extracellular desialylation, the batch cultures were terminated at 96 h, and sialylation analyses were performed when

the cell viabilities was 100%, as seen in Table 6.2. Furthermore, although the glycans at each glycosylation site were found to be incompletely sialylated intracellularly, Asn^{25}-linked glycans were observed to have higher sialic acid content than those of Asn^{97}. We therefore focused on the sialylation of Asn^{97} in this study.

Figure 6.5 shows the separation of the Asn^{97}-linked glycopeptides of IFN-γ from the 0, 2 and 20 mM ManNAc-supplemented cultures. Since complex biantennary structures are the dominant oligosaccharides at each glycosylation site of CHO-derived IFN-γ (James *et al* , 1995; Harmon *et al*, 1996), and the distribution of bi-, tri-, and tetraantennary structures remains relatively unchanged throughout batch CHO culture (Harmon *et al*, 1996), only sialylation of the complex biantennary glycans is considered here. For ease of visualization, the chromatograms were scaled to the maximum absorbance . C_0, C_{1a}, C_{1b}, and C_2 indicate glycopeptides possessing asialo, monosialo (sialic acid on Man(α1-6) branch), monosialo (sialic acid on Man(α1-3) branch), and bisialo complex biantennary structures, respectively The identification of the different sialo structures was achieved using matrix-assisted laser-desorption ionization/time-of-flight mass spectrometry and linkage-specific exoglycosidase digestion which was detailed in Chapter Four. Figure 6.5 shows that the Man(α1-3) branches were more highly sialylated than the Man(α1-6) arms for each culture. This finding is in agreement with our previous report of preferential sialylation of the Man(α1-3) branch of the predominant complex biantennary glycans for CHO-derived IFN-γ in

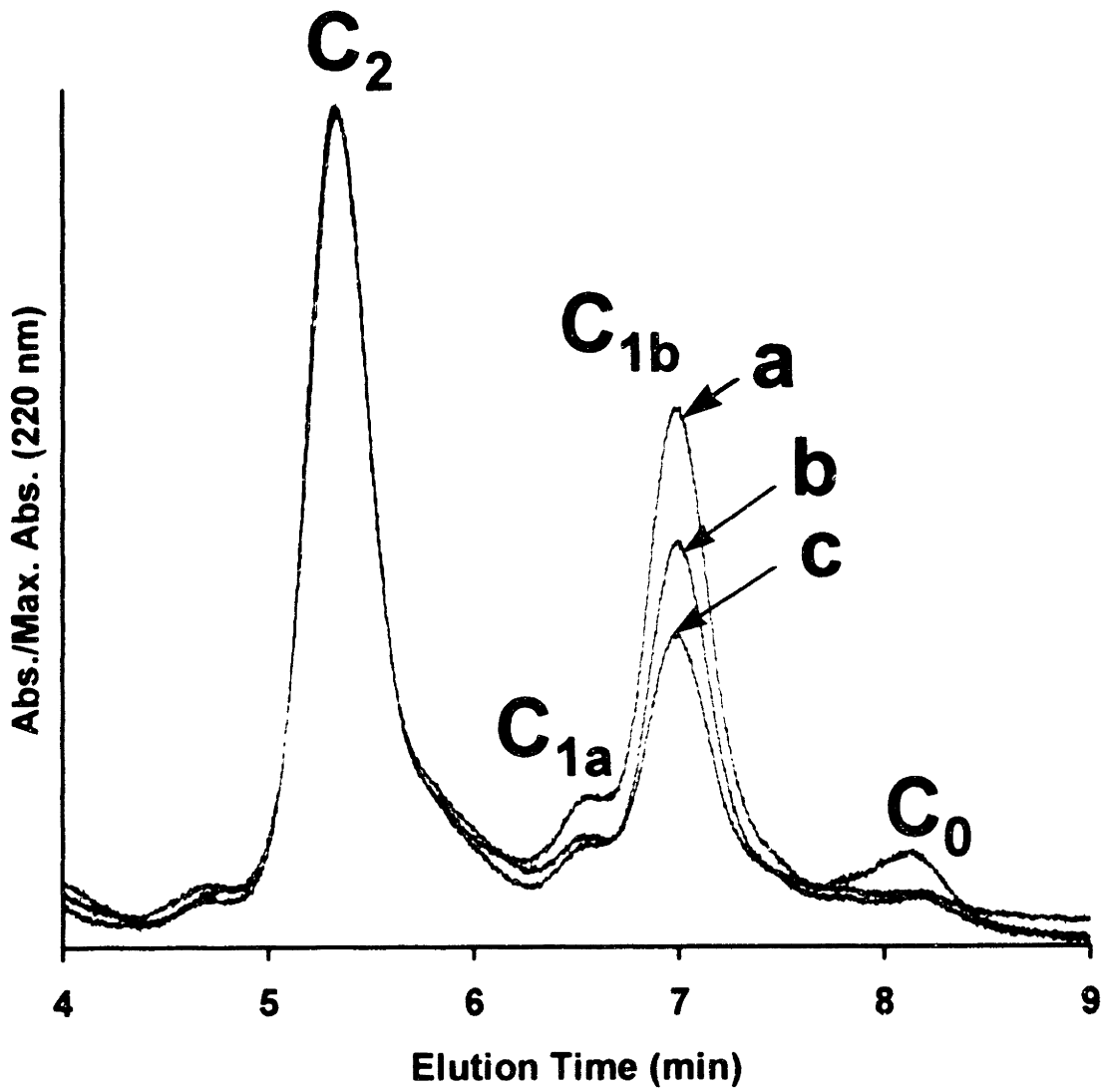

Figure 6.5: Neutral pH/borate-complexation reversed-phase HPLC separations of Asn97-linked IFN-g tryptic glycopeptides from CHO batch cultures supplemented with a) 0, b) 2, c) 20 mM ManNAc. C0, C1a, C1b, and C2 indicate glycopeptides possessing asialo, monosialo (sialic acid on Man(a1-6) branch), monosialo (sialic acid on Man(a1-3) branch), and bisialo complex biantennary glycan structures, respectively.

Chapter Four. In the unsupplemented culture without ManNAc, approximately 35% of the Asn^{97}-linked biantennary glycans were not fully sialylated, as seen in Table 6.3, with the incomplete sialylation percentage of Asn^{97} glycans defined as following:

$$\frac{A_{C1a} + A_{C1b} + A_{C0}}{A_{C2} + A_{C1a} + A_{C1b} + A_{C0}} \times 100\%$$

where A_n is the integrated peak area of fraction *n* from the neutral pH/Borate complexation HPLC chromatogram. The sialylation profile for the culture supplemented with 0.2 mM ManNAc (data not shown) was indistinguishable from that of the control. This finding shows that low concentration of ManNAc feeding did not affect the sialylation of IFN-γ. This result is in agreement with the finding that no increase in the intracellular pool of CMP-sialic acid with 0.2 mM supplemental ManNAc was observed However, when fed with 2 mM ManNAc, the asiolo and monosialo (sialic acid on Man(α1-6) branch) biantennary structures virtually disappeared Furthermore, the monosialo (sialic acid on Man(α1-3) branch) complex biantennary structures, the predominant incompletely sialylated glycans was dramatically decreased and the percentage of overall incompletely sialylated glycans reduced to approximately 26%. At 20 mM supplemental ManNAc, the asiolo and monosialo (sialic acid on Man(a1-6) branch) complex biantennary structures virtually disappeared. This is consistent with the data from 2mM ManNAc treatment It should be noted that the monosialo (sialic acid on Man(α1-3) branch) complex biantennary structures decreased by nearly half compared to the controlled, and the the percentage of overall incompletely

sialylated glycans decreased to approximately 20%. However, no further improvement in sialylation of Asn^{97}-linked glycans was observed with feeding of 40 mM ManNAc (data not shown). The Asn^{25}-linked glycans of CHO-derived IFN-γ are more heavily sialylated than the oligosaccharides at the Asn^{97} site. In this study, less than 10% of the Asn^{25}-linked glycans were incompletely sialylated in each of the ManNAc-supplemented and unsupplemented cultures, and no significant effects due to ManNAc feeding were observed.

The ManNAc feeding described in this study was performed in the batch mode in which ManNAc was fed only at the beginning of the culture. It is possible that a significant portion of the supplemental ManNAc was consumed for sialic acid synthesis during the course of the culture. Furthermore, it was observed that the supplemental ManNAc was incorporated into IFN-γ almost exclusively as sialic acid. The supplemental ManNAc could have been utilized by the CHO cells for metabolic or synthetic pathways other than sialic acid synthesis, or ManNAc could have simply degraded during the course of the culture. Understanding the influence of these effects on product sialylation is necessary to develop an optimized ManNAc feeding strategy in order to achieve maximal product sialylation. Therefore, supernatant was collected every 24 h for the 2 mM ManNAc-supplemented batch exposed to radiolabeled ManNAc, and the percentage of product sialylation originating from the supplemental ManNAc was estimated as previously described. As shown in Figure 6.6, the percentage of product sialylation originating from the supplemental ManNAc remained at 60% throughout the 96-h culture process. This finding suggests that with 2 mM

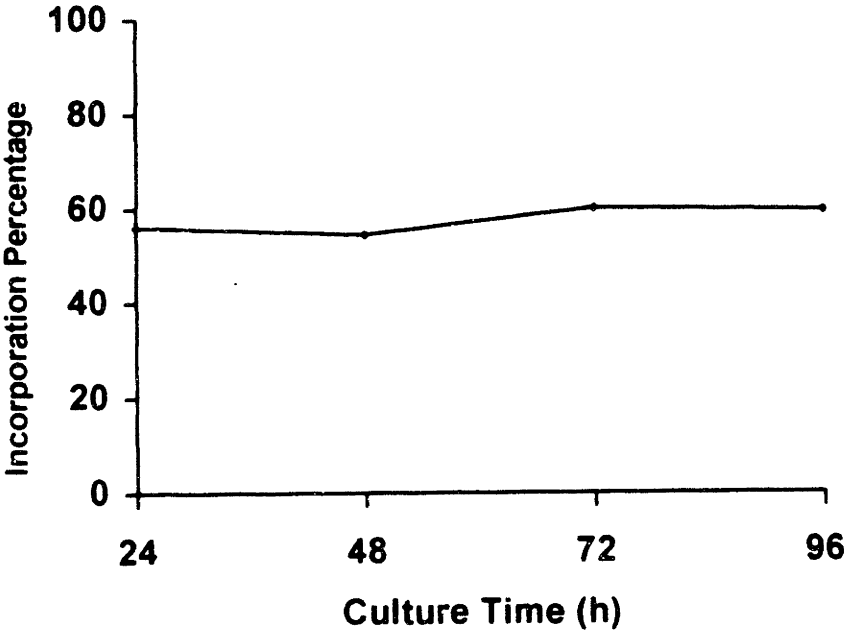

Figure 6.6: Percentage of IFN-γ sialylation originating from supplemental ManNAc throughout four days of batch CHO cell culture.

ManNAc in the culture medium, neither the consumption of ManNAc for sialic acid synthesis nor the utilization of ManNAc by other pathways were great enough to reduce the supply of ManNAc for sialic acid synthesis. As a result, additional feeding of ManNAc during the course of the batch was not required for maximal product sialylation.

6.2.4 Transport of CMP-sialic acid through Golgi vesicles

The possibility of improving product sialylation by increasing the availability of CMP-sialic acid was investigated. ManNAc, a specific precursor for sialic acid synthesis, was shown to increase the intracellular pool of CMP-sialic acid and improve product sialylation. However, although the intracellular pool of CMP-sialic acid increased by nearly thirty-fold by feeding of 20 mM ManNAc, significant incomplete product sialylation remained. There are several possible reasons for the remaining incomplete sialylation. It is possible that the intracellular CMP-sialic acid had limited access to the trans-Golgi, and CMP-sialic acid remained a limiting factor for the sialyltransferase reaction. Due to the sensitivity of the analytical method, intracellular CMP-sialic acid was measured in this study, rather than the localized sialic acid concentration in the trans-Golgi, the site of the sialyltransferase reaction. Publications by Carey *et al* (1980), Hanover and Lennarz (1982), and Sommers and Hirschberg (1982) have demonstrated that CMP-sialic acid is transported into Golgi-derived vesicles. Carey *et al* (1980) suggested that this transport process involves a protein-mediated transport system and that this transport can be saturated due to a limited amount of transport carriers in the Golgi membranes. Capasso and Hirschberg (1984) have

proposed a coupled exchange in the Golgi between CMP-sialic acid and CMP. These findings suggest that the CMP-sialic acid pool inside the trans-Golgi will not be increased by the same magnitude as in the cytoplasm due to limited transport of the precursor to the site of sialylation.

In order to understand the transport of CMP-sialic acid through the Golgi vesicles at the CMP-sialic acid concentrations measured for ManNAc-treated CHO cell, Golgi vesicles were isolated and incubated with radio-labeled CMP-sialic acid. In this study, microsomes (including both ER and Golgi vesicles) were isolated from $9x10^7$ cells using the method developed by Kamath and Narayan (1972), which introduced the use of Ca^{2+} treatment of microsomes in order to allow the use of shorter centrifugation times. Although microsomes were used to study the transport of CMP-sialic acid, the transport is known to be specific for trans-Golgi vesicles only (Capasso and Hirschberg, 1984). The protein concentration of the microsome mixture isolated from $9x10^7$ cells was determined to be 7.1 mg/ml by Bradford protein assay.

Since CMP-sialic acid is known not only for being tranported inside the trans-Golgi but also non-specifically binding to the membrance surface of trans-Golgi (Carey *et al.*, 1980), the transport rate of CMP-sialic acid through the microsome was determined by a differential measurement utilizing the coupled exchange in the Golgi between CMP-sialic acid and CMP. Golgi vesicles were first incubated with radiolabeled CMP-sialic acid without CMP. Therefore, the radioactivity of centrifuged Golgi vesicles after incubation resulted from both transport of CMP-sialic acid inside the Golgi and non-specific binding of CMP-

sialic acid to the Golgi surfaces. At the same time, Golgi vesicles were also incubated with CMP-sialic acid in the presence of 400 mM CMP. Due to the coupled exchange in the Golgi of CMP-sialic acid and CMP, radiolabeled CMP-sialic acid would not be transported inside trans-Golgi but still would non-specifically bind to the Golgi surfaces. By subtracting the latter measurement from the former, the transport rate of CMP-sialic acid could be calculated.

The transport rate of CMP-sialic acid into Golgi vesicles under different concentrations of CMP-sialic acid was measured, as depicted in Figure 6.7. The transport became gradually saturated, especially when the concentration of CMP-sialic acid was over 100 μM. However, based upon the transport curve in Figure 6.7, the transport rate of CMP-sialic acid of CHO cells without ManNAc treatment (*i.e.*, 33 μM CMP-sialic acid suggested a transport rate of 60 dpm/min) was at least double that of the 20 mM ManNAc treated CHO cells (*i.e.*, 900 μM of CMP-sialic acid suggested a transport rate of 120 dpm/min). However, the overall sialylation percentage of Asn^{97}, as described in Chapter Four, was only increased from 84% to 92%. This conclusion suggests not only that further availability of CMP-sialic acid inside trans-Golgi probably would not increase IFN-γ sialylation any further but also that, with 20 mM ManNAc treatment, CMP-sialic acid inside the trans-Golgi might approach saturation for sialyltransferase.

Another factor which must be considered is the steric accesibility of the glycosylation sites. While the Asn^{25} glycosylation site is in a flexible loop between two α-helices, Asn^{97} is contained within an α-helical region (Ealick *et al.*, 1991).

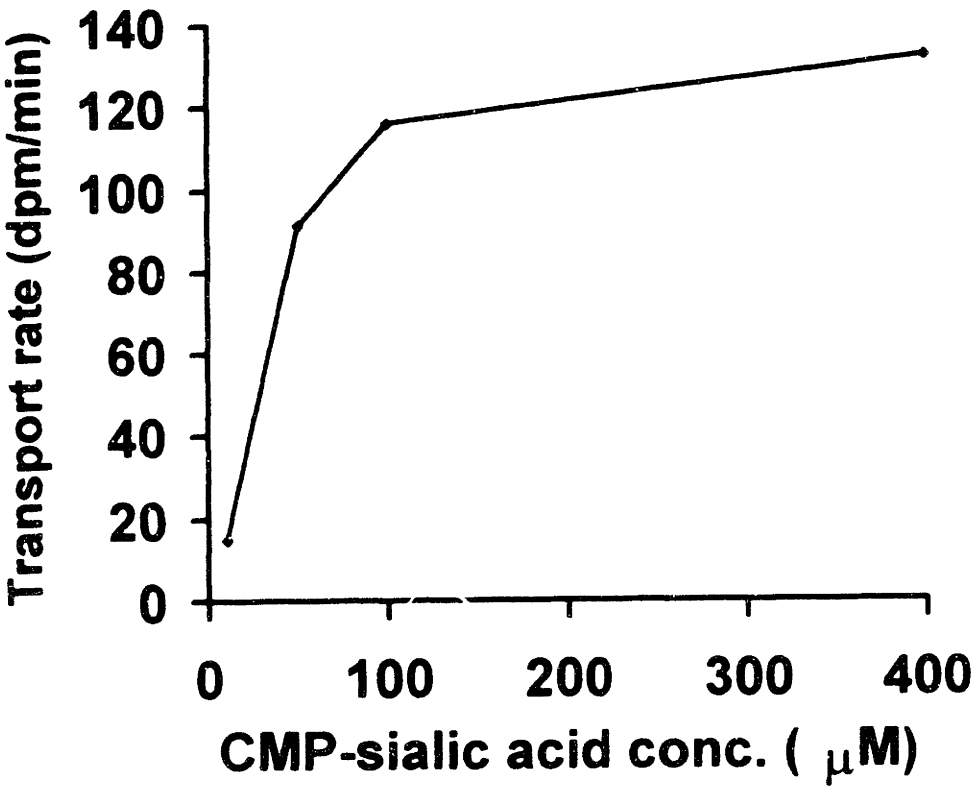

Figure 6.7: *in vitro* CMP-Sialic Acid Transport into Trans-Golgi

Due to its greater accessibility to the various enzymatic processes involved in glycosylation, Asn^{25}-linked oligosaccharides of CHO-derived IFN-γ possess greater average antennarity (James *et al.*, 1995; Harmon *et al.*, 1996) and sialylation, as reported in Chapter Four, than the glycans at Asn^{97}, and fucosylation occurs exclusively at the Asn^{25} site. Furthermore, the Man(α1-3) branch of the predominant complex biantennary glycan offers a more exposed orientation than the Man(α1-6) arm (Joziasse *et al.*, 1985). As a result, 98% of Man(α1-3) branches of biantennary glycans at the Asn^{25} glycosylation site were sialylated while only 68% of the Man(α1-6) arms of Asn^{97}-linked complex biantennary glycans were sialylated in the unsupplemented culture. Although the sialylation of the Man(a1-6) branches of the Asn^{97}-linked glycans increased to 82% with 20 mM ManNAc supplementation, this location remained as the dominant source of incomplete product sialylation

CHAPTER SEVEN: CONCLUSIONS AND RECOMMENDATIONS

7.1 Conclusion

The presence and structure of oligosaccharides in glycoproteins are known to influence the biological properties of therapeutic proteins. The ability to characterize the oligosaccharides in real-time during animal cell cultivation offers the possibility to control and ensure the quality and consistency of the therapeutic proteins. This thesis presents a number of real-time analytical techniques in the quantitative measurement of macro- and microheterogeneity of the glycosylation of Chinese Hamster Ovary (CHO) cell cultures derived interferon-γ (IFN-γ) containing two potential glycosylation site, Asn^{25} and Asn^{97}. The monitoring techniques include tandem microbore chromatography, capillary electrophoresis, continuous peptide digestion and MALDI/TOF mass spectrometry. Rapid and real-time analysis (4 hours) and high sensitivity (0.5 μg) have been achieved to characterize both macro- and microheterogeneity of IFN-γ glycosylation. Both the site occupancy and fractions of biantennary, triantennary and tetraantennary structures of interferon-γ were found to remain unchanged during culture.

Since sialic acid content is known to be a critical determinant of the biological properties of glycoproteins, it is essential to characterize and monitor sialylation patterns of recombinant glycoproteins intended for therapeutic use. In this study, both site- and branch-specific differences in sialylation of human IFN-γ were reported. Sialylation profiles were quantitated by reversed-phase HPLC

separations of the site-specific pools of tryptic glycopeptides representing IFN-γ's two potential N-linked glycosylation sites. Although sialylation at each glycosylation site was found to be incomplete, glycans of Asn^{25} were more heavily sialylated than those of Asn^{97}. Furthermore, Man(α1-3) arms of the predominant complex biantennary structures were more favorably sialylated than Man(α1-6) branches at each glycosylation site. When the sialylation profile was analyzed throughout a suspension batch culture, sialic acid content at each site and branch was found to be relatively constant until a steady decrease in sialylation was observed coincident with loss of cell viability. The introduction of a competitive inhibitor of sialidase into the culture supernatant prevented the loss of sialic acid after the onset of cell death but did not affect sialylation prior to cell death. This finding indicated that incomplete sialylation prior to loss of cell viability could be attributed to incomplete intracellular sialylation while the reduction in sialylation following loss of cell viability was due to extracellular sialidase activity resulting from cell lysis. Thus, both intracellular and extracellular processes defined the sialic acid content of the final product.

Although serum-free media have been widely used in mammalian cell culture for therapeutic protein production, the effects of serum-substitutes on product quality have not been extensively examined. This study observed an adverse effect of Primatone RL, an animal tissue hydrolysate commonly used as a serum-substitute to promote cell growth, on sialylation of interferon-γ (IFN-γ) in CHO cell culture in both batch and fed-batch modes. In batch cultures, decreased sialylation was observed at each of the glycosylation sites of IFN-γ

with the use of elevated concentrations of the peptone. Although poorest sialylation was obtained with the use of a growth-inhibiting concentration of Primatone RL, diminished sialylation was observed at the optimal peptone concentration for cell growth and product yield. Since incubation of the product in Primatone RL-supplemented acellular medium did not result in decreased sialylation, the negative effect of Primatone could not be attributed to extracellular desialylation of IFN-γ by components of the peptone. In the fed-batch mode, a culture utilizing a serum-free feeding medium supplemented with Primatone RL demonstrated poorer sialylation than a similar culture not fed the peptone. The results of both the batch and fed-batch experiments indicate that the adverse effect of Primatone RL was not due solely to ammonia accumulation.

In this study, the incomplete intracellular sialylation of IFN-γ produced by CHO cell culture was minimized by supplementing the culture medium with N-acetylmannosamine (ManNAc), a direct intracellular precursor for sialic acid synthesis. By introducing 20 mM ManNAc into the culture medium, the percentage of incompletely sialylated IFN-γ for the dominant biantennary glycan structure was reduced by nearly 50% at the Asn^{97} glycosylation site. This was achieved without affecting cell growth or product yield. Radiolabeled ManNAc was used to trace the incorporation of ManNAc, and it was found that the supplemental ManNAc was exclusively incorporated into IFN-γ as sialic acid. The intracellular pool of CMP(cytidine 5'-monophosphate)-sialic acid, the nucleotide sugar substrate for sialyltransferase, was also extracted and quantified by HPLC. Feeding of 20 mM ManNAc increased this intracellular pool of CMP-sialic acid

nearly by thirty-fold compared to unsupplemented medium. Further incubation of isolated Golgi vesicles with radio-labeled CMP-sialic acid suggests that the concentration of CMP-sialic acid might approach the saturation of sialyltransferase inside trans-Golgi of CHO cells with the treatment of 20 mM ManNAc.

In conclusion, an analytical methodology has been developed to characterize IFN-γ glycosylation in CHO cell culture, the influence of culture condition on product glycosylation profile has been assess and several cell culture strategies have been explored to improve product glycosylation homogeneity

7.2 Recommendation for future works

The results of this thesis have suggested several further topics for full investigation First of all, with 20mM feeding of ManNAc in culture medium, it was implied that the intracellular availability of CMP-sialic acid might approach saturation for sialyltransferase activity, and, consequently, no further improvement of product sialylation should be expected with even higher availability of CMP-sialic acid The remaining incomplete sialylation might be caused by the inadequacy of sialyltransferase activity As a result, full sialylation could only be achieved through the combination of enhanced sialyltransferase activity and increased availability of CMP-sialic acid It will be interesting to test the possibility of further improvement in product sialylation by sialyltransferase

activity enhancement through either genetic manipulation or promotion of sialyltransferase activity by chemical response

Dexamethasone, which can decrease the activity of oligosaccharaide branching enzyme, has been shown in Chapter Six to reduce the proportion of highly-branched glycoforms of the product. It would be potentially valuable to utilize the impacts of both ManNAc feeding and dexamethasone on product glycosylation in order to produce glycoprotein with bisialo biantennary oligosaccharide structure In this manner, a highly homogeneous and efficacious product may be possible

The analytical methodology developed in this research to fully characterize the product glycosylation has also made research on several related topics feasible The capability of our analytical scheme to characterize and quantify the protein glycosylation heterogeneity provides great opportunities to understand the impact of oligosaccharide structures on pharmacokinetic properties of glycoproteins. The determination of the circulatory half-life of glycoproteins involves several different mechanisms Although glycoproteins can be attacked and removed by asiologlycoprotein receptors on the human hepatocytes, human proteins with molecular weights less than about 70 kDa are continuously removed from the circulation through the kidney. The filtration rate through the kidney glomerular tubules is sensitive to protein tertiary structure as well as molecular weight and can be inhibited by the presence of surface charge (Kaniwar, 1984) Biantennary structures with full sialylation are probably the best structure to avoid the attack of asialoglycoprotein receptors However, the impact on other

mechanisms involved in the clearance of glycoproteins is not clear. Study in this area would provide valuable information oligosaccharide structures which are most ideal for glycoproteins as human therapeutics.

The analytical methodology developed for characterization of IFN-γ glycosylation, including the enzymatic proteolytic digestion, the reversed-phased chromatographic isolation of target peptides and the characterization of relevant peptides by MALDI-TOF, is also applicable to the rapid and sensitive characterization of other important aspects of protein quality, including amino acid sequence integrity. For IFN-γ, the presence of several polypeptide forms, rather than a single form, after the removal of oligosaccharide suggested that C-terminal proteolytic cleavage took place in CHO culture (Curling *et al.*, 1990) Since the integrity of the C-terminal sequence is critical to the biological properties of IFN-γ, it is desirable to understand the influence of cell culture conditions on product peptide integrity and, ultimately, produce IFN-γ in CHO cell culture with C-terminal integrity

Reference

Abeijon, C.; Hirschberg, C. B. Topography of glycosylation reactions in the endoplasmic reticulum *TIBS*. **1992**, 17: 32-36.

Allen, S , Naim, H. Y , Bulleid, N. J. Intracellular folding of tissue-type plasminogen activator----effects of disulfide bond formation on N-linked glycosylation and secretion. *J. Biol. Chem.* **1995**, 270. 4797-4804.

Anderson, D. C.; Goochee, C. F. The effect of ammonia on the O-linked glycosylation of granulocyte colony-stimulating factor produced by Chinese hamster ovary cells *Biotechnol. Bioeng.* **1995**, 47: 96-105.

Aquino, D ; Wong, R., Margolis, R. U , Margolis, R. K. Sialic acid residues inhibit proteolytic degradation of dopamine β-hydroxylase *FEBS Lett* **1980**, *112*: 195-198.

Bocci, V , Pacini, A ; Pessina, G P , Paulesu, L , Muscettola, M , Lunghetti, G Catabolic sites of human interferon-γ *J Gen Virol* **1985**, 66. 887-891

Borys, M C , Linzer, D J H , Papoutsakis, E. T Culture pH affects expression rates and glycosylation of recombinant mouse placental lactogen proteins by Chinese hamster ovary cells. *Bio/Technology* **1993**, 4 459-467

Bulleid, N J , Bassel-Duby, R S., Freedman, R B ; Sambrook, J F , Gething, M J Cell-free synthesis of enzymatically active tissue-type plasminogen activator Protein folding determines the extent of N-linked glycosylation *Biochem J* **1992**, 286. 275-280

Berg D T , Burck, P J , Berg, D H.; Grinnell, B. W Kringle glycosylation in a modified human tissue plasminogen activator improves functional properteis *Blood*, **1993**, 81 1312-1322

Bergman, L. W.; Kuehl, W M Temporal relationship of translation and glycosylation of immunoglobulin heavy and light chains. *Biochem* **1978**, 17 5174-5180

Capasso, J M and Hirschberg, C B Mechanisms of glycosylation and sulfation in the Golgi apparatus Evidence for nucleotide sugar/nucleoside monophosphate and nucleotide sulfate/nucleoside monophosphate antiports in the Golgi apparatus membrane. *Proc Natl. Acad Sci. USA.* **1984**, 81 7051-7055

Carey, D. J.; Sommers, L. W.; Hirschberg, C. B. CMP-N-acetyl-neuraminic acid: Isolation from and penetration into mouse liver microsome. *Cell.* **1980**, 19: 597-605.

Coates, S. W.; Gurney, T. Jr.; Sommers, L. W.; Yeh, M.; Hirschberg, C. B. Subcellular localization of sugar nucleotide synthetases. *J. Biol. Chem.* **1980**, 225: 9225-9229.

Carr, S. A.; Barr, J. R.; Robers, G. D.; Anumula, K. R.; Taylor, P. B. Identification of attachment sites and structural classes of Asparagine-linked carbohydrates in glycopeptides. *Meth. Enz.* **1990**, 193: 501-536.

Castro, P. M. L.; Ison, A. P.; Hayter, P. M.; Bull, A. T. The macroheterogeneity of recombinant human interferon-γ produced by Chinese hamster ovary cells is affected by the protein and lipid content of the culture medium. *Biotechnol. Appl. Biochem.* **1995**, 87: 87-100.

Chotigeat, W.; Watanapokasin, Y.; Mahler, S ; Gray, P.P. Role of environmental-conditions on the expression levels, glycoform pattern and levels of sialyltransferase for hFSH produced by recombinant CHO cells *Cytotechnology*, **1994**,15: 217-221.

Corfield, A. P. and Schauer R. Current aspects of glycoconjugate biosynthesis. *Biol Cellulaire.* **1979**, 36: 213-226.

Curling, E M., Hayter, P.M.; Baines, A J ; Gull, K.; Strange, P. G; Jenkins, N Recombinant human interferon-γ: differences in glycosylation and proteolytic processing lead to heterogeneity in batch culture. *Biochem. J* **1990**, 272: 333-337

Deutscher, S L , Nuwayhih, N.; Stanley, P ; Briles, E. I. B., Hirschberg, C. B. Translocation across Golgi vesicle membranes A CHO glycosylation mutant deficient in CMP-sialic acid transport. *Cell.* **1984**, 39: 295-299.

Devos, R ; Cheroutre, H., Tava, Y.; Degrave, W.; Van Heuverswyn, H.; W. Fiers. Molecular cloning of human interferon cDNA and its expression in eukaryotic cells. *Nucleic Acids Res.* **1982**, 10: 2487-2501.

Dordal, M. S., Wang, F F., Goldwasser, E. The role of carbohydrate in erythropoiein action *Endocrinology* **1985**, 116 2293-2299

Dorner, A. J., Bole, D. G.; Kaufman, R. J. The relationship of N-linked glycosylation and heavy chain-binding protein A association with the secretion of glycoprotein. *J. Cell. Biol.* **1987**, 105: 2665-2674.

Dorner, A. J.; Krane, M. G.; Kaufman, R. J. Reduction of endogenous GPR78 levels improves secretion of a heterologous protein in CHO cells. *Mol. Cell. Biol.* **1988**, 8: 4063-4070.

Drickamer, K. Clearing up glycoprotein hormones. Cell **1991**, 67: 1029-1032.

Easton, E. W.; Bolscher, J. G. M.; van den Eijnden, E. H. Enzymatic amplification involving glycosyltransferases forms the basis for the increased size of asparagine-linked glycans at the surface of NIH 3T3 cells expressing the N-ras proto-oncogene. *Jour. Biol. Chem.* **1991**, 266 (32): 21674-21680.

Ealick, S. E.; Cook, W. J.; Vijay-Kumar, S.; Carson, M.; Nagabhushan, T. L.; Trotta, P. P.; Bugg, C. E. Three-dimensional structure of recombinant human interferon-g. *Science* **1991**, 252. 698-702

Elbein, A. D Glycosidase inhibitors –inhibitors of N-linked oligosaccharide processing *FASEB J* **1991**, 5 3044-3-63.

Ezekowitz, R. A B , Stahl, P. D. The structure and function of vertebrate mannose lectin-like proteins *J. Cell. Sci. Suppl.* **1988**, 9 121-133

Farrar, M A., Schreiber, R D. The molecular cell biology of interferon-γ and its receptor *Annu Rev. Immunol* **1993**, 11 571-611.

Fennie, C , Lasky, L A. Model for intracellular folding of the human immunodeficiency virus type 1 gp120 *J Virol.* **1989**, 63: 639-646

Ferwerda, W.; Blok, C. M., van Rinsum, J Synthesis of N-acetylneuraminic acid and of CMP-N-acetylneuramnic acid in the rat liver cell *Biochem. J* **1983,** 216 87-92.

Fuhrmann, U., Bause, E., Legler, G., Ploegh, H Novel mannosidase inhibitor blocking conversion of high mannose to complex oligosaccharides *Nature (London)* **1984**, 307: 755-758.

Galili, U.; Macher, B.A., Buehler, J ; Shohet, S B. Human natural anti-alpha-galactosyl IgG. 2. The specific recognition of alpha(1-3)linked galactose residues *J. Exp. Med.* **1985**, 162 573-582.

Gawlitzek, M., Valley, U.; Nimtz, M.; Wagner, R ; Conradt, H.S. Characterization of changes in the glycosylation pattern of recombinant proteins from BHK-21-cells due to different culture conditions. *J. Biotechnol.* **1995**, 42 117-131.

Goldwasser, E.; Kung, C.K.-H; Eliason, J. On the mechanism of erythropoietin-induced differentiation. *J. Biol. Chem.* **1974**, 249: 4202-4206.

Grabenhorst, E., Hoffmann, A., Nimtz, M., Zettlmeissl, G., Conradt, H. S. Construction of stable BHK-21 cells coexpressing human secretory glycoproteins and human Gal(β1-4)GlcNAc-R α2,6-sialyltransferase. *Eur. J. Biochem.* **1995**, 232: 718-725.

Grabenhorst, E.; Hofer, B.; Nimtz, M.; Jager, V.; Conradt, H.S. 1993 Biosynthesis and secretion of human interleukin-2 glycoprotein variants from baculovirus-infected sf21cells-characterization of polypeptides and post-translational modifications. *Eur. J. Biochem.* **1993**, 215: 189-197.

Gramer, M. J.; Goochee, C. F Glycosidase activities in Chinese hamster ovary cell lysate and cell culture supernatant *Biotechnol Prog* **1993**, 9: 366-373.

Gramer, M J , Goochee, C. F.; Chock, V. Y., Brousseau, D. T , Sliwkowski, M B Removal of sialic acid from a glycoprotein in CHO cell culture supernatant by action of an extracellular CHO cell sialidase *Bio/Technology* **1995**, 13 692-698

Gramer, M J , Goochee, C F Glycosidase activities of the 293 and NS0 cell-lines and of an antibody –producing hybridoma cell line *Biotechnol Bioeng* **1995**, 43 423-428

Gravel, Y and von Heijne, G Sequence differences between glycosylated and non-glycosylated Asn-X-Thr/Ser acceptor sites. Implication for protein engineering *Protein Eng* **1990**, 3: 433-442.

Grzesiek, S , Dobeli, H , Gentz, R , Garotta, G.; Labhardt, A. M., Bax, A ^{1}H, ^{13}C, and ^{15}N backbone assignments and secondary structure of human interferon-γ. *Biochem.* **1992**, 31. 8180-8190.

Hahn, T. J. and Goochee, C.F. Growth-associated glycosylation of transferrin secreted by HepG2 cells *J. Biol. Chem* **1992**, 267: 23982-23987

Hanover, J. A. and Lennarz, W J. 1982 Transmembrane assembly of N-linked glycoproteins. Studies on the topology of saccharide-lipid systhesis *J. Biol Chem.* **1982**, 257. 2787-2794

Harmon, B J , Gu, X , Wang, D. I. C. Rapid monitoring of site-specific glycosylation microheterogeneity of recombinant human interferon-γ. *Anal. Chem.* **1996**, 68: 1465-1473

Harms, E.; Kreisel, W.; Morris, H. P. and Reutter, W. Biosynthesis of N-Acetylneuraminic acid in Morris hepatomas. *Eur. J. Biochem.* **1973**, 32: 254-262.

Hart, G. W. 1992. Glycosylation. *Current Opinion in Cell Biology* 1992, 4: 1017-1023.

Hayter, P M., Curling, F. M.; Baines, A. J.; Jenkins, N.; Salmon, I.; Strange, P. G.; Tong, J. M.; Bull, A. T. Glucose-limited chemo-stat culture of Chinese hamster ovary cells producing recombinant human interferon-γ *Biotechnol. Bioeng.* **1992**, 39: 327-335

Hayter, P M.; Curling, E.M ; Gould, M L., Baines, A. J.; Jenkins, N., Salmon, I ; Strange, P G , Bull, A. T The effect of dilution rate on CHO cell physiology and recombinant interferon-γ production in glucose-limited chemostat cultures *Biotechnol Bioeng* **1993**, 42 1077-1085

Hermentin, P , Witzel, R , Vliegenthart, J F , Kamerling, J P ; Nimtz, M , Conradt, H S A strategy for the mapping of N-glycans by high-pH anion-exchange chromatography with pulsed amperometric detection *Anal Biochem* **1992**, 203 281-289

Hirschberg, C B and Yeh, M Sialic acid uptake by BHK cells and subsequent incorporation into glycoproteins and glycolipids *J Supramol Struct* **1977**, 6 571-577

Hiyama, J , Weisshaar, G , Renwick, A G The asparagine-linked oligosaccharides at individual glycosylation sites in human thyrotrophin *Glycobiology* **1992**, 2 401-409.

Hooker, A D ; Goldman, M H., Markham, N H , James, D C , Ison, A P , Bull, A T., Strange, P G ; Salmon, I , Baines, A J , Jenkins, N *N*-Glycans of recombinant human interferon-γ change during batch culture of Chinese hamster ovary cells. *Biotechnol Bioeng* **1995**, 48: 639-648

Hokke, C H , Bergwerff, A. A.; Vandedem, G W K.; Kamerling, J P , Vliegenthart, J F G Structural-analysis of the sialylated N-linked and O-linked carbohydrate chains of recombinant-human-erythropoietin expressed in chinese-hamster ovary cells-sialylation patterns and branch location of dimeric N-acetyllactosamine units *Eur J. Biochem* **1995**, 228: 981-1008

Hsieh, Y L F., Wang, H., Elicone, C.; Mark, J , Martin, S.A.; Regnier, F Automated analytical systems for the wxamination of protein primary structure *Anal Chem* **1996**, 68 455-462

Huberty, M. C , Vath, J. E.; Yu, W.; Martin, S. A. Site-specific carbohydrate identification in recombinant proteins using MALD-TOF MS. *Anal Chem.* **1993**, 65: 2791-2800.

James, D C ; Freedman, R. B ; Hoare, M.; Ogonah, O. W.; Rooney, B. C.; Larionov, O. A., Dobrovolsky, V N.; Lagutin, O. V.; Jenkins, N. N-Glycosylation of recombinant human interferon-γ produced in different animal expression systems. *Bio/Technology* **1995**, 13: 592-596.

Jan, D. C-H., Jones, S. J.; Emery, A N ; Al-Rubeai, M Peptone, a low-cost growth-promoting nutrient for intensive animal cell culture. *Cytotechnology* **1994**, 16 17-26

Jenkins, N , Castro, P. M L , Menon, S ; Ison, A P , Bull, A T Effect of lipid supplements on the production and glycosylation of recombinant interferon-γ expressed in CHO cells *Cytotechnology* **1994a**, 15. 209-215

Jenkins, N , Curling, E M A Glycosylation of recombinant proteins problems and prospects *Enzyme Microb Technol.* **1994b**, 16 354-364

Joziasse D H , Schiphorst, W E C M , van den Eijnden, D H , van Kuik, J A , van Halbeek, H , Vliegenthart, J F G Branch specificity of bovine colostrum CMP-sialic acid N-acetyllactosaminide α2-6-sialyltransferase *J Biol Chem* **1985**, 260 714-719

Kagawa, Y , Takasaki, S , Utsumi, J.; Hosoi, K., Shimizu, H., Kochibe, N , Kobata, A. Comparative-study of the asparagine-linked sugar chains of natural human interferon-beta-1 and recombinant human interferon-beta-1 produced by 3 different mammalian cells *J Biol Chem.* **1988**, 263 17508-17515

Kaluza, G , Rott, R , Schwarz, R T. Carbohydrate-induced conformational changes of semliki forest virus glycoproteins determin antigenicity *Virology* **1980**, 102 286-299

Kamath, S A., Narayan, K A. Interaction of Ca^{2+} with endoplasmic reticulum of rat liver: a standardized procedure for the isolation of rat liver microsomes *Anal Chem.* **1972**, 48: 53-61

Kaniwar, Y S biology of disease biophysiology of glomerular filtration and proteinuria *Lab. Invest* **1984**, 51 7-21

Kean, E L 1972 CMP-sialic acid synthetase of nuclei *Methods Enzymol* **1972**, XXVIII 413-421

Kohn, P ; Winzler, R. J , Hoffman, R. C Metabolism of D-glucosamine and N-Acetyl-D-glucosamine in the intact rat. *J. Biol Chem.* **1962**, 237: 304-308

Kornfeld, R and Kornfeld S Assembly of asparagine-linked oligosaccharides. *Ann Rev. Biochem.* **1985**, 54: 631-664.

Kurota, N., Orita, T ; Hattori, K.; Oheda, M.; Ochi, N.; Yamazaki, T Structural characterization of natural and recombinant human granulocyte colony stimulating factors *J. Biochem.* **1990**, 107 486-492

Lau, J T Y , Welpy, J K , Shenbaganurthi, P.; Naider, F.; Lennarz, W J 1983 Substrate recognition by oligosaccharyl transferase: inhibition of co-translational glycosylation by acceptor peptides *J Biol Chem* **1983**, 258 15255-15260

Lawson, E Q , Hedlund, B E , Ericson, M E , Mood, D A , Litman, G W , Middaugh, R Effect of carbohydrate on protein solubility *Arch Biochem Biophys* **1983**, 220 572-575

Lee, E U , Roth, J , Paulson, J C Alteration of terminal lycosylation sequences on N-linked oligosaccharides of Chinese hamster ovary cells by expression of b-galactosidase a2,6-sialyltransferase *J Biol Chem* **1989**, 264 13848-13855

Lifely, M R , Hale, C , Boyce, S , Keen, M J , Phillips, J Glycosylation and biological activity of CAMPATH-1H expressed in different cell lines and grown under different culture conditions *Glycobiology* **1995**, 5 813-822

Lin, A A., Kimura, R , Miller, W M Production of tPA in recombinant CHO cells under oxygen-limited conditions *Biotechnol Bioeng* **1993**, 42 339-350

Lund, J T , Takahashi, N , Nakagawa, H , Goodall, M , Bentley, T , Hindley, S A Control of IgG/Fc glycosylation a comparison of oligosaccharides from chimeric human/mouse and mouse subclass immunoglobulin Gs *Mol Immunol* **1993**, 30 741-748

Miletich, J P , Broze Jr , G J Protein C is not glycosylated at asparagine 329. *J. Biol. Chem* **1990**, 265. 11397-11404.

Mizrahi, A Primatone RL in mammalian cell culture media *Biotechnol Bioeng.* **1977**, 19 1557-1561

Monica, T. J , Williams, S B , Goochee, C. F , Maiorella, B L Characterization of the glycosylation a human-IgM produced by a human-mouse hybridoma *Glycobiology* **1995**, 5 175-185

Mortz, E , Sareneva, T , Julkunen, I ; Roepstorff, P Does matrix-assisted laser desorption/ionization mass spectrometry allow analysis of carbohydrate

heterogeneity in glycoproteins? A study of natural human interferon-γ *J. Mass Spect.* **1996**, 31: 1109-1118.

Mutsaers, J. H. G M.; Kamerling, J. P.; Devos, R.; Guisez, Y ; Fiers, W , Vliegenthart, J F G Structural studies of the carbohydrate chains of human γ-interferon. *Eur. J. Biochem.* **1986**, 156: 651-654.

Nakao, H.; Hishikawa, A.; Karasuno, T.; Nishiura, T.; Iida, M., Kanayama, Y.; Yonezawa, T., Tarui, S., Taniguchi, N. Modulation of N-acetyl-glucosaminyltransferase III, IV and V activities and alteration of the surface oligosaccharide structure of a myeloma cell line by interleukin 6 *Biochem Biophys Res Commun* **1990**, 172: 1260-1266

Noguachi, A ; Mukuria, C. J ; Suzuki, E., Naiki, M Immunogenicity of N-glycolylneuraminic acid-containing carbohydrate chains of recombinant human erythropoietin expressed in chinese hamster ovary cells *J. Biochem* **1995**, 117 59-62

Olden, K , Pratt, R M , Yamada, K. M Role of carbohydrate in biological function of the adhesive glycoprotein fibronectin *Proc Natl Acad Sci* **1979**, 76 3343-3347

Oheda, M , Hasegawa, M , Hatto ri, K , Kuboniwa, H , Kojima, T , Orita, T , Tomonou, K., Yamzaki, T , Ochi, N O-linked sugar chain of human granulobyte colony-stimulating factor protects it against polymerization and denaturation allowing it to retain its biological activity *J Biol. Chem.* **1990**, 265 11432-11435

Parekh, R B , Dwek, R A., Rudd, P M , Thomas, J R , Rademacher, T W , Warren, T , Wun, T -C , Hebert, B ; Reitz, B , Palmier, M., Ramabhadran, T , Tiemeier, D. C N-glycosylation and in vitro enzymatic activity of human recombinant tissue plasminogen activator expressed in Chinese hamster ovary cells and a murine cell line *Biochem* **1989**, 28 7670-7679

Patel, T P , Parekh, R B ; Moellering, B J ; Prior, C P. Different culture methods lead to differences in glycosylation of a murine IgG monoclonal antibody *Biochem. J* **1992**, 285 839-845

Patterson, D H , Tarr, G E.; Regnier, F. E , Martin, S A C-terminal ladder sequencing via matrix-assisted laser desorption mass spectrometry coupled with carboxypeptidase Y time-dependent and concentration-dependent digestions. *Anal Chem* **1995**, 67: 3971-3978

Paulson, J. C. and Colley, K J. 1989 Minireview: Glycosyltransferases. *J Biol Chem.* **1989**, 264 17615-17618

Peutt, D. Conformational studies on glycosylated bovine pancreatic ribonuclease. *J. Biol. Chem.* **1973**, 248. 3566-3572.

Pless, D. D.; Lennarz, W J Enzymatic conversion of proteins to glycoproteins *Proc. Natl. Acad Sci USA* **1977**, 74. 134-138.

Pumper, R. W Adaptation of tissue culture cells to a serum-free medium *Science* 1958, **128** 363

Reuter, G., Schauer, R Determination of sialic acids *Methods Enzymol* **1994**, 230 168-199

Rice, K G , Rao, N B N , Lee, Y C Large-scale preparation and characterization of N-linked glycopeptides from bovine fetuin *Anal Biochem* **1990**, 184 249-258

Righetti, P R *Isoelectric Focusing Theory, Methodology and Applications*, Elsevier Amsterdam, **1983**

Rijcken, W R P, Overdijk, B , Eijnden, D H V D Ferwerda, W The effect of increasing nucleotide-sugar concentrations on the incorporation of sugars into glycoconjugates in rat hepatocytes *Biochem J* **1995**, 305 865-870

Rijcken, W R P, Overdijk, B , Eijnden, D H V D, Ferwerda, W Pyrimidine nucleotide metabolism in rat hepatocytes evidence for compartmentation of nucleotide *Biochem J* **1993**, 293 207-213

Rinderknecht, E , O'Connor, B H , Rodriguez, H Natural human interferon-γ complete amino acid sequence and determination of sites of glycosylation. *Jour Biol Chem* **1984**, 259 6790-6797

Rohrer, J S , Cooper, G A , Townsend, R R Identification, quantitation, and characterization of glycopeptides in reversed-phase HPLC separations of glycoprotein proteolytic digests *Anal Biochem* **1993**, 212 7-16

Ryll, T and Wagner, R. 1991. Improved ion-pair high-performance liquid chromatographic method for the quantification of a wide variety of nucleotides and sugar-nucleotides in animal cells. *J. Chromatogr* **1991**, 570 77-88

Sairam, M R , Linggen, J , Bhargavi, G N Alterations in antigenic structure of gonadotropins following deglycosylation *Bioscience Reports* **1988**, 8 271-278.

Sareneva, T , Pirhonen, J , Cantell, K , Kalkkinen N I, Julkunen, I Role of N-glycosylation in the synthesis, dimerization and secretion of human interferon-γ *Biochem J* **1994**, 303 831-840

Sareneva, T.; Pirhonen, J.; Cantell, K.; Julkunen, I. N-glycosylation of human interferon-γ glycans at Asn-25 are critical for protease resistence *Biochem. J.* **1995**, 308: 9-14

Sasaki, H., Ochi, N.; Dell, A., Fukuda, M. Site-specific glycosylation of human recombinant erythropoietin analysis of glycopeptides or peptides at each glycosylation site by fast atom bombardment mass spectrometry. *Biochemistry* **1988**, 27 8618-8626

Scahill, S J., Devos, R., Van Der Heyden, J., Fiers, W. Expression and charaterization of the product of a human immune interferon cDNA gene in Chinese hamster ovary cells *Proc Natl Acad Sci USA* **1983**, 80 4654-4658

Schachter H and Roden L In *Metabolic Conjugation and Metabolic Hydrolysis* III, Fishman, W., Ed., Academic Press San Diego, CA, 1973 17-34

Schauer, R Sialic acids as antigenic determinants of complex carbohydrates *Adv Exp Med Biol* **1988**, 228 47-72

Schlaeger, E -J., Schumpp, B Propagation of a mouse myeloma cell line J558L producing human CD4 immunoglobulin G1 *J Immunol Methods* **1992**, 146 111-120

Shelikoff, M., Sinskey, A J., Stephanopoulos, G The effect of protein synthes is inhibitors on the glycosylation site occupancy of recombinant human prolactin *Cytotechnology* **1994**, 15 195-208

Schoop, H J., Schauer R, Faillard, H Die oxydative entstehung von *N*-glykolyl-neuraminsaure aus *N*-acetyl-neuraaminsaure *Z Physiol Chem* **1969**, 350 155-162

Skehel, J J., Stevens, D J., Daniels, R S., Douglas, A R., Knossow, M., Wilson, I A Wiley, D C A carbohydrate side chain on hemagglutinins of Hong Kong influenza viruses inhibits recognition by a monoclonal antibody. *Proc Natl Acad Sci USA* **1984**, 81 1779-1783

Sliwkowski, M B., Gunson, J V; Warner, T. G Sialylation and mannose phosphorylation as a function of culture conditions for recombinant human deoxyribonuclease produced in CHO cells *J Cell Biochem Suppl.* **1992**, 16 150

Smith, P L., Kaetzel, D., Nilson, J., Baenziger, J U The sialylated oligosaccharides of recombinant bovine lutropin modulate hormone bioactivity *J Biol. Chem* **1990**, 265 874-881

Sommers, L W. and Hirschberg, C. B. Transport of sugar nucleotide into rat liver Golgi. *J. Biol Chem.* **1982**, 257: 10811-10817.

Spellman, M. W ; Basa, L. J.; Leonard, C K.; Chakel, J. A., O'connor, J V ; Wilson, S ; van Halbeek, H Carbohydrate structures of human tissue plasminogen activator expressed in Chinese hamster ovary cells. *J. Biol.Chem* **1989**, 264: 14100-14111.

Sutton, C. W., O'Neill, J A . Cottrell, J S. Site-specific characterization of glycoprotein carbohydrates by exoglycosidase digestion and laser desorption mass spectrometry *Anal Biochem* **1994**, 218. 34-46

Tachibana, H , Taniguchi, K , Ushio, Y ; Teruya, K , Osada, K , Murakami H Changes of monosaccharide availability of human hybridoma lead to alteration of biological properties of human monoclonal-antibody *Cytotechnology* **1994**, 16 151-157

Takeuchi, M , Takasadi, S , Miyazaki, H . Kato, T , Hoshi, S , Kochibe, N , Kobata, A Comparative study of the asparagine-linked sugar chains of human erythropoietins purified from urine and the culture medium of recombinant Chinese hamster ovary cells *J Biol Chem* **1988**, 26 3657-3663

Tandai, M , Endo, T , Sasaki, S , Masuho, Y , Kochibe, N, Kobata, A, Structural study of the sugar moieties of monoclonal antibodies secreted by human-mouse hybridoma *Arch Biochem Biophys 1991*, 291 339-348

Taylor, W G "Feeding the baby"-serum and other supplements to chemically defined medium *J Natl Cancer Inst* **1974**, 53 1449-1457.

Teige, M , Weidemann, R , Kretzmer, G Problems with serum-free production of antithrombin III regarding proteolytic acitivity and product quality *J Biotech* **1994**, 34 101-105

Townsend, R R , Hardy, M R , Cumming, D A , Carver, J P, Bendiak, B Separation of branched sialylated oligosaccharides using high-pH anion-exchange chromatography with pulsed amperometric detection. *Anal Biochem* **1989**, 182. 1-8

Treuheit, M J., Costello, C E., Halsall, H B Analysis of the five glycosylation sites of human α1-acid glycoprotein. *Biochem J* **1992**, 283 105-112

Treuheit, M J , Costello, C E , Kirley, T L Structures of the complex glycans found on the β-subunit of (Na, K)-ATPase* *J Biol Chem* **1993**, 268 13914-13919

Tsuda, E , Kawanishi, G ; Ueda, M ; Masuda, S , Sasaki, R The role of carbohydrate in recombinant human erythropoietin *Eur J Biochem* **1990**, 188 405-411

van den Eijnden, D H , Joziasse, D H , Dorland, L , van Halbeek, H , Vliegenthart, J F G , Schmid, K Specificity in the enzymic transfer of sialic acid to the oligosaccharide branches of bi- and triantennary glycopeptides of α1-acid glycoprotein *Biochem Biophys Res Commun* **1980**, 92 839-845

van den Eijnden, D H 1973 The subcellular localization of cytidine 5'-monophospho-N-acetylneuraminic acid synthetase in calf brain *J Neurochem* **1973**, 19 1649-1658

van Rinsum, J , van Dijk, W , Hooghwinkel, J M , Ferwerda, W Subcellular localization and tissue distribution of sialic acid precursor forming enzymes *Biochem J* **1983**, 210 21-28

Wang F -F C , Hirs, C H W Influence of the heterosaccharides in porcine pancretic ribonuclease on the conformation and stability of the protein *J Biol Chem* **1977**, 252 8358-8364

Warner, T G , Chang, J , Ferrari J , Harris, R , McNerney, T , Bennett, G , Burnier, J Sliwkowsli, M B Isolation and properties of a soluble sialidase from the culture fluid of Chinese hamster ovary cell *Glycobiology* **1993**, 3 455-463

Watson, E , Yao, F Capillary electrophoretic separation of recombinant granulocyte-colony-stimulating glycoforms *J Chromatogr* **1993**, 630 442-446

Weiss, P , Ashwell, G , The asialyglycoprotein receptor properties and modulation by ligand *Prog Clin Biol Res* **1989**, 300 169-184

Wittwer, A J and Howard, S C Glycosylation at Asn-184 inhibits the conversion of single-chain to two-chain tissue-type plasminogen activator by plasmin Biochem **1990**, 29 4175-4180

Xie, L 1996 Stoichiometric medium design and nutritional control in fed-batch cultivation of aminal cells, Ph D thesis, Massachusetts Institute of Technology, Cambridge, MA, USA

Xie, L and Wang, D I C Stoichiometric analysis of animal cell growth and its application of medium design *Biotechnol Bioeng* **1994a**, 43 1164-1174

Xie, L and Wang, D I C Fed-batch cultivation of animal cells using different medium design concepts and feeding strategies *Biotechnol Bioeng* **1994b**, 43 1175-1189

Xie, L. and Wang, D. I. C. Applications of improved stoichiometric model in medium design and fed-batch cultivation of animal cells in bioreactor *Cytotechnology* **1994c**, 15. 17-29.

Yamaguchi, K , Akai, K.; Kawanishi, G ; Ueda, M.; Masuda, S. and Sasaki, R Effects of site-directed removal of N-glycosylation sites in human erythropoietin on its production and biological properties *J Biol. Chem* **1991**, 266. 20434-20439

Yamashita, K , Ohkura, T ; Tachibana, Y., takasaki, S , Kotata, A Comparative study of the oligosaccharides released from baby hamster kidney cell and their polyoma transformant by hydrazinolysis *J Biol Chem* **1984**. 259 10834-10840

Yamashita, K. Tachibana, Y , Nakayama. T , Kitamura. M , Endo. Y , Kobata. A Structural studies of the sugar chains of human parotid α-amylase *J Biol Chem* **1980**. 255 5635-5642

Yan, S C B , Razzano, P , Chao, Y B . Walls, J D , Berg. D T , McClure D B . Grinnell. B W Characterization and novel purification of recombinant human protein-C from 3 mammalian-cell lines *Bio/Technology* **1990**. 8 655-661

Yet, M -G . Wold. F The distribution of glycan structures in individual N-glycosylation sites in animal and plant glycoproteins *Arch Bioch Biophys* **1990**. 278 356-364

Yohe, H C . Ueno. K. Chang. N -C , Glaser. G H . Yu, R K Incorporation of *N*- acetylmannosamine into rat rain subcellular gangliosides effect of pentylenetetrazol-induced convulsions on brain gangliosides *J Neurochem* **1980**. 34. 560-568

Zhang. Y . Zhou. Y . Yu. J Effects of peptone on hybridoma growth and monoclonal antibody formation *Cytotechnology* **1994**. 16 147-150

THESIS PROCESSING SLIP

FIXED FIELD ill _____ name _____

index _____ biblio _____

▶COPIES Archives Aero Dewey Eng Hum

Lindgren Music Rotch Science

TITLE VARIES ▶☐ _____

_____

_____

NAME VARIES ▶☐ _____

_____

IMPRINT (COPYRIGHT) _____

▶COLLATION _____

_____

▶ADD DEGREE _____ ▶DEPT _____

SUPERVISORS _____

_____

_____

_____

_____

_____

_____

_____

_____

NOTES

cat'r date

page

▶DEPT _____

▶YEAR _____ ▶DEGREE _____

▶NAME _____